

Alma Mater Studiorum – Università di Bologna

**DOTTORATO DI RICERCA IN  
MECCANICA E SCIENZE AVANZATE DELL'INGEGNERIA**

Ciclo XXXII

**Settore Concorsuale: 09/C2**

**Settore Scientifico Disciplinare: ING-IND/18**

**INTEGRATED DESIGN OF ATMOSPHERIC PRESSURE NON-EQUILIBRIUM  
PLASMA SOURCES FOR INDUSTRIAL AND BIOMEDICAL APPLICATIONS**

**Presentata da: Filippo Capelli**

**Coordinatore Dottorato  
Prof. Marco Carricato**

**Supervisore  
Prof. Vittorio Colombo**

**Esame finale anno 2020**



# Index

Abstract .....	5
Chapter 1 .....	7
1.1 This thesis.....	9
1.2 Outline.....	10
1.3 References .....	11
Chapter 2 .....	15
2.1 Sterilization methods for packaging .....	Errore. Il segnalibro non è definito.
2.1.1 Thermal treatments.....	Errore. Il segnalibro non è definito.
2.1.2 Chemical treatments .....	Errore. Il segnalibro non è definito.
2.1.3 Radiation treatments .....	Errore. Il segnalibro non è definito.
2.2 Plasma assisted treatments for bacterial inactivation .....	Errore. Il segnalibro non è definito.
2.2.1 Corona discharges.....	Errore. Il segnalibro non è definito.
2.2.2 Atmospheric-Pressure Plasma Jets....	Errore. Il segnalibro non è definito.
2.2.3 Resistive Barrier Discharges .....	Errore. Il segnalibro non è definito.
2.2.4 Dielectric Barrier Discharges .....	Errore. Il segnalibro non è definito.
2.3 References .....	Errore. Il segnalibro non è definito.
Chapter 3 .....	29
3.1 Plasma reactive components .....	Errore. Il segnalibro non è definito.
3.2 References .....	Errore. Il segnalibro non è definito.
Chapter 4 .....	35
4.1 Effect of water vapor .....	Errore. Il segnalibro non è definito.
4.2 Pathogen selection .....	Errore. Il segnalibro non è definito.
4.3 Biological protocol.....	Errore. Il segnalibro non è definito.
4.4 Biological results.....	Errore. Il segnalibro non è definito.
4.5 Discussion .....	Errore. Il segnalibro non è definito.
4.6 References .....	Errore. Il segnalibro non è definito.

Chapter 5 .....	47
5.1 Proof of concept.....	48
5.2 Temperature analysis .....	50
5.3 Electrical measurement .....	53
5.4 Discussion on results and dielectric material choice .....	55
5.5 Cooling system .....	57
5.6 Chemistry analysis .....	58
5.6.1 OAS .....	63
5.6.2 OAS results and discussion .....	68
5.7 Process characterization conclusions .....	75
5.8 References .....	76
Chapter 6 .....	79
6.1 Global model .....	Errore. Il segnalibro non è definito.
6.1.1 Input parameters .....	Errore. Il segnalibro non è definito.
6.1.2 Global model results.....	Errore. Il segnalibro non è definito.
6.2 Fluid model.....	Errore. Il segnalibro non è definito.
6.2.1 Input parameters .....	Errore. Il segnalibro non è definito.
6.2.2 Fluid model results .....	Errore. Il segnalibro non è definito.
6.3 Conclusions .....	Errore. Il segnalibro non è definito.
6.4 References .....	Errore. Il segnalibro non è definito.
Chapter 7 .....	91
7.1 Further investigation .....	92
7.2 About disinfection treatment.....	93

# Abstract

In this dissertation are reported the most relevant results obtained during my three years Ph.D. project. An open-air plasma source has been developed to treat plastic and metallic films typically used in food packaging manufacturing. Among others, the DBD configuration was chosen due to its many advantages such as high intensity and uniformity of the treatment, possibility of operating in ambient air as well as ease of scale up.

Biological experiments were performed to assess the microbial reduction induced by the plasma treatment. Different operative conditions have been tested in order to identify the most efficient configuration and two distinct behaviours have been observed: low-power density treatment allowed to achieve microbial inactivation values below  $\log 2$  independently on treatment time; high-power density treatment where the microbial reduction grew with increasing treatment time.

Subsequently, the plasma discharge has been characterized by means of three investigation methods: thermal, electrical and optical absorption spectroscopy (OAS) analysis. The thermal and electrical analyses were employed to identify the best dielectric materials for food packaging manufacturing purposes. Once defined the optimal DBD configuration, OAS was used to measure the absolute concentration of ozone and nitrogen dioxide. Results showed that at low-power density the chemistry is governed by ozone; while at high-power density ozone is consumed by the poisoning effect and only nitrogen dioxide is detectable.

Lastly, a numerical simulation has been used to deeper investigate the chemistry governing the plasma discharge; by means of PLASIMO a global model and a fluid model were implemented.



# Chapter 1

## Introduction

“*What should we call the main part of the discharge?*” [1]. The Nobel prize winner Irving Langmuir asked and answered this question back in 1928; he was working in the General Electric Research Laboratory on the extension of lifetime of tungsten filament light bulbs and he was looking for a word to describe the gas discharge he was studying. As many know, he decided to use the word “plasma” due to the similarities he saw between that multicomponent, strongly interacting ionized gas and the blood plasma.

More than 90 years have passed, and the term “plasma” is well accepted by the scientific community, however the definition of what is a plasma has been shaped through research in the last hundreds of years, starting from the Benjamin Franklin’s lightning experiment (1752) until now.

*Nowadays*, we refer to plasma as the fourth state of matter: plasma is an ionized gas and consists of neutral, reactive and charged species. Ionization itself is an extremely wide concept and therefore we can say that more than 99% of visible matter in the universe is in the plasma state [2]. Plasma can be observed in nature as lightning or as Northern light in proximity of the poles; in the everyday life we are used to see plasma in neon lamps, besides from that plasma applications are spread all around the industrial world.

“Ionized” means that at least one electron is not bound to an atom or molecule, converting the atom or molecule into positively charged ion [2]. A gas can be more or less ionized depending on the energy applied to it; therefore we can divide plasmas in two groups, weakly and strongly ionized: weakly ionized plasmas are those with a low ratio between ionized and non-ionized particles (ionization degree), usually this ratio is in the range  $10^{-7}$ – $10^{-4}$ . When the ionization degree is closer to unity, we have a completely ionized plasma [2]. An ionization degree is not the only characteristic that a gas should have to be called plasma; a plasma is a macroscopically neutral gas, which means that the balance of electrically positive and negative species must be almost null.

As in any gas, temperature in plasma is determined by the average energies of its particles (neutral and charged) and their relevant degrees of freedom (translational, rotational, vibrational, and those related to electronic excitation). Thus, plasmas, as multi-component systems, are able to exhibit multiple temperatures [2]. Following this concept, plasmas can be divided in two other categories: *equilibrium* plasmas and *non-equilibrium* plasmas. equilibrium plasmas are strongly ionized, and the temperatures of neutral species, ions and electrons are almost equal. Local Thermodynamic Equilibrium can be assumed (these plasmas are also known as LTE-plasmas), consequently the macroscopic temperature of the gas is high:

$$T_e \approx T_n \approx T_i \approx T_g$$

Where  $T_e$ ,  $T_n$ ,  $T_i$  and  $T_g$  are temperatures of electrons, neutral species ions and gas respectively. Gas temperature may reach values of several eV (1 eV is about 11600 K); consequently, these plasmas are also called *hot* plasmas or *thermal* plasmas. Applications are typically conducted at atmospheric pressure and include cutting and welding of metals, thermonuclear plasma systems, waste destruction, nanoparticle synthesis, plasma spray and others. Although it is not known on a global scale, thermal plasmas are involved in each automotive and shipbuilding industries; moreover, one of the most exploited methods of production of optical fiber implies the usage of a hot plasma.

*Non-equilibrium* plasmas (also known as *cold*, *non-thermal* or *non-LTE* plasmas) are plasmas in which the electron temperature is orders of magnitude greater than the temperature of any other species; as a result, there is no LTE and the macroscopic gas temperature is lower than in hot plasmas:

$$T_e \gg T_n \approx T_i \approx T_g$$

*Historically*, cold plasmas were produced in low pressure environment and used for applications such as microelectronics manufacturing, ozone generation, light generation and surface functionalization. It's worth reminding that most computer and smart phones hardware have undergone production processes relying on plasma technology [3].

In *order* to ionize a gas energy, either thermal or electrical, is needed; to generate non-equilibrium plasmas, usually a high electric field is applied to a gas by means of two electrodes; when the potential difference applied to the gas exceed the breakdown voltage some atoms and molecules are ionized. This breakdown voltage was described by Paschen [4] and depends on the product of the gas pressure and the distance

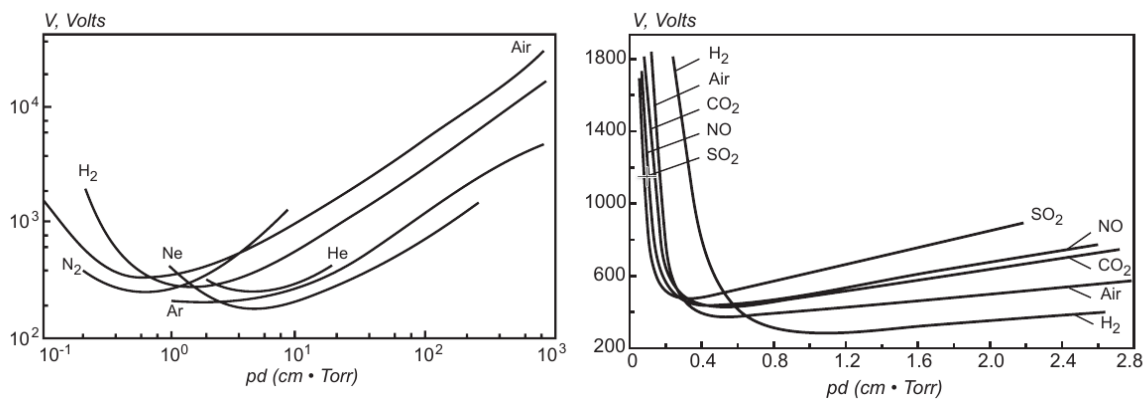


Figure 1.1 Breakdown Paschen curves for different atomic and molecular gases. [5]

between electrodes. These two parameters together define the distance that an electron will travel in the gas before colliding with another particle; this distance along with the electrical force applied to the electron give us information about the energy transferred in the collision: if this energy is higher than a certain threshold the affected



atom or molecule will be ionized. In order to reach that energy threshold value, the distance between two collisions cannot be too small; consequently, the voltage breakdown is higher for shorter inter electrode distances. On the other hand, an increase in pressure would lead to more frequent collisions, therefore a shorter distance travelled by electrons between collisions, hence a lower probability to successfully ionize an atom/molecule. Hence, the U shape for the breakdown graph that can be seen in Figure 1.1.

In order to sustain a non-equilibrium plasma, a pulsed power supply is often used; in fact, if the voltage applied to the electrodes exceed the breakdown voltage for a long period, the ionization may reach a high degree changing the gas condition from non-LTE to LTE. At low pressure, a stable plasma generation can be achieved imposing a low voltage over a gap of several centimetres; as the pressure raises also the breakdown voltage raises: at atmospheric pressure the breakdown value over a few millimetres gap is of several kV [5,6].

Plasma grants possibilities that are attractive for different applications in distinct fields: (1) the temperature of at least one of its component and energy density can significantly exceed those of conventional chemical technologies; (2) plasmas are able to produce very high concentrations of energetic and chemically active species (e.g., electrons, ions, atoms, radicals, excited states and photons); (3) plasma systems can essentially be far from thermodynamic equilibrium, keeping bulk temperature as low as room temperature. These plasma features allow significant intensification of traditional chemical processes and crucial increase of their efficiencies [5].

In recent years, a great effort has been made in cold plasma research to eliminate the constraint of working at low pressure ; there are mainly two reason behind this worldwide trend: first of all, working at atmospheric pressure implies freedom from vacuum systems which are expensive and extremely sensitive; moreover, working at high pressure allows treatment on living tissues, paving the way for medical applications,.

Thanks to the work conducted by research groups and companies, the field of application of cold atmospheric pressure (CAP) is widening day by day; starting from assisted combustion [7], surface disinfection [8], tissue engineering [9] decontamination of thermosensitive material [10] food [11–13] and packaging sanitation[14–16] surface functionalization in implantology [17,18], treatment and deposition of polymers [19–21]. Finally, the use of non-thermal plasmas has gained significant interest in the medical field [22–25], showing promising future applications in wounds healing [8,26,27] and cancer therapies [28–30].

## 1.1 This thesis

The focus of my Ph.D. research was to study, design and optimize cold atmospheric pressure plasma processes for disinfection and sterilization purposes. The main core of the project was to find out if CAPs could be efficiently used for bacterial inactivation in a very specific application: disinfection of films used as food packaging. This task

required to study and understand which plasma source configuration could be used for such applications.

A process optimization phase followed; this phase consisted in characterizing the plasma in order to better understand the behaviour of the discharge under various different operative conditions. The knowledge acquired during this investigation allowed to identify the plasma characteristics that are involved in microbial inactivation and how to maximize their production, enhancing the process efficacy; this improvement enabled to meet the requirements of the industrial process: short treatment time and high inactivation levels.

Conclusions about the applicability and convenience of using plasma assisted decontamination processes are also given.

## 1.2 Outline

In this section an overview of the thesis will be given in order to help the reader to go through it without losing perspective on the final aim of the whole dissertation. After this brief introduction, which has the purpose to clarify the main goal of my research, the reader will find a more structured explanation of what can be found in literature about packaging disinfection. The aim of this second chapter is to underline the limits of applicability of conventional treatments and to highlight the main advantages of CAPs. At the end of this chapter a description of the plasma source used is presented.

The third chapter is meant to explain the optimization approach followed during this project; an iterative approach was used which required to repeat the same steps over and over: design of the plasma source, biological test to assess the treatment efficacy, plasma characterization to link inactivation efficacy with operative conditions. Later in this chapter, a complete analysis of what are the traits of CAPs that may lead to inactivation is reported. On chapter 4 the biological protocol is shown along with the main bacterial inactivation results.

Chapter 5 exposes every diagnostic technique used to characterize the plasma process. In this thesis are reported: temperature measurements, electrical measurements, UV analysis and chemical analysis of the gas phase by means of optical absorption spectroscopy (OAS). This last method of measurements is explained in detail being the most powerful one.

On chapter 6 a different approach to the same problem is reported: numerical simulation. The plasma discharge was simulated by means of the code PLASIMO (<https://plasimo.phys.tue.nl/>); this kind of approach allows, after validation, to predict the whole chemistry of a process. Additionally, by changing input parameters the user can predict the behaviour of different discharges without performing every characterization test.

The closing chapter goes again through the whole research project in order to underline the main results and conclusions achieved; moreover, an overview on future possible applications of disinfection plasma treatment is given, reporting those industrial sectors which may take advantage from this new method of sanitation.

### 1.3 References

- [1] Tonks L 1967 The Birth of “Plasma” *Am. J. Phys.* 35 857
- [2] Tendero C, Tixier C, Tristant P, Desmanson J and Leprince P 2006 Atmospheric pressure plasmas: A review *Spectrochim. Acta - Part B At. Spectrosc.* 61 2–30
- [3] Raizer Y P 1991 Gas discharge physics
- [4] Meek J M 1940 A theory of spark discharge *Phys. Rev.* 57 722–8
- [5] Fridman A 2008 *Plasma Chemistry*
- [6] Kogelschatz U 2003 Dielectric-barrier Discharges: Their History, Discharge Physics, and Industrial Applications 23 1–46
- [7] Starikovskaia S M 2014 Plasma-assisted ignition and combustion: nanosecond discharges and development of kinetic mechanisms *J. Phys. D. Appl. Phys.* 47 353001
- [8] O’Connor N, Cahill O, Daniels S, Galvin S and Humphreys H 2014 Cold atmospheric pressure plasma and decontamination. Can it contribute to preventing hospital-acquired infections? *J. Hosp. Infect.* 88 59–65
- [9] Fazel-Rezai R 2011 *Biomedical Engineering: Frontiers and Challenges*
- [10] Bekeschus S, Schmidt A, Weltmann K D and von Woedtke T 2016 The plasma jet kINPen – A powerful tool for wound healing *Clin. Plasma Med.* 4 19–28
- [11] Misra N N, Patil S, Moiseev T, Bourke P, Mosnier J P, Keener K M and Cullen P J 2014 In-package atmospheric pressure cold plasma treatment of strawberries *J. Food Eng.* 125 131–8
- [12] Basaran P, Basaran-Akgul N and Oksuz L 2008 Elimination of *Aspergillus parasiticus* from nut surface with low pressure cold plasma (LPCP) treatment *Food Microbiol.* 25 626–32
- [13] Perni S, Shama G and Kong M G 2008 Cold atmospheric plasma disinfection of cut fruit surfaces contaminated with migrating microorganisms *J. Food Prot.* 71 1619–25
- [14] Chipera S, Chen W, Mejlholm O, Dalgaard P and Stamate E 2011 Atmospheric pressure plasma produced inside a closed package by a dielectric barrier discharge in Ar/CO<sub>2</sub> for Bacterial Inactivation of Biological Samples *Plasma Sources Sci. Technol.* 20 025008
- [15] Ziuzina D, Patil S, Cullen P J, Keener K M and Bourke P 2013 Atmospheric

- cold plasma inactivation of *Escherichia coli* in liquid media inside a sealed package *J. Appl. Microbiol.* 114 778–87
- [16] Muranyi P, Wunderlich J and Langowski H C 2010 Modification of bacterial structures by a low-temperature gas plasma and influence on packaging material *J. Appl. Microbiol.* 109 1875–85
- [17] Lappalainen R and Santavirta S S 2005 Potential of coatings in total hip replacement *Clin. Orthop. Relat. Res.* 72–9
- [18] Ong J L, Carnes D L and Bessho K 2004 Evaluation of titanium plasma-sprayed and plasma-sprayed hydroxyapatite implants in vivo *Biomaterials* 25 4601–6
- [19] Liguori A, Traldi E, Toccaceli E, Laurita R, Pollicino A, Focarete M L, Colombo V and Gherardi M 2015 Co-Deposition of Plasma-Polymerized Polyacrylic Acid and Silver Nanoparticles for the Production of Nanocomposite Coatings Using a Non-Equilibrium Atmospheric Pressure Plasma Jet *Plasma Process. Polym.* 1–10
- [20] Liguori A, Pollicino A, Stancampiano A, Tarterini F, Focarete M L, Colombo V and Gherardi M 2016 Deposition of Plasma-Polymerized Polyacrylic Acid Coatings by a Non-Equilibrium Atmospheric Pressure Nanopulsed Plasma Jet *Plasma Process. Polym.* 13 375–86
- [21] Beier O, Pfuch A, Horn K, Weisser J, Schnabelrauch M and Schimanski A 2013 Low temperature deposition of antibacterially active silicon oxide layers containing silver nanoparticles, prepared by atmospheric pressure plasma chemical vapor deposition *Plasma Process. Polym.* 10 77–87
- [22] Fridman A and Friedman G 2012 *Plasma medicine*
- [23] Fridman G, Friedman G, Gutsol A, Shekhter A B, Vasilets V N and Fridman A 2008 Applied plasma medicine *Plasma Process. Polym.* 5 503–33
- [24] Kong M G, Kroesen G, Morfill G, Nosenko T, Shimizu T, Van Dijk J and Zimmermann J L 2009 Plasma medicine: An introductory review *New J. Phys.* 11
- [25] von Woedtke T, Reuter S, Masur K and Weltmann K D 2013 Plasmas for medicine *Phys. Rep.* 530 291–320
- [26] Wu A S, Kalghatgi S, Dobrynin D, Sensenig R, Cerchar E, Podolsky E, Dulaimi E, Paff M, Wasko K, Arjunan K P, Garcia K, Fridman G, Balasubramanian M, Ownbey R, Barbee K A, Fridman A, Friedman G, Joshi S G and Brooks A D 2013 Porcine intact and wounded skin responses to atmospheric nonthermal plasma *J. Surg. Res.* 179 e1–12

- 
- [27] Boekema B K H L, Vlig M, Guijt D, Hijnen K, Hofmann S, Smits P, Sobota A, Van Veldhuizen E M, Bruggeman P and Middelkoop E 2015 A new flexible DBD device for treating infected wounds: In vitro and ex vivo evaluation and comparison with a RF argon plasma jet *J. Phys. D. Appl. Phys.* 49 44001
- [28] Lee H J, Shon C H, Kim Y S, Kim S, Kim G C and Kong M G 2009 Degradation of adhesion molecules of G361 melanoma cells by a non-thermal atmospheric pressure microplasma *New J. Phys.* 11
- [29] Collet G, Robert E, Lenoir A, Vandamme M, Darny T, Dozias S, Kieda C and Pouvesle J M 2014 Plasma jet-induced tissue oxygenation: Potentialities for new therapeutic strategies *Plasma Sources Sci. Technol.* 23
- [30] Vandamme M, Robert E, Lerondel S, Sarron V, Ries D, Dozias S, Sobilo J, Gosset D, Kieda C, Legrain B, Pouvesle J M and Pape A Le 2012 ROS implication in a new antitumor strategy based on non-thermal plasma *Int. J. Cancer* 130 2185–94



## Chapter 2

### 2.0 Bacterial inactivation

Bacterial inactivation is a major concern both in the industrial and in the biomedical fields; scientists and researchers all around the world have been seeking for effective and reliable sterilization methods for hundreds of years.

In the industrial field, a great effort was and still is devoted to find new and more efficient sterilization methods for the food packaging sector; in fact, packaging plays an important role in the food manufacturing process, to protect from microorganisms and chemical changes, preserving foods from external agents, hence lengthening the shelf life of products. One of the most used methods in the food processing industry is “aseptic packaging”; this method involves the filling and sealing of a microbiologically stable (i.e. commercially sterile) product into sterilized containers under conditions that prevent microbial recontamination of the product, the containers, and their closures [1].

The bacterial inactivation topic is crucial also in the biomedical field for different reasons: as shown by the World Health Organization in the “Prevention of hospital-acquired infections” [2], 8.7% of hospital patients had nosocomial infections; at any time over 1.4 million people worldwide suffer from complications acquired in hospital due to bacterial infections. L.T. Curtis underlines that in the US alone, nosocomial infections cause about 1.7million infections and 99000 deaths per year; moreover, each nosocomial infection increased medical costs by \$12,197 [3]. Bacteria are transmitted between patients through several pathways: direct contact between patients (hands, saliva droplets or other body fluids); in the air (droplets or dust contaminated by a patient’s bacteria); via staff contaminated through patient care (hands, clothes, nose and throat) who become transient or permanent carriers, subsequently transmitting bacteria to other patients by direct contact during care; via objects contaminated by the patient (including equipment); via the staff’s hands, visitors or other environmental sources (e.g. water, other fluids, food) [4].

With this basis, it is easy to understand why the pursuit of new, efficient, reliable and flexible bacterial inactivation methods is so interesting.

#### 2.1 Sterilization methods for packaging

As reported by Ansari *et alii* in their “Overview of sterilization methods for packaging materials used in aseptic packaging systems” [1], there are several key factors that a sterilization method should have:

- rapid microbicidal activity;

- compatibility with treated surfaces, especially packaging material and equipment;
- minimum residue, easily removed from surface;
- present no health hazard to the consumer;
- no adverse effect on product quality in the case of unavoidable residue or erroneous high concentration;
- present no health hazard to operation personnel around the packaging equipment;
- compatible with environment;
- non-corrosive to surfaces treated;
- reliable and economical.

As can be expected, none of the common sterilization systems in use today fulfills all the request shown above. Conventional sterilization methods can be divided in three main categories: thermal, radiation and chemical treatments.

### 2.1.1 Thermal treatments

Traditionally, bacterial inactivation has been delivered through heating processes. Experience has shown that moist heat has a greater efficacy than dry heat to kill microorganisms; among others, spores present the highest thermal resistance and are often used as a benchmark to evaluate the efficacy of a sterilization process. “Dry heat produces microbial death as a result of dehydration followed by protein oxidation. Death by moist heat is caused by denaturation and coagulation of essential cell proteins” [5].

The main drawbacks of thermal processes are long treatment times and the dependence on the material to be treated; the velocity of microbial destruction depends on how rapidly the heat is transferred to the cell from the thermal carrier. For these types of treatments, it is essential to consider the nature of the surface to be treated. Metal containers, with their high conductivity are easier to thermally sterilize than are carton and plastics packaging. Moreover, plastic materials have often a low thermal stability and cannot be exposed to high temperature for the time needed to achieve sterilization.

On the positive side, thermal processes do not deposit any residues on the surface of the treated material and are environmentally friendly.

Among thermal processes it is worth mentioning treatments with saturated steam: these methods use humid air with a temperature between 121°C and 165°C. Treatments are usually performed under pressure, with a highly variable timing related to the level of inactivation desired: from a few seconds to several tens of minutes.

Other types of thermal processes are those using *superheated steam and hot air*; these treatments use dry heat and are less effective than those with humid air; consequently, higher temperatures are needed to achieve sterilization. Temperatures may vary between 145°C and 250°C. When materials susceptible to water are used, such as paper containers, treatments with hot air may be the only viable option.



The last thermal methods to be reported are those based on extrusion heating; these processes exploit the heat used to produce the packaging materials to deliver also the sterilization. Usually, this technology is used in form-fill-seal packaging systems.

## 2.1.2 Chemical treatments

These methods use chemicals in the form of liquid or gas for bacterial inactivation; there is a wide variety of chemicals which can be used for this purpose: ethylene oxide, peracetic acid, beta propiolactone, alcohol, chlorine, ozone etc.

Among others, hydrogen peroxide is the most interesting to be used for industrial applications; packaging is sprayed or dipped into an aqueous solution of 10-30% of hydrogen peroxide. This sterilizing agent has a slow effect on spore at low temperature; the efficacy of the treatment can be enhanced greatly increasing the temperature up to 60-90°C with hot air.

Chemical packaging sterilization may be the only viable path when thermosensitive materials are used; on the other hand, there are several drawbacks that cannot be ignored. First, there is a major concern about the toxicity of the chemicals involved in the process: there are regulations stating the maximum concentration of residues that can be found on the product after treatment, in order not to harm the customer. For this reason, cleaning of the packaging after treatment is often needed. The safety of workers must be guaranteed. Finally, the chemical procurement is an expense which must be reported.

## 2.1.3 Radiation treatments

Several different electromagnetic radiations are used for sterilization. Radiations are characterized by frequency, wavelength, penetrating power and energy range; known biocidal radiation are infrared, ultraviolet and  $\gamma$  rays. As for thermal processes, the efficacy of a sterilization treatment is a function of the energy delivered to the substrate (i.e. type of radiation, intensity and exposure time).

A huge advantage using these kinds of treatments is that radiation does not leave any residues on the treated surface, nor affect the surrounding environment.

On the other hand, irradiation may affect part of the material properties, compromising its use; furthermore, all electromagnetic radiation is a line-of-sight technology, reducing its industrial applicability.

The best known and used biocidal radiation is the UV which use rays with wavelengths between 200 and 315 nm [1]. The optimal effect of this treatment can be achieved using UV-C rays (250 – 280 nm). UV radiation is frequently also combined with chemical processes to enhance the sterilization effect and to minimize the quantity of chemicals involved in the process; resulting in a minor quantity of residues to be removed.

Infrared rays lie in the waveband 0.8 – 15  $\mu\text{m}$ ; this kind of radiation is absorbed by the treated surface and converted into heat, increasing the material temperature. This method relies greatly on the geometry and physical properties of the package.

Another excellent sterilizing method involve ionizing radiation; unlike the UV, this radiation penetrates deeply into objects. Among ionizing radiation, the most employed is the  $\gamma$  rays. Even if the efficacy of this technology is well known, it is not well spread in the industry field, due to several disadvantages that are worth mentioning: to avoid

any hazard for workers and the environment a heavy shielding must be used; moreover the initial installation cost is large. Finally, treated containers have to be moved from the sterilizing facilities to a location where they are filled with foods; it is difficult to ensure the packaging sterility during the phase.

Lastly, short pulses of light can be used for sterilization purposes; this technology employs highly energetic broad spectra rays; materials are flashed from 1 to 20 times with exposure times between 1  $\mu$ s to 0.1 s. This sterilization method acts only in line of sight, hence can be applied only on containers with a geometry which does not allow shadowing on the product.

## 2.2.0 Plasma assisted treatments for bacterial inactivation

Although plasma applications have been present in the industrial field for decades, the interest about plasma disinfection has grown only recently. Many research papers can be found in literature showing CAP applicability to the biomedical field; this wide emerging field (known as plasma medicine) includes large scale disinfection, wound healing, cancer treatment, tissue engineering and pharmacology [6].

The knowledge of plasma medicine on interaction between plasma and microorganisms and disinfection methods to avoid infections can be used to study, design and implement CAP industrial applications for packaging materials sterilization.

Many authors have investigated the possibility to kill microorganisms using plasma; the most relevant results are reported here: Pervin Basaran *et alii* obtained a log 5 decrease of *A. parasiticus* on contaminated hazelnuts, peanuts, and pistachio nuts [7]. Deng *et alii* achieved a log 4 reduction on *B. subtilis* spores using an atmospheric-helium plasma plume with 10 minutes of treatment [8]. Guimin *et alii* produced a log 5.38 reduction on *S. aureus* with a treatment time of 90 s and a log 5.36 reduction on *E. coli* with 60 s of treatment using a coaxial dielectric barrier discharge plasma jet in argon [9]. Kirkpatrick *et alii* used an atmospheric pressure argon DBD and reached a log 5 reduction on *E. coli* with 20 minutes of treatment [10]. Klämpf *et alii* reached a log 6 reduction on *C. albicans* with 30 s of treatment using a cold atmospheric surface micro-discharge plasma [11].

There are several key factors which make plasma extremely appealing for sterilization processes, the first of which is the high reactivity of plasma itself. Plasma is composed by several reactive components whose combined effects make it aggressive towards living organisms; this fact allows to achieve sterilization within short treatment times and consequently raises the interest for industrial applications.

Another important trait that makes plasma a possible future alternative for disinfection treatments is the production of gaseous residues; so, there is no need for packaging cleaning after the disinfection treatment. The only precaution that the process designer must take is related to the flow of gases inside the machine. The absence of a washing phase improves the treatment in two distinct ways: economically,

reducing both treatment times and the needed equipment; secondly, the risk of recontamination during the cleaning of the packaging is removed.

Although plasma may not be the best option for any sterilization treatment, it is very appealing for treatment of thermo-sensitive materials. Nowadays materials science is chasing the possibility to avoid plastic materials preferring new environmental-friendly materials; these materials have often low mechanical and thermal resistance; therefore, thermal sterilization is forbidden.

There are several different plasma source architectures that can be used for sterilization purposes, any of which has a wide range of operative conditions; this large collection of sources and processes allows the treatment of almost any kind of material and geometry known. In 2002 Laroussi reported on the most promising plasma decontamination processes [12], later in 2008 Moreau *et alii* returned on this subject [13]. A brief review of the most relevant plasma sources for bacterial inactivation is reported here.

### 2.2.1 Corona discharges

This plasma source architecture consists in a high voltage pin electrode facing a ground electrode; the enhancement of the electrical field close to the sharp end of the pin induce the ionization the gas. This discharge is usually RF-driven to create plasma at atmospheric pressure; furthermore, a process gas is often needed, such as argon or helium. Nevertheless, an atmospheric pressure air plasma can be produced also by means of a kHz pulsed AC power supply.

Siemens was the first to generate ozone in order to disinfect water supplies using a corona discharge [14]. A pulsed atmospheric pressure corona discharge inactivated microbial spores in less than 1 s [15].

A more sophisticated architecture uses an array of multiple pins to create a large volume plasma; Mohamed *et alii* proposes the use of an atmospheric pressure large volume air plasma generated by a 100 ns, 1-kHz high voltage pulse for the sterilization of fruits [16].

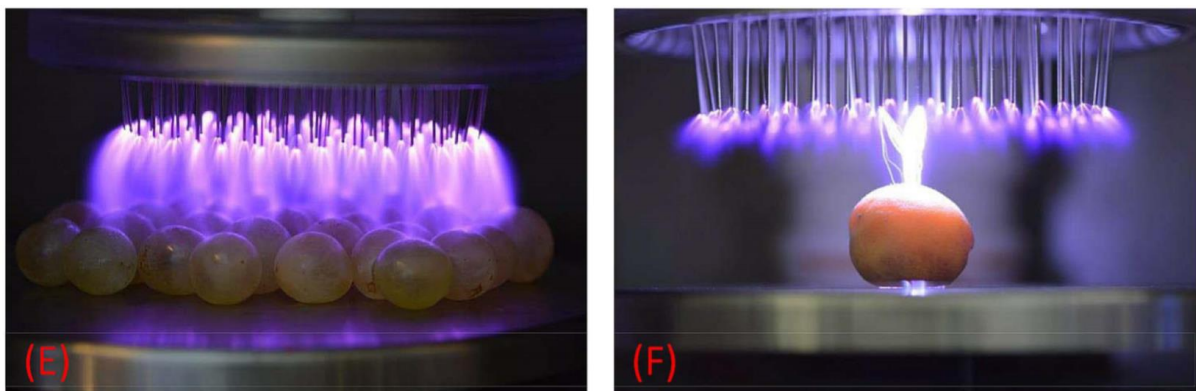
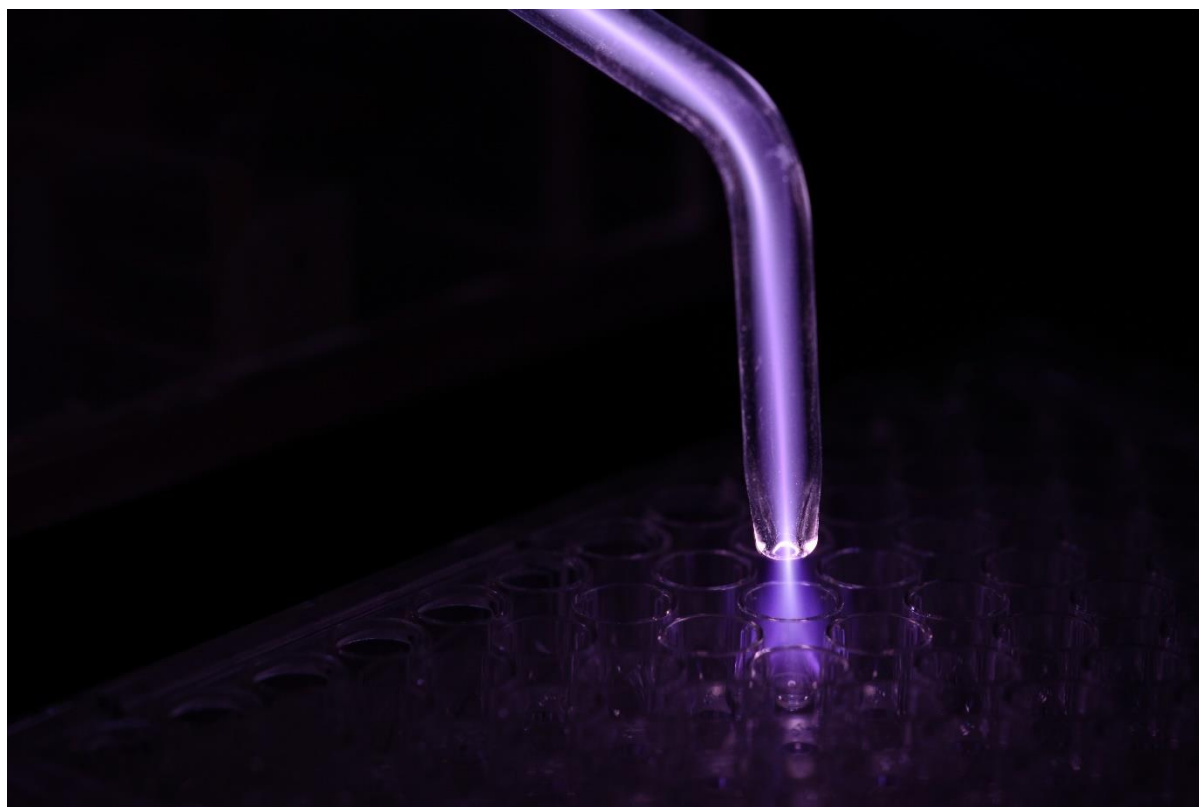


Figure 2.1 Multipin-corona discharge treatment of grapes [17]

## 2.2.2 Atmospheric-Pressure Plasma Jets

The atmospheric-pressure plasma jet is a capacitively coupled device consisting of two coaxial electrodes between which a gas flows; usually the central electrode is connected to the high voltage power supply while the external electrode is grounded. The electric field accelerates free electrons of the gas inducing ionization, ionization waves allow for electric field propagation in the gas flow. With this architecture plasma application (to the bio-interface) can be uncoupled from plasma generation. For this kind of plasma source, the most used process gas is helium; argon may be also interesting.



*Figure 2.2 Atmospheric pressure plasma jet treatment of liquids [18]*

Herrmann *et alii* reported a log 7 reduction of *B. globigii* in about 30 s of treatment with an atmospheric pressure plasma jet [19].

## 2.2.3 Resistive Barrier Discharges

This type of plasma source is composed by two planar electrodes facing each other; at least one of these electrodes must be covered with a resistive layer, this layer limits the discharge current and therefore prevents arcing. power supplies for these devices can be both DC and low-frequency AC. Using ambient air as plasma gas, the gap between electrodes cannot exceed a few mm; using helium, plasma can be produced in larger volumes.

Laroussi *et alii* [20] reported a log 4 reduction of vegetative *B. subtilis* cells in about 10 min using a gas mixture of 97%–3% helium-oxygen.

#### 2.2.4.0 Dielectric Barrier Discharges

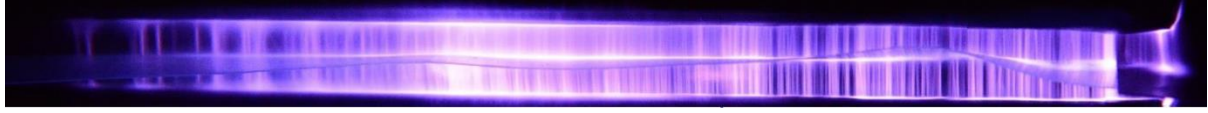


*Figure 2.3 Dielectric barrier discharge*

This family of plasma sources, also known as DBD, is similar to the resistive barrier discharge; it consists in two planar electrodes facing each other; at least one of these electrodes must be covered with a dielectric layer. One or both electrodes are powered; as soon as the voltage imposed to the gap overcomes the breakdown voltage of the gas, the discharge is ignited. After ignition, charged particles are collected on the dielectric surface. This accumulation of charge creates a voltage drop, which contrasts the applied voltage and therefore, induces a discharge current decrease and then the discharge extinguishment. During the second half cycle of the applied power, the voltage increases again, and the discharge reignites. This process is repeated during each period of the applied potential waveform.

DBDs can be divided into two categories: volume discharge (VD) and surface discharge (SD). VD-DBDs consist in two electrodes facing each other, one of which must be covered with a dielectric layer. In VDs, plasma is generated in the interelectrode gap. SD-DBDs are composed by the same essential elements; however, the layout is different: high voltage and ground electrode are in contact by means of a dielectric layer, plasma is generated on the edge of the ground electrode. To maximize the plasma generation surface, the ground electrode has usually the shape of a mesh.

From a practical point of view VD- and SD-DBDs are very different one from another. The plasma generation gap of VD at atmospheric pressure never exceed a few mm; this implies that treated object cannot be thicker than that. This fact limits applications to gases, powders and films. On the other hand, the fact that plasma is well confined in the gap between electrodes maximize the quantity of reactive components that have an active role in the process: electrons, ions, chemical species, excited species, electromagnetic field, UV radiation, visible radiation and thermal radiation.

##### 2.2.4.1 VD-DBDs

These devices can be operated both at low pressure (micro-electronics, light applications) and at high pressure (surface modification, ozone generation, wastewater treatment, exhaust gas control). At low pressure, the discharge is diffuse (also known as glow discharge), hence treatments are highly homogeneous. The low-pressure condition implies a low concentration of species (electrons, ions, atoms and molecules); ionization is easier to achieve but collisions between species and substrate are rarer

than those at high pressure. At high pressure, the discharge is filamentary: there are high intensity streamers (micro-discharges) that connect electrodes, these current channels are of short duration (1-10 ns [21]), which is inversely proportional to the gas pressure. Filaments have a radius of approximately 100  $\mu\text{m}$  and appear to be randomly well distributed in the treatment volume.

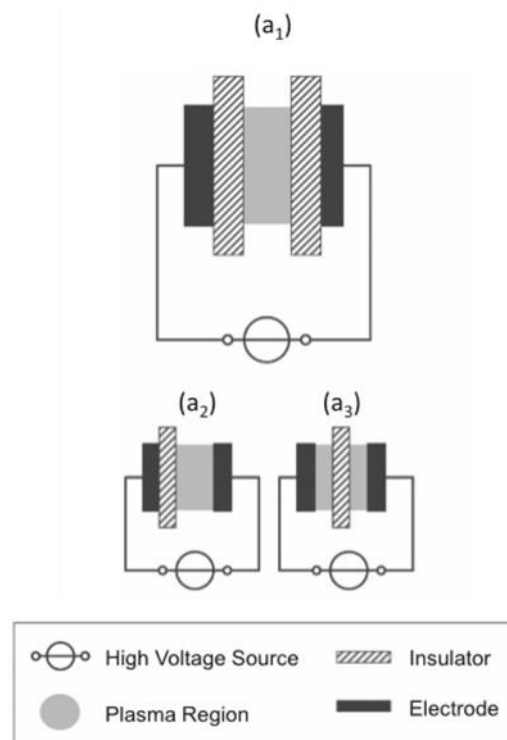


Figure 2.4 VD-DBD main layouts [22]

Low pressure VDs are not the best option for sterilization for several reasons: first, the vacuum system is expensive, sophisticated and hard to handle. Treatment times are longer than those at atmospheric pressure to achieve similar results; there are two factors that explain this fact: vacuum systems need time to reach low pressure condition; particles are scarcely dense in low pressure plasmas, therefore bacterial destruction is rarer, hence slower. Moreover, low pressure reactors must be sealed during operation, this means that continuous treatments are forbidden. Finally, vacuum systems cannot (easily) be used for the treatment of living tissues.

Some scientists tried to combine the high efficacy and convenience of atmospheric pressure VDs with the homogeneousness of glow discharges. One of the early examples of glow VD plasma at atmospheric pressure was reported by Donohoe *et alii*, who used a large gap pulsed-barrier discharge in a mixture of helium and ethylene to polymerize ethylene [23]. Laroussi *et alii* [20] used of the glow discharge at atmospheric pressure to destroy cells of *P. fluorescens*. They obtained full destruction of  $4 \times 10^6/\text{ml}$  in less than 10 min. The reaction chamber was filled mostly with helium and an admixture of air.

### 2.2.4.2 SD-DBDs

SD-DBDs generate plasma on the ground electrode surface; therefore, there are no strong limitations to the possible geometries to be treated. The main disadvantage of this layout is that part of the plasma reactive agents is not involved in the treatment: electrons, ions and electromagnetic field are concentrated in proximity of the ground electrode; consequently, their direct effects on substrates are neglected. SD treatments rely mainly on chemical species produced in the plasma; consequently, the process efficacy is directly connected to the treatment volume and the diffusion velocity of those species. This fact makes an accurate process design mandatory in order to guarantee uniformity of treatment of substrates.

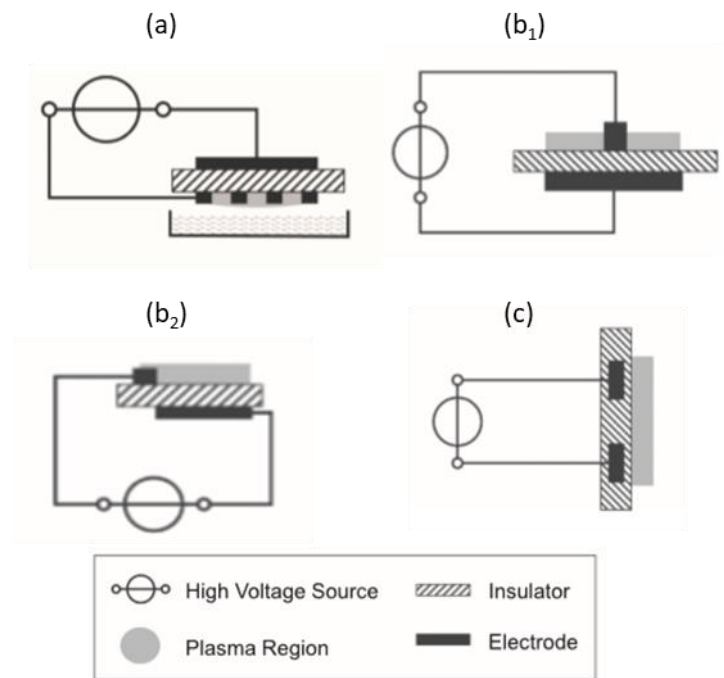
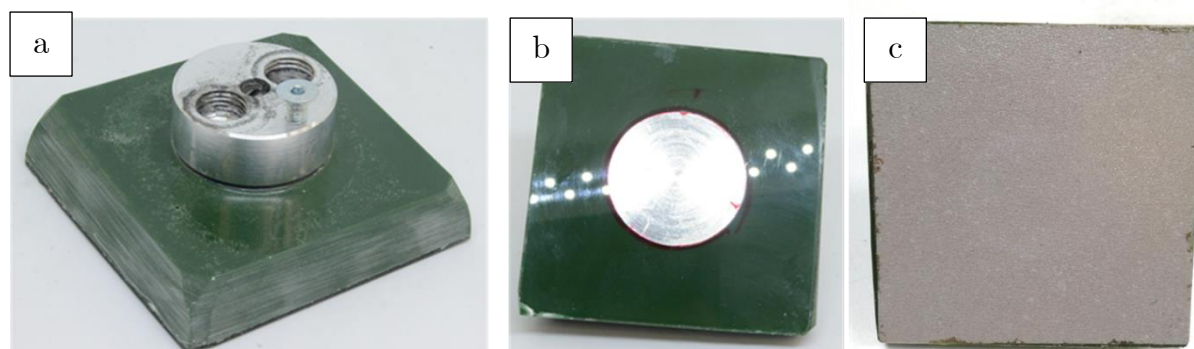


Figure 2.5 SD-DBD main layout [22]

### 2.2.4.3 IAP VD-DBD

In this section the DBD designed, realized and used for experiments will be presented. The layout is that of a VD-DBD: two planar electrodes facing each other; the dielectric layer is attached to the high voltage electrode. The high voltage electrode has a circular shape with a radius of 19 mm; the grounded electrode is a stainless-steel square 80 mm wide.





*Figure 2.6 IAP VD-DBD, a) top view of the cylindrical high voltage electrode embedded in the resin; b) bottom view of the high voltage electrode with glass dielectric; c) bottom view of the high voltage electrode with gres dielectric.*

4 different dielectrics with different thickness were tested; here is presented the material used for biological tests (test and results about dielectric material analysis will be presented on chapter 4). A ceramic material is used as a dielectric, with a thickness of 3 mm. The high voltage electrode is covered with an episodic resin to avoid free discharge. The interelectrode gap is set to 1 mm; there is no confinement of the treatment volume, therefore air may flow freely.

The power supply used for the whole experimental campaign is the AlmaPULSE (AlmaPlasma srl, Italy). This AC current generator is specifically designed for cold atmospheric plasma applications. AlmaPULSE is a flexible tool for R&D and lab scale investigations. The AlmaPULSE allows to modify several parameters: maximum potential, pulses frequency, duty-cycle and treatment time. Changing the potential and the frequency input values AlmaPULSE, it is possible to adjust the power absorbed by the plasma source (hence the power delivered by the plasma to the substrate).



*Figure 2.7 AlmaPULSE (by AlmaPlasma srl)*

## 2.3 References

- [1] Ansari I A and Datta A K 2003 an Overview of Sterilization Methods for *Trans IChemE* 81
- [2] Ducloux G, Fabry J, Nicolle L and others 2002 Prevention of hospital acquired infections: a practical guide WHO/CDS/CSR/EPH/2002.12
- [3] Curtis L T 2008 Prevention of hospital-acquired infections: review of non-pharmacological interventions *J. Hosp. Infect.* 69 204–19
- [4] Reed D and Kemmerly S A 2009 Infection Control and prevention: A review of hospital-acquired infections and the economic implications *Ochsner J.* 9 27–31
- [5] Parrott E L 1970 *Pharmaceutical technology* (Burgess)
- [6] Fridman A and Friedman G 2012 *Plasma medicine*
- [7] Basaran P, Basaran-Akgul N and Oksuz L 2008 Elimination of *Aspergillus parasiticus* from nut surface with low pressure cold plasma (LPCP) treatment *Food Microbiol.* 25 626–32
- [8] Deng X, Shi J and Kong M G 2006 Physical mechanisms of inactivation of *Bacillus subtilis* spores using cold atmospheric plasmas *IEEE Trans. Plasma Sci.* 34 1310–6
- [9] Search H, Journals C, Contact A, Iopscience M, Sci P and Address I P Bacteria Inactivation Using DBD Plasma Jet in Atmospheric  $\mu$  i Ó £ ì , 83
- [10] Kirkpatrick M and Odic E 2007 Atmospheric Pressure Humid Argon DBD Plasma for the Application of Sterilization - Measurement and Simulation of Hydrogen, Oxygen, and Hydrogen Peroxide Formation *Int. J. Plasma Environ. Sci. Technol.* 1 96–101
- [11] Klämpfl T G, Isbary G, Shimizu T, Li Y F, Zimmermann J L, Stolz W, Schlegel J, Morfill G E and Schmidt H U 2012 Cold atmospheric air plasma sterilization against spores and other microorganisms of clinical interest *Appl. Environ. Microbiol.* 78 5077–82
- [12] Laroussi M 2002 Nonthermal decontamination of biological media by atmospheric-pressure plasmas: Review, analysis, and prospects *IEEE Trans. Plasma Sci.* 30 1409–15
- [13] Moreau M, Orange N and Feuilloley M G J 2008 Non-thermal plasma technologies : New tools for bio-decontamination 26 610–7

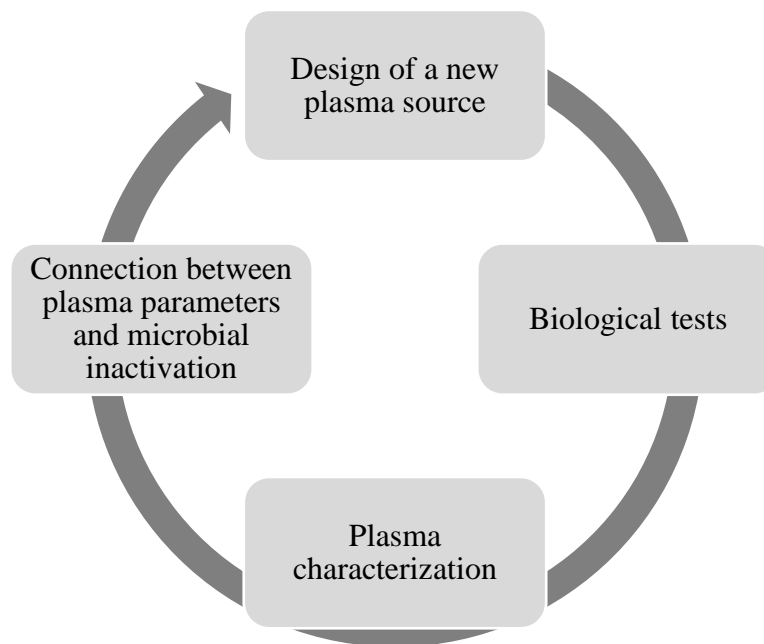
- 
- [14] Siemens W 1857 Ueber die elektrostatische Induction und die Verzögerung des Stroms in Flaschendrähnen *Ann. Phys.* 178 66–122
- [15] Menashi W P 1968 Treatment of surfaces
- [16] Belgacem Z Ben, Carre G, Charpentier E, Le-Bras F, Maho T, Robert E, Pouvesle J M, Polidor F, Gangloff S C, Boudifa M and Gelle M P 2017 Innovative non-thermal plasma disinfection process inside sealed bags: Assessment of bactericidal and sporicidal effectiveness in regard to current sterilization norms *PLoS One* 12 1–18
- [17] Mohamed A-A H, Al-Mashraqi A A, Shariff S M, Benghanem M, Basher A H and Ouf S A 2014 Pressure Air Plasma *IEEE Trans. Plasma Sci.* 10 2488–9
- [18] Boselli M, Colombo V, Gherardi M, Laurita R, Liguori A, Sanibondi P, Simoncelli E and Stancampiano A 2015 Characterization of a Cold Atmospheric Pressure Plasma Jet Device Driven by Nanosecond Voltage Pulses *IEEE Trans. Plasma Sci.* 43 713–25
- [19] Herrmann H W, Henins I, Park J and Selwyn G S 1999 Decontamination of chemical and biological warfare (CBW) agents using an atmospheric pressure plasma jet (APPJ) *Phys. Plasmas* 6 2284–9
- [20] Laroussi M 1995 Sterilization of tools and infectious waste by plasmas *Bull. Amer. Phys. Soc. Div. Plasma Phys* 40 1685–6
- [21] Fridman A 2008 *Plasma Chemistry*
- [22] Brandenburg R 2018 Corrigendum: Dielectric barrier discharges: progress on plasma sources and on the understanding of regimes and single filaments (Plasma Sources Science and Technology (2017) 26 (053001) DOI: 10.1088/1361-6595/aa6426) *Plasma Sources Sci. Technol.* 27
- [23] Donohoe K G and Wydeven T 1979 Plasma polymerization of ethylene in an atmospheric pressure-pulsed discharge *J. Appl. Polym. Sci.* 23 2591–601



## Chapter 3

# Process design and optimization

The final aim of this project was to design, realize and optimize plasma sources for disinfection processes; this kind of research required an iterative approach. Starting from a literature analysis and previous experience, a plasma source was designed and realized; later biological tests were performed to assess the antimicrobial effect of the plasma treatment. Finally, the plasma was characterized by means of several techniques to find a relation between plasma parameters and microbial inactivation. Using the information gained, a new plasma source was designed, in order to optimize the characterized plasma process; subsequently, the whole procedure started again.



The analysed process was a plasma assisted disinfection treatment of packaging film materials; these films were used in a form-fill-seal implant which realize food containers. Two different materials were treated: one polymeric and one metallic.

Firstly, a DBD was realized using PMMA; the purpose of this plasma source was to verify if a VD-DBD was suitable for this kind of application. Biological tests were performed varying operative conditions in order to identify the optimum working condition; to modify the plasma dose delivered to the substrate 4 main parameters were changed: maximum voltage, pulse frequency, duty cycle and treatment time.

Different analyses were performed to evaluate the efficacy of each reactive components of the plasma.

### 3.1 Plasma reactive components

As already stated, plasma is a multicomponent mixture in a gaseous state. Lot of its components are highly energetic and reactive; the possibility to exploit one or more of these aggressive agents for different purposes widen the field of possible applications. A great effort has been devoted to study and understand how distinct plasma components act in disinfection and sterilization processes; in this section a comprehensive exposure of these components and their importance will be reported.

As reported by Woedtke *et alii* [1], the main reactive components of a CAP are electrons, ions, reactive neutral species, excited species, UV-radiation, thermal radiation, electromagnetic fields and electric current.

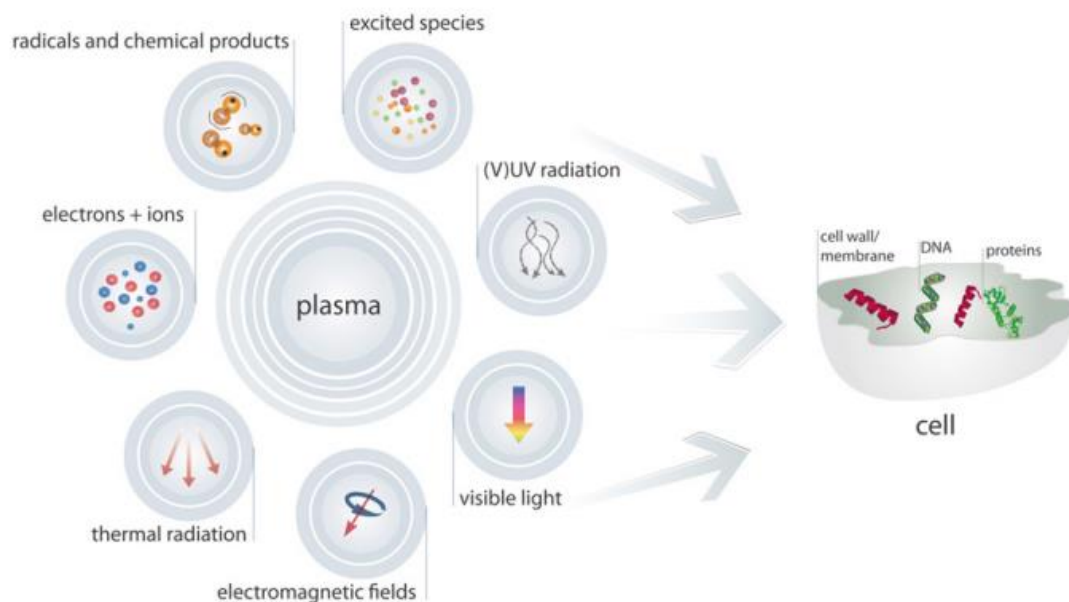


Figure 3.1 Plasma sterilizing agents [1]

#### *Reactive neutral species*

It is known that reactive species, generated in plasma through electron-impact excitation and dissociation, play an important role in disinfection treatment. This kind of species are produced and induced by the chemistry which regulates the plasma discharge. It is possible to modify the chemical kinetics of these species by varying operative conditions such as gas flow rate or input power; obviously, the main characteristic that affects the production of different neutral species is the choice of the process gas.

Many studies and tests for medical applications involve the use of noble gases such as helium and argon; noble gases are easier to ionize, the voltage needed to ignite plasma is lower compared to the one needed to ignite plasma in air. The possibility to generate plasma at relative low voltage is extremely appealing for biomedical purposes;

in the biomedical field in fact, the patient safety must always be guaranteed. On the other hand, these kinds of plasmas produce reactive neutral species only when the noble gases meet air; this fact implies that the concentrations of reactive neutral species are remarkably lower compared to those of air plasmas.

For disinfection and sterilization of non-living materials it is more convenient to use air as process gas; air is drastically cheaper than helium or argon and leads to higher concentrations of reactive neutral species.

Logically, for air plasmas, the main reactive species produced are those of oxygen and nitrogen (RONS). At low power densities, the chemistry is governed by ozone (a thorough chemistry analysis is reported on chapter 5) which interacts with (micro)organisms and therefore its maximum concentration in ambient air is regulated by law. At higher power densities, nitrogen species dominate the chemistry: NO has a high biocidal impact and it is short living; NO<sub>2</sub> derives from NO but it is long living, therefore its concentration in the atmosphere is regulated by law, just as ozone.

Herrmann et alii [2] experimentally proved that reactive oxygen species (ROS) have a strong germicidal effect; he compared the bacterial inactivation results obtained with and without oxygen using a plasma jet. This fact is associated with the presence of the metastable singlet state of oxygen (O●), and ozone (O<sub>3</sub>).

Another strong disinfectant species is the hydroxyl radical (OH●); this molecule is produced only when water is present in the discharge. Kuzmichev et alii [3] studied moistened air treatment and concluded that “the best bactericidal effects are achieved in moistened oxygen and air.”

### *UV-radiation*

UV light is used for sterilization process and for therapeutic applications such as induction of vitamin D production, treatment of psoriasis and vitiligo. Low quantities of UV radiation are emitted by plasmas; nevertheless, this radiation must be considered due to its high interaction with biomolecules. UV affects bacteria cells inducing the formation of thymine dimers in the DNA, inhibiting the bacteria’s ability to replicate. The capability of UV to inactivate cells depends on 2 factors: wavelength and dose. In fact, not all the UV light may damage microorganism; the wavelength germicidal range is 220-280 nm. Moreover, the dose of the radiation (expressed in watt\*s/cm) in this range must exceed a certain threshold.

As for many disinfectants UV light can be helpful to destroy bacteria, but it can also be harmful for users. Limits of exposure are set by the International Commission on Non-Ionizing Radiation Protection: 30 J m<sup>2</sup> in the spectral region of 180–400 nm within an 8 h-period and 104 J/m<sup>2</sup> in the region of 315–400 nm [4].

Laroussi [5] assessed that UV radiation was not the main disinfectant agent by comparing the bacterial inactivation produced by a low-pressure mercury-vapor lamp and an atmospheric pressure cold plasma. Herrmann et alii [2] shown no substantial reduction in the initial concentration of *B globigii* exposed to a plasma jet with the plasma effluent blocked by a quartz window. The scarcely pronounced effect of plasma produced UV can be found in the low emissivity of CAPs in the germicidal range. Most

gases used at atmospheric pressure do not emit any appreciable dose of UV radiation in the germicidal wavelengths.

### *Electric current*

Electric current is present in most plasma discharges; the use of electricity in medicine has a long history and many therapeutic effects also in wound healing are reported and applied today. For biomedical applications, this current must be limited to be harmless; for treatment on non-living materials, the current must be limited to avoid damaging the substrate.

### *Charged Particles*

In CAPs the bombardment of microorganism by charged particles should play no role in the destruction of cells; in fact, the average energy of ions is close to room temperature. Only electron average energy is in the eV range; nevertheless, their kinetic energies is low due to their light mass. Consequently, the majority of researchers neglect the role of ions and electrons in sterilization.

Completely disagreeing with this approach, Mendis et alii [6] suggested that charged particles might play a very significant role in the rupture of the outer membrane of bacterial cells. This rupture is provoked by the electrostatic force caused by charge accumulation on the outer surface of the membrane.

### *Thermal radiation*

Thermal radiation is known to have an impact on microorganisms; as shown previously, a great variety of conventional sterilization treatments rely on this energy vector to destroy bacteria. However, to achieve sterilization it has been shown that the temperature must be higher than 121°C for several minutes. Even if thermal radiation is a component of CAP, the temperature increase is usually in the rage of 20-30°C; that means that most of the treatments produce a macroscopic temperature of 50-60°C. In this temperature range no bacteria can be eliminated by means of only thermal radiation; for this reason, most researcher neglect the role of temperature.

## 3.2 References

- [1] von Woedtke T, Reuter S, Masur K and Weltmann K D 2013 Plasmas for medicine Phys. Rep. 530 291–320
- [2] Herrmann H W, Henins I, Park J and Selwyn G S 1999 Decontamination of chemical and biological warfare (CBW) agents using an atmospheric pressure plasma jet (APPJ) Phys. Plasmas 6 2284–9
- [3] Kuzmichev A I, Soloshenko I A, Tsiolko V V, Kryzhanovsky V I, Bazhenov V Y, Mikhno I L and Khomich V A 2000 Features of sterilization by different types of atmospheric pressure discharges Proceeding of 7th International Symposium on High Pressure, Low Temperature Plasma Chemistry. Greifswald, Germany
- [4] ICNIRP I 1996 Guidelines on UV radiation exposure limits Heal. Phys 71 978–



---

82

- [5] Laroussi M and Leipold F 2004 Evaluation of the roles of reactive species, heat, and UV radiation in the inactivation of bacterial cells by air plasmas at atmospheric pressure *Int. J. Mass Spectrom.* 233 81–6
  
- [6] Mendis D A, Rosenberg M and Azam F 2000 A note on the possible electrostatic disruption of bacteria *IEEE Trans. plasma Sci.* 28 1304–6



## Chapter 4

# Biological tests

In the biomedical field there is a clear distinction between the concepts of sterilization, disinfection and decontamination. In the frame of this project, a disinfection process has been developed: i.e. a process aimed to the elimination of most, if not all pathogenic microorganisms, excluding spores. There is no international standardization about the reduction level which must be achieved in a disinfection process; common values are around log 4-5 [1].

The most important feature of a disinfection process is the repeatability and reliability of the induced microbial inactivation.

Disinfection is a complex task to accomplish; the life or death of microorganisms depends on many variables, some of which can be classified as process operative conditions (or inputs) and can be modified without any drawback, while others are fixed by industrial requirements.

### *Operative conditions*

Dealing with an open-air VD-DBD, the main input parameter which may be varied is the electric power density, which is defined over the plasma generation surface; using the AlmaPULSE, this input may be adjusted manipulating 3 different factors: maximum voltage (kV), pulse frequency (kHz) and duty-cycle (%). To analyze how the power density affected the disinfection efficacy, two power density values have been used for the experiments.

The treatment volume is also an important characteristic of a process; in this research this feature was kept constant to a cylinder ( $\phi$  39 mm, thickness 1 mm). A deeper investigation of this parameter and considerations on how it can affect applications will be given in chapter 5 (paragraph 5.3, electrical measurement).

Finally, the choice of the dielectric material alters considerably the discharge. In this frame, the physical quantities which describe the behaviour of a particular material are the dielectric strength (MV/mm) and the thickness (mm); knowing these characteristics, the input potential needed to ignite plasma can be predicted. In addition, the choice of the dielectric material affects also the mechanical properties of the plasma source, which cannot be underestimated. In this chapter, results are shown for treatment performed using a ceramic dielectric; in chapter 5 the choice of this material is discussed.

### *Industrial requirements*

There are several parameters which may vary from one application to another: considerations on this topic usually rely on economic analysis. As already

highlighted, plasma technologies depend largely on the discharge gas and pressure. Although historically low-pressure processes have found extensive use, CAPs are more appealing when applicable. Regarding the process gas, it is obvious that air is the cheapest gas available, therefore the most convenient; in addition, the presence of oxygen and nitrogen is needed to enhance the antimicrobial effect of a plasma treatment. The adoption of air as process gas can also imply the presence of water vapor in the discharge; it has been proven that the presence of water in the discharge has a huge impact in the chemistry and in the decontamination efficacy of a CAP treatment (this topic is discussed in the next paragraph). Finally, using air at atmospheric pressure allows open-air configuration, which enables continuous treatment of material, a crucial aspect from a productivity point of view. In this work, each experiment was performed in open air.

One of the most important characteristics of a disinfection process is the treatment time; this parameter is strictly connected the microbial inactivation rate and must be chosen accordingly with the desired level of disinfection. From an industrial perspective, the choice between two disinfection methods is done on an efficiency basis: for equal expenses and values of inactivation the shortest treatment time is the best choice. In this work, treatment times in the range 0.1 - 8 seconds were tested; 8 seconds was the maximum treatment time allowing a sufficient packaging production rate.

Another key aspect with direct implications on the choice of the disinfection method is the packaging material. As mentioned in chapter 2, different materials require different process specifications; in this work two substrate were tested: a polymeric film and an aluminum one.

Biological analysis starts with the selection of the microorganisms to be treated; this decision is made to better represent the real environment of the process, trying to simulate the most probable scenario. Later in this chapter, the choice of microbes to be treated is explained.

## 4.1 Effect of water vapor

In fundamental research, scientists usually try to find a connection between a varying parameter and the obtained results. To do this, they try to fix every other possible parameter to limit the variability of the system that they are studying. Following this concept, it is easy to understand why most scientific papers about plasma treatment are realized using a process gas different from air. Air is a very uncertain mixture; everybody knows that 78% of air is made of molecular nitrogen, 21% of molecular oxygen, almost 1% of argon and smaller quantities of other gases; it is also known that water is present in air in the state of vapor and that the % of relative humidity changes constantly. Unfortunately, for plasma process, a small variation in the gas composition may lead to completely different results; the need for repeatable conditions is the reason why most researchers use synthetic air when dealing with air plasma.

When the research shifts from fundamentals towards applications, the urgency of investigating real industrial conditions cannot be ignored; many works studied the dependency of microbial inactivation from the relative air humidity. Here are reported the most relevant.

Hähnel *et alii* studied the influence of air humidity on the reduction of *Bacillus atrophaeus* spores at atmospheric pressure using a SD-DBD; they varied the relative humidity from 0 to 70% in a controlled volume and came to the conclusion that the air humidity has a strong influence on the microbial reduction rate. They also highlighted that higher concentration of water vapor leads to higher killing rates of the microorganisms [2]. Hähnel explained the increase of reduction rate with the improved production of OH radicals; he also reported that LIF experiments are needed to investigate this phenomenon more deeply.

Maeda *et alii* used an atmospheric pressure humid air plasma to inactivate *E. coli* [3], they studied the efficacy of the process varying the relative humidity from 0 to 70%. They found that the best inactivation results could be obtained with a relative humidity of 43.

Also Muranyi *et alii* studied the influence of relative gas humidity on the inactivation efficiency of a low temperature gas plasma [4]. They used a cascaded DBD fed with synthetic air against *Aspergillus brasiliensis* and *Bacillus subtilis* spores; they discovered that the efficacy of the process was not only connected with relative humidity, but also with the pathogen under investigation. More precisely, the best results against *A. brasiliensis* were obtained working with high humidity; on the contrary, to inactivate *B. subtilis* it was better working in low humidity condition.

The last work worth mentioning is from Purevdorj *et alii*; they investigated the effect of feed gas composition of plasma on *Bacillus pumilus* spore mortality [5]. They tested a wide variety of feed gases at low pressure (50 Pa); the best inactivation results were obtained using air with a 0.05 molar fraction of water vapour. The great increase of efficacy obtained raising the molar fraction of water vapor in the feed gas from 0 to 0.05 allowed Purevdorj to assert that radicals are deeply involved in spore mortality. In fact, the presence of water in the gas discharge leads to the production of H and OH radicals by electron impact.

From an industrial point of view, the fact that water vapor increases the efficacy of plasma assisted disinfection treatments is positive, since the use of dry synthetic air would have implied additional costs. Biological tests were performed in open air in the Langmuir bioplasma bacterial lab of DIN & CIRI-MAM departments of the Bologna University, where relative humidity lies normally in the range 60-80%.

## 4.2 Pathogen selection

Disinfection processes are always under investigation, the research for novel disinfection methods never stops. There are different international standards for validation and routine control of these processes, most of which require to test the

biological effect of the treatment under examination against the most resistant microorganisms.

Nowadays, the standard procedures for verifying the efficacy of sterilization methods are based on the inactivation of *B. atrophaeus* spores, *B. coagulans* spores, *C. sporogenes* spores and *G. stearothermophilus* spores [6].

Plasma assisted disinfection treatments require to be tested on a variety of microorganisms. In fact, plasma relies on several disinfecting agents to achieve microbial inactivation; these agents may have a different effect on specific types of pathogens due to their peculiar metabolic and morphologic properties [7]. As reported by Madigan *et alii*, the most relevant microbial properties that affect the efficacy of different disinfecting agents are the thickness of cell walls and their chemical composition, the structure of membranes, the DNA protection structures and the ability of aerobic or anaerobic respiration [8]. The international standard (ISO 14937) suggests the use of microorganisms that have a high resistance to the investigated disinfecting agent, that are usually present on the materials to be treated and in the environment in which the product is manufactured, and that cover a broad range of types (*e.g.* aerobic and anaerobic bacteria, spores, fungi, yeasts, parasites and viruses). The ISO standard requires also to check the efficacy against Gram-positive and Gram-negative vegetative bacteria. Regulatory guidelines specify the importance to check the efficacy against mesophilic bacteria and fungi that grow under aerobic conditions, which are commonly used as indicator of environmental conditions and microbial presence during packaging production process. For these reasons, in this work a Gram-positive (*S. aureus*) and a Gram-negative (*E. coli*) aerobic bacteria were tested. *S. aureus* has implications in hygiene control, and it is also a key cause of food poisoning, as it produces heat-stable enterotoxins. Its prevalence is widespread as it commonly found in the human mucous membranes and skin. *E. coli* is a noxious foodborne pathogen transmitted by water and different kinds of food; while most *E. coli* strains are a component of human intestinal microbiota and do not constitute a health risk, other strains represent a health problem because of their ability to survive under stress conditions and to secrete toxins that cause enterohemorrhagic gastroenteritis. Additionally, experiments were conducted using *C. albicans* and *A. brasiliensis* as indicator organisms for aerobic yeasts and moulds, respectively. Some yeasts and moulds produce toxic mycotoxins, most of which are heat-resistant, and they may represent a problem for packaging industries. Particularly, *C. albicans* is a polymorphic fungus that grows as yeast in normal environmental conditions; this ubiquitous microorganism can survive up to four months on inanimate surfaces. *A. brasiliensis* is a mould that produce black spores which are readily dispersed in the surroundings; it is ubiquitous in the soil and it is commonly reported as contaminant of indoor environments.

### 4.3 Biological protocol

#### *Microbial strains and growth conditions*

For microbiological experiments, *Staphylococcus aureus* ATCC 6538, *Escherichia coli* ATCC 11775, *Candida albicans* ATCC 10231 and *Aspergillus brasiliensis* ATCC 16404 (here referred to as *S. aureus*, *E. coli*, *C. albicans* and *A. brasiliensis*) were purchased from American Type Culture Collection (Manassas, VA, USA). *S. aureus* was grown on tryptic soy agar for 24 h, *E. coli* on nutrient agar for 24 h, *C. albicans* on sabouraud dextrose agar for 48 h and *A. brasiliensis* on malt extract agar for 48 h (Biolife Italiana, Milan, Italy). All strains were incubated at 37°C.

#### *Microbiological analysis*

The following biological protocol was used to perform disinfection tests in the Langmuir bioplasma bacterial lab of DIN & CIRI-MAM departments of the Bologna University. Every experiment was performed in triplicate.

Colonies from agar plates were transferred in sterile 0,9% NaCl solution to reach a concentration of approximately  $5 \times 10^8$  colony forming units (CFU) per mL reading the suspension turbidity with a McFarland Densitometer (Densitometer DEN-1B, Biosan SIA, Riga, Latvia).

Disks of polymeric material (diameter of 27 mm, thickness of 300  $\mu\text{m}$ ) were used as germ carriers. The disks were washed with ethanol 70%, exposed to UV radiation for 1 h and placed into sterile petri dishes. 20  $\mu\text{L}$  of microbial suspension were dispensed in 20 drops on the food-contact surface of each disk to reach a microbial concentration of  $10^6$  CFU/cm<sup>2</sup>. Disks were dried for 15 min at 37°C to achieve complete evaporation of the saline solution. Four disks were plasma treated for each experiment (treatment times and plasma doses were varied and are reported in the next section with results); three control samples (no plasma treatment) were included in the experiment. To recover microorganisms from the surface of the disks and to obtain a uniform suspension, each disk was placed in a 50 mL centrifuge tube containing 5 mL of a PBS + 0,1% Tween 80 solution and then the tube was shaken by means of a vortex for 1 minute. This suspension was serially diluted and plated on agar plates. Plates were incubated at 37°C to evaluate the CFU formation by counting the colonies and the counted CFU were expressed as CFU/mL. Finally, the Log Reduction was calculated for each plasma treatment using the follow equation:

$$\text{Log R} = \text{Log}_{10} N_0 - \text{Log}_{10} N_t$$

where  $N_0$  and  $N_t$  are the microbial concentrations of the untreated and treated samples respectively. Standard deviation was calculated based on Log R values obtained for each plasma treatment.

## 4.4 Biological results

The experimental campaign lasted 3 years, several different plasma source architectures were tested; after identifying the VD-DBD as the most suitable plasma source, many different materials and operative conditions were investigated. For clarity of exposure, all the results that led to the final process configuration are left out.

The plasma source used to produce these results is the IAP VD-DBD shown in paragraph 2.2.4.3. The treatment time was varied between 0.1 and 8 seconds. Two distinct power densities were used: 1.5 and 13.4 W/cm<sup>2</sup>, to produce these power densities the pulse frequency was kept constant at 20 kHz while the voltage amplitude of the input waveform varied.

Experiments were performed on 2 different substrates: a polymeric film and an aluminum one; since results are extremely close, only results obtained with the polymeric film are presented here.

The inactivation produced on *S. aureus*, *E. coli* and *C. albicans* followed the same trend; for sake of simplicity only results with *S. aureus* are shown here.

In table 4.1 and 4.2, Log R values are reported for 1.5 W/cm<sup>2</sup> and 13.4 W/cm<sup>2</sup> respectively.



Table 4.1 Log R obtained with a power density of 1.5 W/cm<sup>2</sup>

Treatment time [s]	Initial bacterial concentration [CFU/mL]	Final bacterial concentration [CFU/mL]	LOG R	Experiment average Log R	Standard deviation	Operative condition average Log R	Standard deviation
0.1	1,08E+06	302000	0,55	0,55	0,03	0,46	0,10
		332000	0,51				
		283000	0,58				
		303000	0,55				
0.1	8,87E+05	394000	0,35	0,44	0,06		
		302000	0,47				
		279000	0,50				
		315000	0,45				
0.1	3,63E+05	191000	0,28	0,37	0,11		
		185000	0,29				
		110000	0,52				
		143000	0,40				
0.5	7,27E+05	12100	1,78	1,68	0,15		
		18400	1,60				
		10600	1,84				
		22700	1,51				
0.5	8,97E+05	22100	1,61	1,53	0,26		
		25000	1,55				
		14900	1,78				
		60000	1,17				
0.5	1,20E+06	21900	1,74	1,60	0,27		
		18500	1,81				
		27900	1,63				
		73000	1,22				
1	7,47E+05	82000	0,96	1,07	0,11		
		72000	1,02				
		47000	1,20				
		58000	1,11				
1	8,97E+05	18600	1,68	1,81	0,18		
		13500	1,82				
		18600	1,68				
		7900	2,06				
1	3,63E+05	13200	1,44	1,16	0,40		
		29200	1,09				
		12300	1,47				
		88000	0,62				
1	1,20E+06	39000	1,49	1,32	0,12		
		57000	1,32				
		72000	1,22				
		66000	1,26				
4	9,27E+05	22000	1,62	1,50	0,09		
		30000	1,49				
		29000	1,50				
		37000	1,40				
4	9,33E+05	26000	1,56	1,64	0,11		
		23000	1,61				
		16000	1,77				
4	8,87E+05	83000	1,03	1,44	0,28		
		28000	1,50				
		21000	1,63				
		21600	1,61				
8	1,08E+06	50000	1,34	1,63	0,21		
		22900	1,67				
		21800	1,70				
		16100	1,83				
8	8,87E+05	48000	1,27	1,55	0,30		
		15100	1,77				
		12500	1,85				
		42000	1,32				
8	3,63E+05	1300	2,45	2,11	0,32		
		3100	2,07				
		5700	1,80				
8	1,85E+06	10200	2,26	2,14	0,09		
		12500	2,17				
		14500	2,11				
		16800	2,04				
8	1,96E+06	83000	1,37	1,41	0,06		
		71000	1,44				
		65000	1,48				
		86000	1,36				

Table 4.2 Log R obtained with a power density of 13.4 W/cm<sup>2</sup>

Treatment time [s]	Initial bacterial concentration [CFU/mL]	Final bacterial concentration [CFU/mL]	LOG R	Experiment average Log R	Standard deviation	Operative condition average Log R	Standard deviation
0.1	1,08E+06	137000	0,90	0,87	0,08	0,82	0,15
		178000	0,78				
		116000	0,97				
		164000	0,82				
0.1	8,87E+05	101000	0,94	0,89	0,12		
		87000	1,01				
		165000	0,73				
		121000	0,86				
0.1	3,63E+05	46000	0,90	0,71	0,19		
		83000	0,64				
		118000	0,49				
		54000	0,83				
0.5	3,94E+05	3200	2,09	2,17	0,36		
		4400	1,95				
		4600	1,93				
		806	2,69				
0.5	7,47E+05	62000	1,08	1,09	0,09		
		53000	1,15				
		52000	1,16				
		83000	0,95				
0.5	8,97E+05	61000	1,17	0,98	0,17		
		123000	0,86				
		143000	0,80				
		75000	1,08				
0.5	1,08E+06	71000	1,18	1,13	0,09		
		78000	1,14				
		69000	1,20				
		109000	1,00				
1	9,27E+05	31000	1,48	1,53	0,11		
		21000	1,64				
		23000	1,61				
		37000	1,40				
1	9,33E+05	24000	1,59	1,89	0,21		
		9900	1,97				
		8100	2,06				
		10900	1,93				
1	8,97E+05	63000	1,15	1,18	0,03		
		57000	1,20				
		65000	1,14				
		55000	1,21				
1	1,85E+06	218000	0,93	1,23	0,23		
		95000	1,29				
		108000	1,23				
		62000	1,48				
4	7,81E+05	5700	2,14	3,27	0,78		
		98	3,90				
		330	3,37				
		171	3,66				
4	8,07E+05	981	2,92	3,38	0,39		
		142	3,75				
		510	3,20				
		188	3,63				
4	7,27E+05	1300	2,75	3,23	0,78		
		1900	2,58				
		379	3,28				
		35	4,32				
8	1,20E+06	1	6,08	5,34	0,95		
		10	5,08				
		1	6,08				
		94	4,11				
8	1,85E+06	1	6,27	6,27	0,00		
		1	6,27				
		1	6,27				
		1	6,27				
8	1,96E+06	1	6,29	5,75	0,66		
		7	5,45				
		22	4,95				
		1	6,29				

## 4.5 Discussion

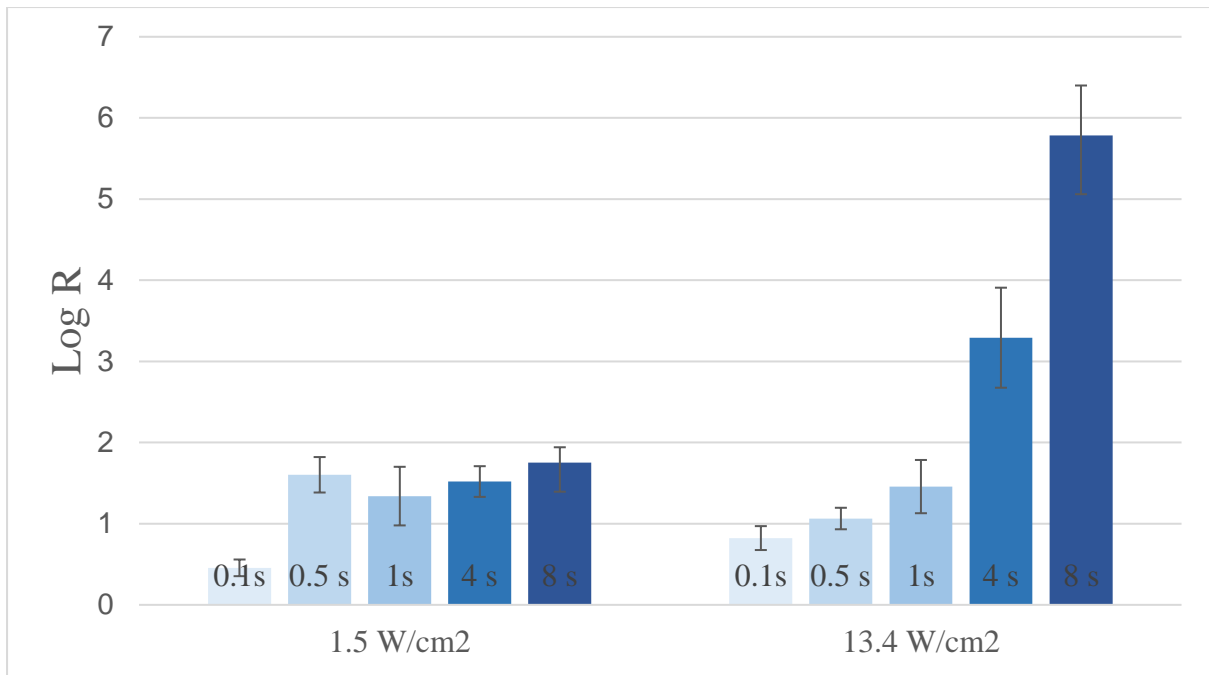
Data from tables 4.1 and 4.2 were used to draw graphs. In graph 4.3, results are grouped according to power density; the group on the left shows the inactivation achieved with the lower power density ( $1.5 \text{ W/cm}^2$ , obtained by imposing a voltage on the current generator of 10 kV). The first thing that can be highlighted is that, in this condition the Log R never exceeded the value of 2, independently from the treatment time. Secondly, it is interesting to notice that for low power density, the bacterial inactivation is not related to the treatment time; whereas, for higher power density ( $13.4 \text{ W/cm}^2$ , obtained by imposing a voltage on the current generator of 20 kV), the microbial inactivation increases with treatment time.

Graph 4.4 reports on the inactivation results obtained for identical treatment times and varying power densities; it can be noticed that, for treatment shorter or equal to 1 s, there is no difference between the inactivation level reached using different power densities. The greater disinfection efficacy of the high-power process is appreciable only for treatment times of  $4/8 \text{ s}$ .

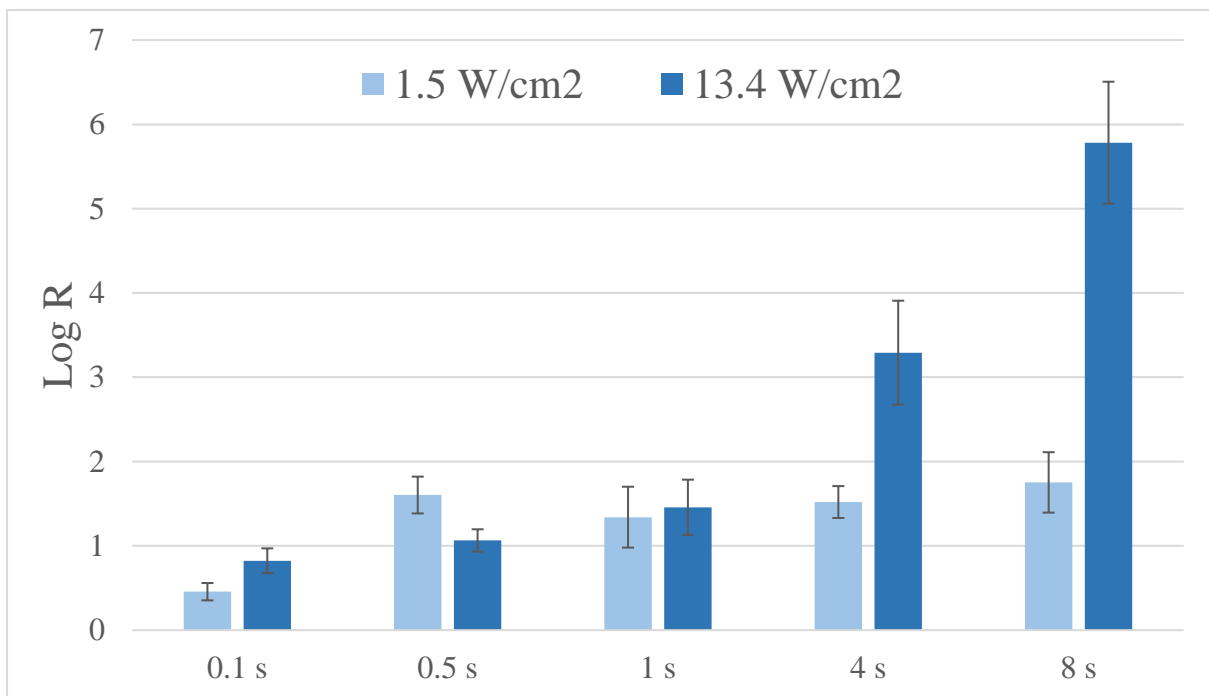
Graph 4.5 shows the same results in a 2-D chart; consequently, it is possible to underline the time dependent trend of the Log R results. For the low-power process, it is difficult to find a trend which fits each result, the best approximating curve is a logarithmic trend (blue line): this trend reaches a plateau almost immediately and the value of Log R remains stable. For the case of high-power densities, the behavior is almost perfectly represented by a linear relation (orange line).

A final remark has to be made about the maximum inactivation level achievable with this experiment: considering the fact that the Log R is calculated starting from the initial concentration of bacteria dispensed on the substrate, the maximum value of inactivation achievable is equal to the logarithm of that concentration. In this series of test, the order of magnitude of the initial concentration of bacteria was of  $10^6$ , consequently the best result achievable was close to  $\text{Log R} = 6$ .

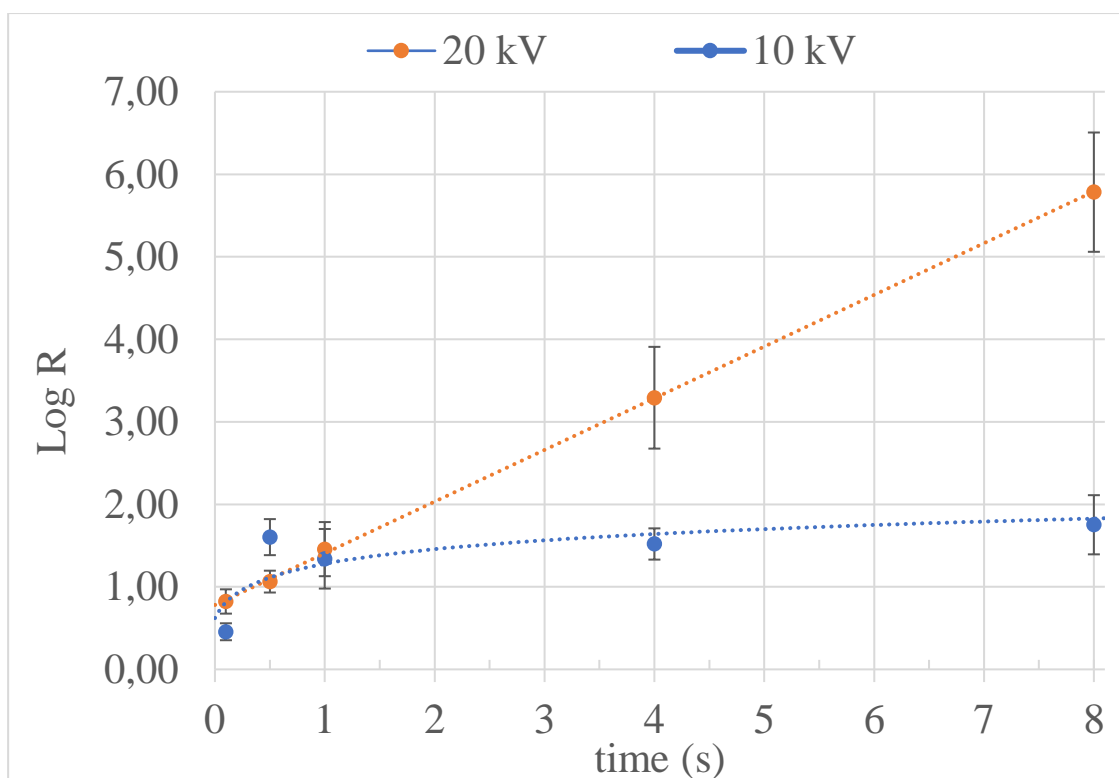
In addition, spores of *A. brasiliensis* have also been tested; as known spores are harder to destroy than vegetative cells. As expected, inactivation results for spores of *A. brasiliensis* are negligible, independently from operative conditions; consequently, those results are not reported.



Graph 4.3 Log R results plotted grouping same power density treatment



Graph 4.4 Log R results plotted pairing same treatment time



Graph 4.5 Log R results plotted over treatment time

Ehlbeck *et alii* [9] published a review on low temperature atmospheric pressure plasma for microbial decontamination; they stated that to understand the relation between the microbial reduction and process parameters (e.g. exposure time, plasma characteristics), it is crucial to study the reduction factors. Following Ehlbeck's idea, chapter 5 and 6 try to establish a connection between microbial reduction and process characteristics.

## 4.6 References

- [1] Widmer A F and Frei R 2011 Decontamination, disinfection, and sterilization *Manual of Clinical Microbiology, 10th Edition* (American Society of Microbiology) pp 143–73
- [2] Hähnel M, Von Woedtke T and Weltmann K D 2010 Influence of the air humidity on the reduction of Bacillus spores in a defined environment at atmospheric pressure using a dielectric barrier surface discharge *Plasma Process. Polym.* 7 244–9
- [3] Maeda Y, Igura N, Shimoda M and Hayakawa I 2003 Inactivation of Escherichia coli K12 using atmospheric gas plasma produced from humidified working gas *Acta Biotechnol.* 23 389–95
- [4] Muranyi P, Wunderlich J and Heise M 2008 Influence of relative gas humidity on the inactivation efficiency of a low temperature gas plasma *J. Appl. Microbiol.* 104 1659–66
- [5] Purevdorj D, Igura N, Ariyada O and Hayakawa I 2003 Effect of feed gas composition of gas discharge plasmas on Bacillus pumilus spore mortality *Lett. Appl. Microbiol.* 37 31–4
- [6] Anon Sterilization of health care products — Moist heat — Part 1: Requirements for the development, validation and routine control of a sterilization process for medical devices ISO 17665-1:2006
- [7] Hury S, Vidal D R, Desor F, Pelletier J and Lagarde T 1998 A parametric study of the destruction efficiency of Bacillus spores in low pressure oxygen-based plasmas *Lett. Appl. Microbiol.* 26 417–21
- [8] Martinko J M and Parker J 2006 *Brock biology of microorganisms* (Pearson Prentice Hall Upper Saddle River)
- [9] Ehlbeck J, Schnabel U, Polak M, Winter J, Von Woedtke T, Brandenburg R, Von Dem Hagen T and Weltmann K D 2011 Low temperature atmospheric pressure plasma sources for microbial decontamination *J. Phys. D. Appl. Phys.* 44

## Chapter 5

# Process characterization

In this chapter each diagnostic technique used to study the plasma processes will be discussed. As already said, CAP treatments are complex processes to analyse and develop; consequently, the optimization of a process of this kind is an interdisciplinary work.

The first plasma source realized was intended to demonstrate the efficacy of VD-DBD plasma treatment for disinfection purposes; materials involved were not meant for continuous operation, hence for an industrial application process. Later, a great effort was spent to create a robust plasma source: a device able to operate for several hours and also able to produce repeatable plasma conditions, hence repetitive results. For this purpose, two distinct analysis were needed: temperature measurements, to assess the heat produced during the treatment and to identify the maximum thermal resistance of the device; electrical measurement to evaluate the electrical power absorbed by the DBD, hence the power conveyed by the plasma to the substrate. These analyses allowed to choose the best layout for the DBD, in terms of structural and functional materials.

Once fixed the plasma source, the chemical characterization of the plasma began with the aim of finding a correlation between biological results and the chemical kinetics of certain active species. Additionally, a correlation between process operative conditions and the chemistry of the treatment was found.

The chemical analysis was performed by means of optical absorption spectroscopy (OAS), a powerful method which allows to measure the absolute concentration of a species in a gas. This technique is non-intrusive, calibration-free and provides results in real time; all factors that make it ideal for process investigation. One of the few drawbacks of OAS technique is that not every chemical species can be analysed and measured; that is the reason why OAS investigation was followed by another analysis: numerical simulation, a type of approach which allowed to assess the chemistry governing the plasma discharge.

## 5.1 Proof of concept

The first step of this entire project was to identify the most suitable plasma source to produce the most efficient antimicrobial treatment on a film (polymeric or metallic); this phase consisted mainly in a literature analysis of already known plasma processes. First of all, a non-equilibrium plasma was needed; in fact, plastic materials have low thermal resistance and cannot withstand high temperatures without being damaged.

Following all the considerations made in chapter 2 about the characteristics of a convenient disinfection treatment, low pressure plasmas were excluded: vacuum systems are expensive and not suitable for a massive production of low-value goods such as food containers; on the other hand, low pressure plasmas are the best choice for the manufacturing of high-value goods, as in microelectronics.

Among the various CAP sources, the VD-DBD was chosen as the most suitable due to several winning characteristics:

- VD-DBD treatments exploit each biocidal agent present in CAP; not knowing which plasma agents was the most relevant, none could be left out.
- From an industrial perspective, one of the most interesting features of DBDs is that they may be operated in an open volume, without the need of a vessel; this fact enables the possibility to perform non-stop treatments.
- VD-DBD effective area is not limited to a small spot, unlike corona and jet discharges; this device can be scaled at will increasing the size of the electrodes, with the only drawback of a greater power consumption. In film process, an increase of electrodes areas corresponds to an increase of plasma dose given to the substrate. This dose growth leads to a disinfection enhancement.
- With the proper precautions, DBDs can be used to treat both dielectric and conductive materials; in the frame of this project, both plastic and metallic films were processed.
- Finally, DBDs can be operated in air. this is which a crucial characteristic for disinfection efficacy, simplicity of operation and economical convenience.

The first VD-DBD realized (figure 5.1) for this work was made of PMMA, a plastic material easy to work by mechanical machining but with low thermal resistance. The choice to use this material was made out of convenience reasons: fast machining, cheap and transparent; this last characteristic allowed to analyse the generation of plasma in terms of brightness (i.e. intensity) and homogeneousness. In order not to obstruct the view of the discharge, the high voltage electrode was made of salted water.



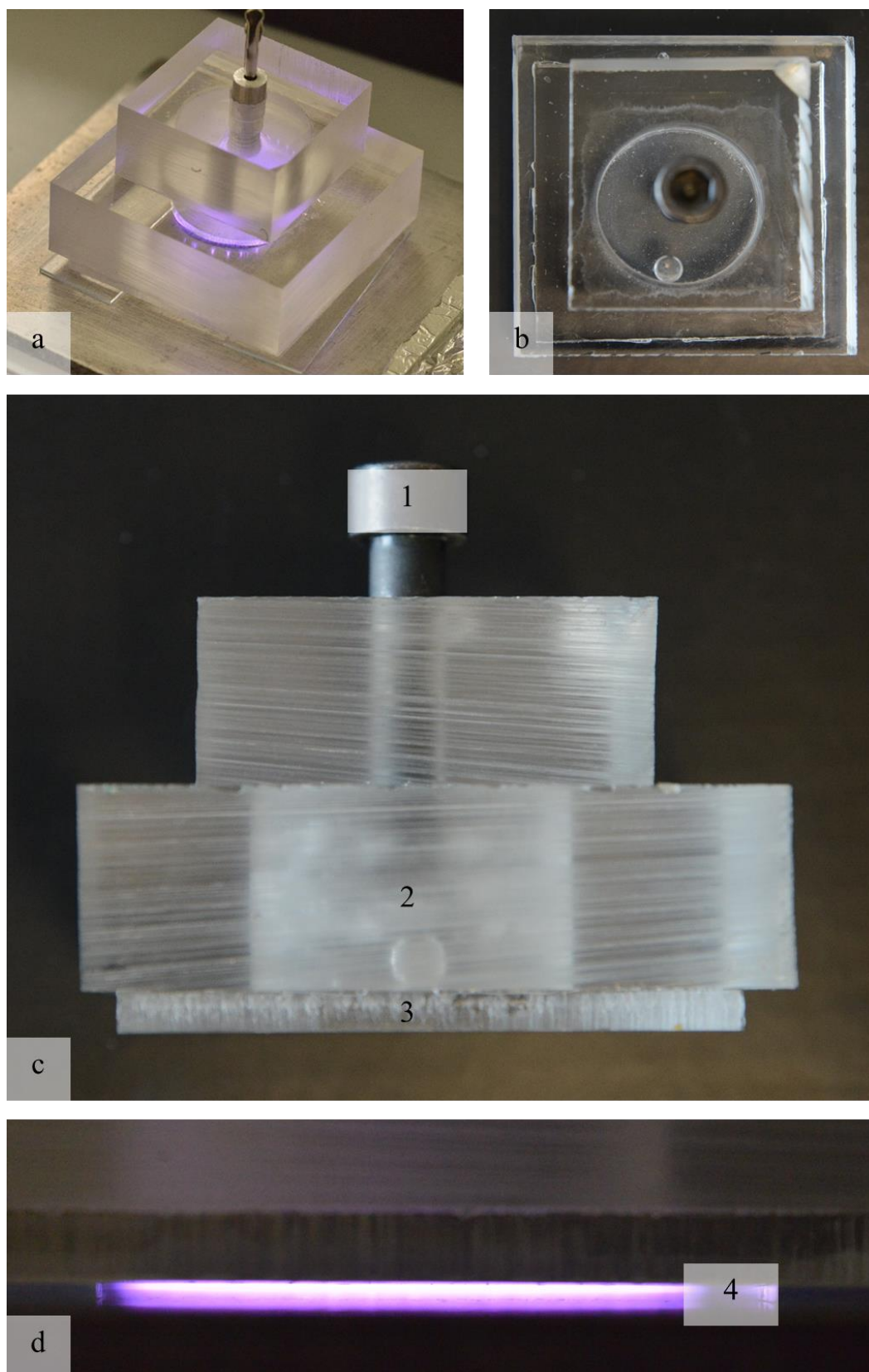


Figure 5.1 a) PMMA DBD; b) top view; c) side view: 1. High voltage electrical connection; 2. Salted water; 3. PMMA dielectric layer; d) plasma side view: 4. plasma

In this configuration, PMMA simultaneously fulfilled the task of dielectric layer (mandatory in a DBD architecture) and water container; the thickness of the dielectric layer was varied between 3 and 5 mm, while the gap between electrodes was kept constant at 1 mm.

AlmaPULSE was used as power supply and several operative conditions were varied to identify the working range of the DBD: maximum voltage, pulse frequency and duty-cycle.

This device could generate plasma in a wide range of electrical conditions and the first results of microbial inactivation were promising; on the other hand, the disadvantages of this plasma source were consistent and could not be ignored. Firstly, due to the electrical power absorbed by the DBD, the water of the high voltage electrode was heated by the Joule effect; after tens of seconds, the water reached boiling temperature. Secondly, in order to guarantee the same electrical conditions at each test, the salted water had to be changed daily to avoid problems of evaporation or water-salt separation. Finally, the heating produced by the current flowing through the plasma warmed up the PMMA; after several minutes of (non-consecutive) operation, the layer between the high voltage water and the plasma region started to melt. This phenomenon was recognizable due to a change of colour of the PMMA.

After proving the efficacy of CAP for microbial inactivation a better plasma source had to be made; in fact, even if decent levels of disinfection were achieved, no real application could be realized with those conditions. There are few characteristics that define a plasma source which can be implemented in the industrial field: the DBD must work continuously for a consistent number of hours; packaging machines work from a minimum of 8 hours a day to a maximum of 24 hours a day. The plasma source must produce the same discharge from ignition to the end of production (excluding the warm-up time). To create a DBD with these characteristics a different dielectric material had to be used; moreover, the high voltage electrode had to be changed with a more reliable one. Three distinct materials were tested, and the water electrode was substituted with an aluminium one; to analyse the performance of the new dielectrics temperature measurements and electrical measurements were performed.

## 5.2 Temperature analysis

The analysis about temperatures reached by the DBD was carried out in order to assess two phenomena: how the electrical input set of the power supply affected the final temperature reached by the DBD and how much power was transferred to the substrate during the plasma treatment. The first topic was interesting because it allowed to observe temperature trend of the dielectric material and to identify the electrical working range of the DBD; out of these limits, the electrical dissipation led to overheating and breakage. The second topic was directly connected to the disinfection: it is known that high temperature may lead to microbial death; it was therefore essential to measure the temperature of the process to evaluate if any inactivation effect was of thermal nature.

Due to process characteristic and DBD layout, this measurement could not be performed online during treatment. Temperatures were measured by means of an Optris pyrometer (OPTCTL-LT-CF1, temperature range  $-50\div 950^{\circ}\text{C}$ ): a pyrometer or infrared thermometer is a device for non-contact temperature measurement.



*Figure 5.2 Optris pyrometer*

The pyrometer measures the electromagnetic radiation radiated from an object and connects that to the temperature of the object. The electromagnetic radiation is focused and converted by an infrared detector into an electrical signal. The signal has to be multiplied by a proportional correction factor; this factor takes into account the emissivity,  $\epsilon$  of the object: a dimensionless number, which may assume any value between 0 and 1. An object that emits a radiation equals to the radiation that it absorbed is called a *black body*, it is purely theoretical and it is considered to have an  $\epsilon = 1$ . Real objects are considered *grey objects* and have an emissivity lower than the unity ( $0 < \epsilon < 1$ ); the value of  $\epsilon$  is defined by the ratio between the radiation emitted from the *grey object* and the radiation emitted from a *black object* which has the same temperature of the first.

The 3 tested materials were mica, gres and glass: for each material a different value of  $\epsilon$  was found in literature [1]. Mica sheets were available only with a thickness of 2 mm; two thickness of gres were tested (3 and 4 mm); glass was the easiest material to find and 4 thickness were tested (2, 3, 4 and 5 mm).

The breakage of the dielectric layer usually was connected to the heating of the material; this heating is strictly connected with the current flowing in the system, therefore the limitations on operative conditions are linked to the maximum power density flowing through the discharge.

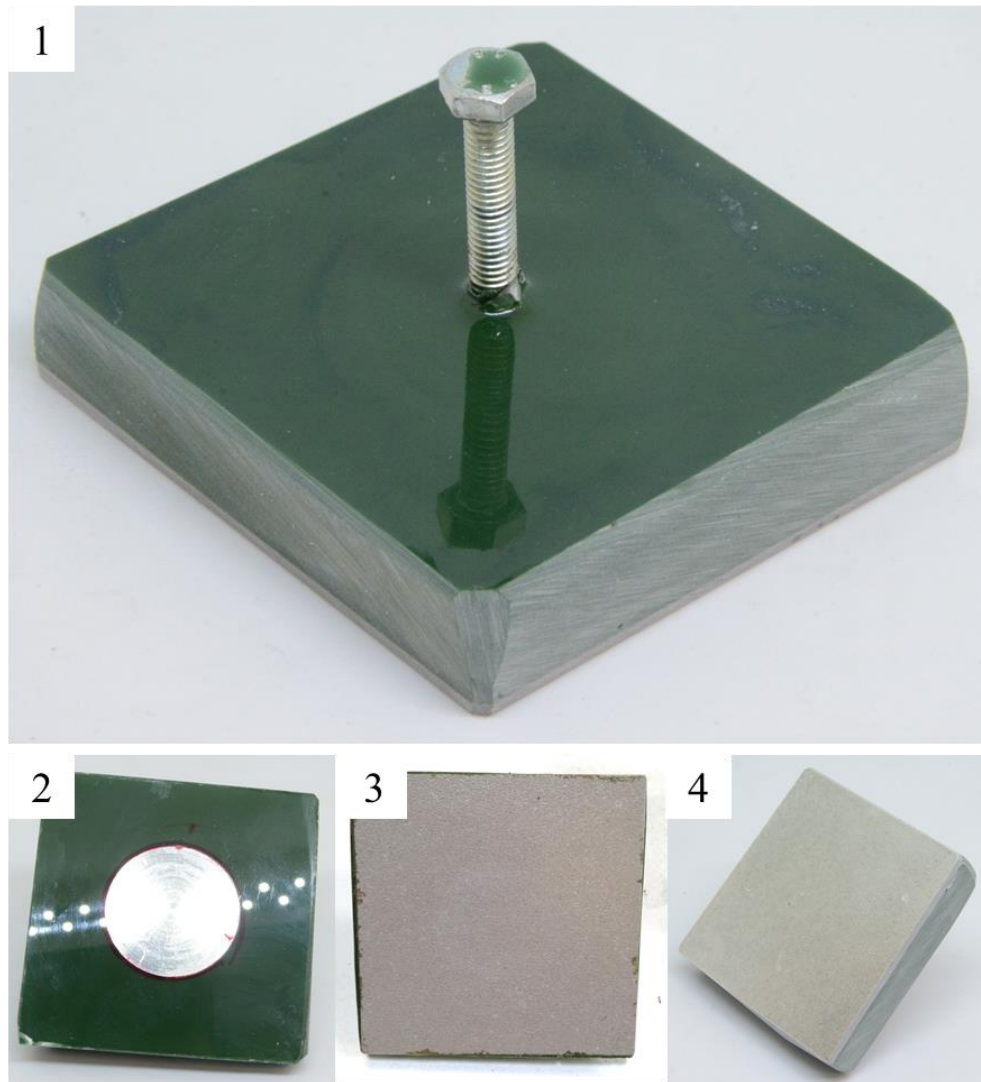
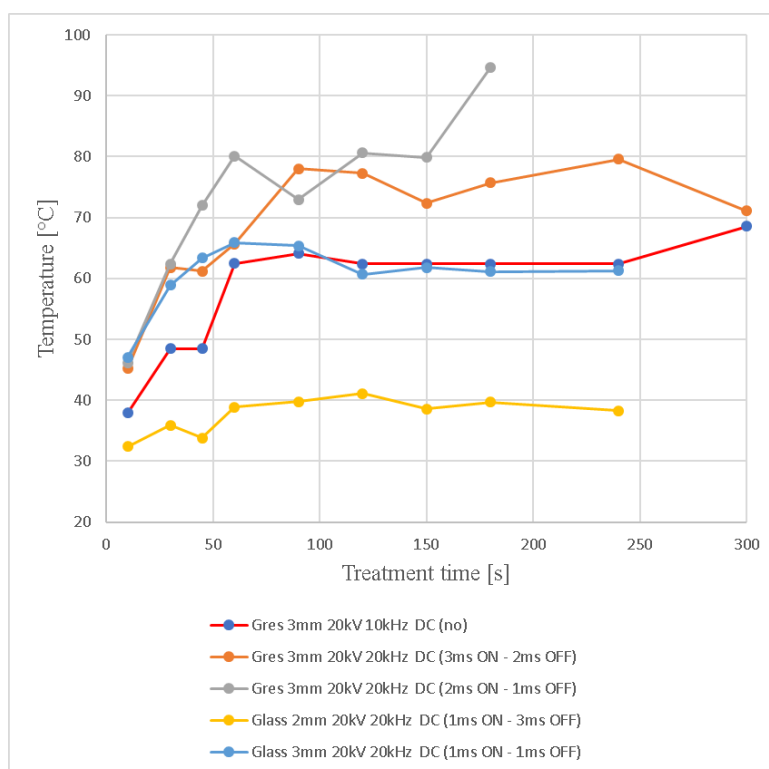


*Figure 5.3 1. Top view of an aluminium high voltage electrode with stainless steel high voltage connection; the electrode is covered with resin to avoid free discharges; this electrode was coupled with different dielectric layers. 2-3-4 bottom views of the electrode paired with glass, gres and mica layer, respectively.*

Experiments consisted in treatment of 300 seconds; every 30 seconds, the plasma was switched off and the high voltage electrode was placed on a pedestal that had the task of maintaining the proper distance between the dielectric material and the IR probe. After sampling, the high voltage electrode was placed on the ground electrode and the power supply was switched on again. Several electrical input conditions were tested with each dielectric material to identify which was the maximum power density usable with each plasma source.

Graph 5.4 is an example of temperature measurements obtained with the pyrometer: firstly, temperature trends shows a quick raise during the initial 60 seconds of treatment; after that, a temperature plateau is reached; secondly, the temperature never exceeds 80°C; this implies that the thermal factor cannot be the main cause of microbial inactivation, if ever. For treatment of this duration (maximum 8 seconds) a higher temperature would be needed to kill microorganisms.



Graph 5.4 temperature trend of the dielectric material

### 5.3 Electrical measurement

AlmaPULSE is a current generator in which the amplitude and the frequency of the potential waveform can be varied; the current provided to the discharge is dictated by the plasma source configuration (geometry and material). So, the electrical power absorbed by the plasma source and the power involved in the discharge cannot be directly controlled from the power supply; it is necessary to measure the power absorbed by the plasma source for every different configuration (dielectric material and electrical input).

From CAP literature, it is clear that there are mainly two methods to analyse electrically a plasma process: the first relies on the direct sampling of potential and current curve [2,3]; the second involves the design of an equivalent circuit to estimate the capacity of the discharge (Lissajous method) [2,4,5]. Although the second method is more precise, providing the real value of power of the plasma discharge, the first method is faster and easier to use. The big disadvantage of the first measurement is that it can calculate the electric power absorbed by the plasma source instead of the power of the discharge; the former is always greater than the latter. Nevertheless, this technique provides reliable and repeatable values of power which can be used to compare two different discharges.

#### *Measurements setup*

Three devices were needed to run the electrical measurements: a current probe, a high voltage probe and an oscilloscope. The setup can be seen in figure 5.5. Current was measured by means of a current probe (Pearson current monitor model 6585) on

the high voltage cable; the voltage was also measured on the high voltage cable, by means a differential probe (Tektronix P6015A 1000X). Both probes were connected to a fast oscilloscope (Tektronix DPO4034) to monitor waveforms and to save data. Data were later processed through MATLAB to calculate the power absorbed by the DBD.

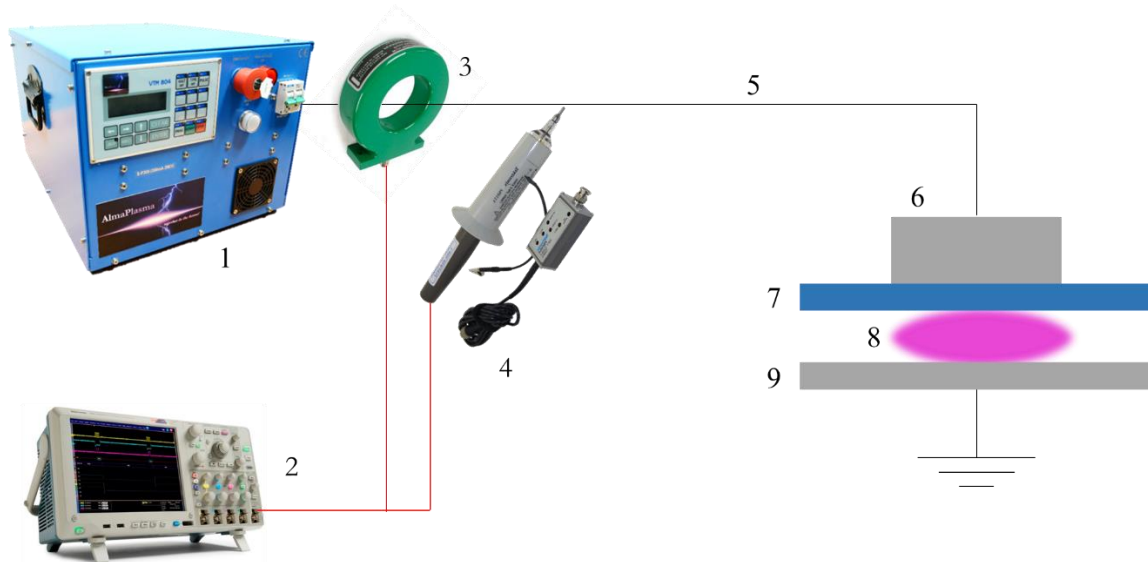
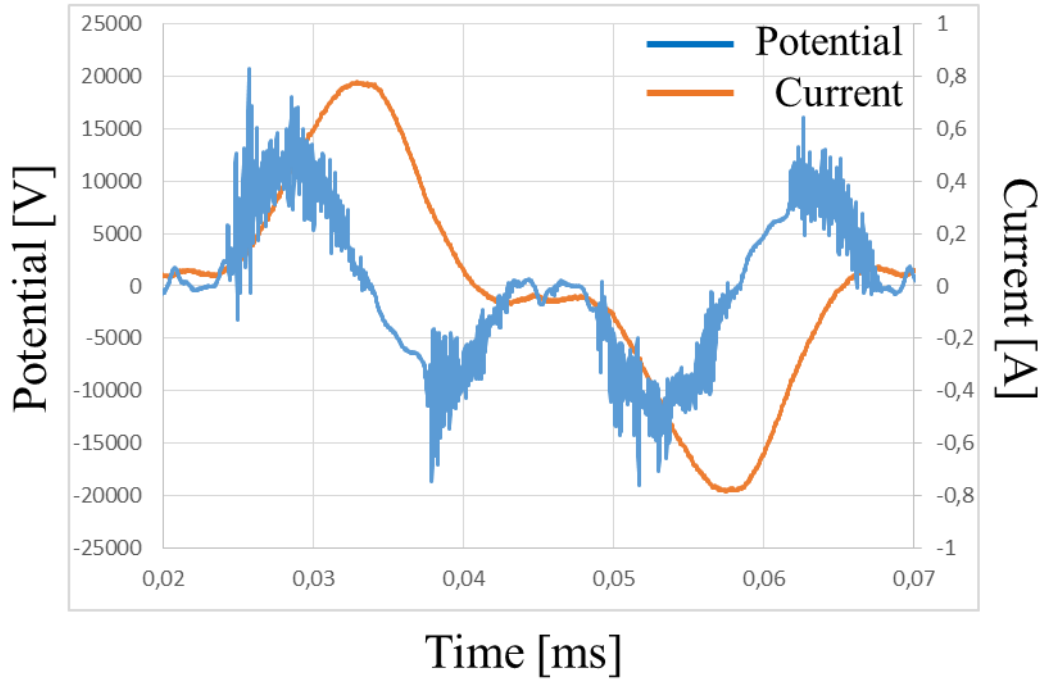


*Figure 5.5 Electrical measurements setup: 1. AlmaPULSE; 2. Oscilloscope; 3. Current probe; 4. High voltage probe; 5. High voltage cable; 6. High voltage electrode; 7. Dielectric layer; 8. Plasma; 9. Ground electrode.*

Graph 5.6 shows the voltage and current curves acquired during one complete period is reported ( $50 \mu\text{s}$ ) using the 3 mm gres electrode; the potential amplitude was set to 20 kV while the pulse frequency was set to 20 kHz. At atmospheric pressure, the DBD source produces a streamer-like discharge consisting in thousands of fast micro discharges (1-10 ns); every streamer produces a spike in the current waveform. It can be noted that, during a single potential period there are four streamer-generation phases; these periods occur simultaneously with voltage gradients.



Graph 5.6 Voltage and current waveforms of a gres-DBD

To calculate the electrical power absorbed by the plasma source a simple algorithm was used; after sampling, data series were trimmed in order to have only one pulse for each series of data; electrical power ( $P$ ) was calculated using the following formula:

$$P = \frac{1}{T} \int_0^T V * I dt$$

Where  $T$  is the period of a voltage pulse,  $V$  is the potential and  $I$  is the current. The current measured and used in this method includes both the discharge current and the displacement current. The power density was calculated dividing  $P$  for the surface of the high voltage electrode.

## 5.4 Discussion on results and dielectric material choice

To define which dielectric material was most suitable for the application under examination, temperature results had to be paired with electrical results; in fact, different materials and thicknesses led to different maximum temperatures; these temperatures are comparable only for equal power density. The goal of this investigation was to find the best compromise between plasma power density and heating.

There are several insights that is worth highlighting with the aim of reaching a final choice of the dielectric material. Most of these remarks are connected to the concept of dielectric strength (DS): for a specific configuration of dielectric material and electrodes, the DS is the minimum applied electric field that results in breakdown. It is known that glass has a lower dielectric strength compared to mica and gres, which have similar DS. Remarks:

- For a single material and electrical input, the power density was higher for thinner dielectric layer; simultaneously, the maximum temperature achieved by the dielectric was greater. Conversely, an increase in the thickness of the dielectric layer led to a lower value of power density, hence a lower heating of the DBD (i.e. maximum temperature).
- For equal thickness and electrical input, the highest power density was associated to the glass-DBD; while mica and gres showed similar results. This fact implies that to achieve the same power density of the glass-DBD, both mica- and gres-DBD needed higher electrical input (or interelectrode potential). Again, this fact is strictly related to the concept of DS.
- Higher values of power density led to a greater heating; hence higher maximum temperature reached. Nevertheless, this close connection between power density and heating does not follow the same trend for any materials: while gres and mica behave almost equally; for equal values of power density and thickness, glass reached drastically lower temperature.

On this basis, glass-DBD showed the best results: higher power density achieved and lower heating during operation; unfortunately, glass proved to have poor mechanical properties and while the glass-DBD showed no problem during operation, the dielectric layer broke during the cooling phase (after treatment): the different thermal expansion factors plus the different thermal inertias of the glass layer and the aluminium electrode led to the formation of cracks in the glass layer. This fact forced to reduce the electrical input to the glass-DBD; doing so, the power density decreased together with the maximum temperature. Practically, in order to avoid breakage, the intensity of the plasma had to be reduced drastically; consequently, the glass-DBD was not the best choice for this particular application, not being able to produce discharges with the same power density of gres and mica DBD.

Mica and gres showed a similar behaviour under almost every circumstance: DS, power consumption, heating, mechanical resistance. The choice between these two materials was made out of different considerations: gres is a ceramic material and shows almost no difference between the first to the hundredth treatment performed; on the other hand, mica consists in numerous thin layers packed together and showed visible damages after a few hours of treatment. In this frame, the gres-DBD was chosen as the most suitable and a 3 mm layer was preferred to a 4 mm one since no mechanical differences were reported between these two configurations; on the other hand, the power density absorbed for equal electrical inputs was greater for the thinner layer. Considering that the AlmaPULSE has a maximum voltage limit input, the thinner gres layer allows to reach higher absolute values of power density compared to the 4 mm layer.



## 5.5 Cooling system

Temperature analysis showed a constant heating by power dissipation to materials constituting the DBD; although this heating was not strongly affecting the discharge generation, it could not be neglected since a plasma assisted industrial processes must operate for several hours continuously.

In this frame, the high voltage electrode was redesigned in order to allow the cooling of the metallic component. Practically, a U-shaped channel was drilled in the high voltage electrode to allow the flow of a cooling fluid. At first, compressed air was used to cool the electrode; but, due to the low heating exchange surface and the low heating exchange factor of air, the efficacy of this system was almost null. The same idea was followed using a cooling dielectric liquid (water and glycol); the efficacy of this system was extremely higher than the previous one and allowed to keep the temperature of the high voltage electrode constant at  $\sim 25^{\circ}\text{C}$  (room temperature).

Being purely metallic, the ground electrode had a higher heat exchange factor compared to the high voltage electrode (and a lower thermal inertia); therefore, the cooling effect of the ambient air was enough to allow continuous operation on a lab scale DBD.

In figure 5.7 a rendering of the final DBD source is reported; in the sectional view the O-ring element needed to ensure the sealing of the cooling system is shown.

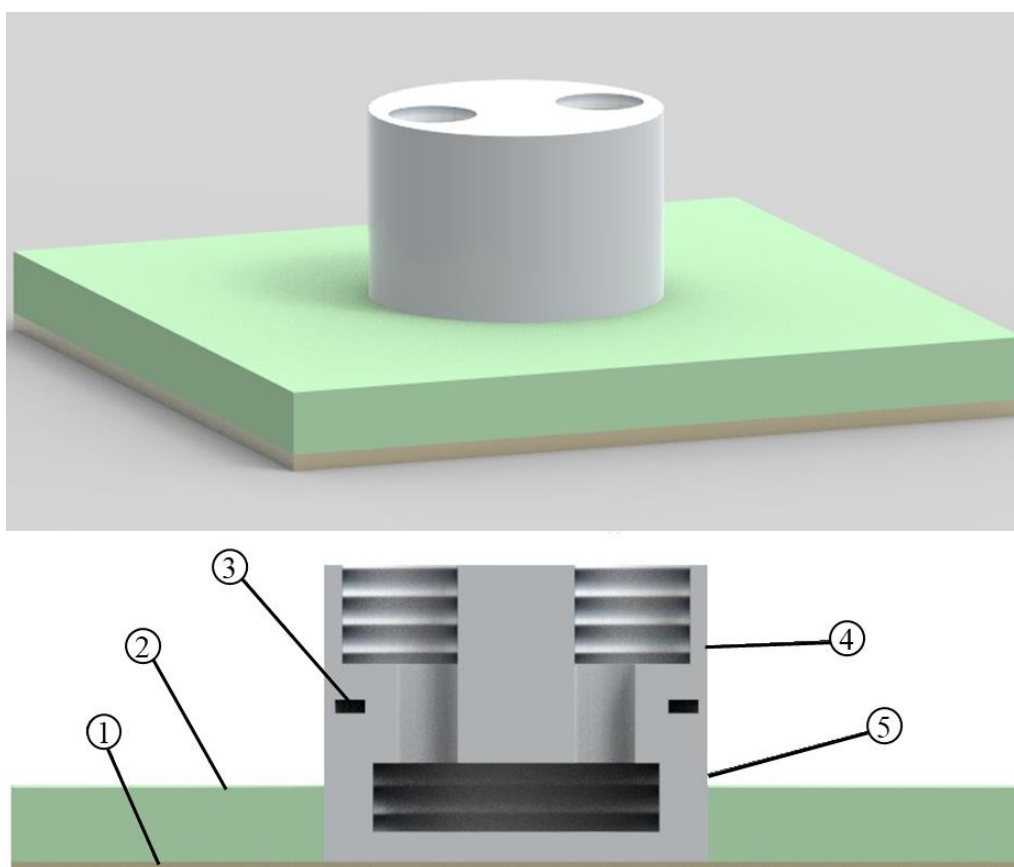
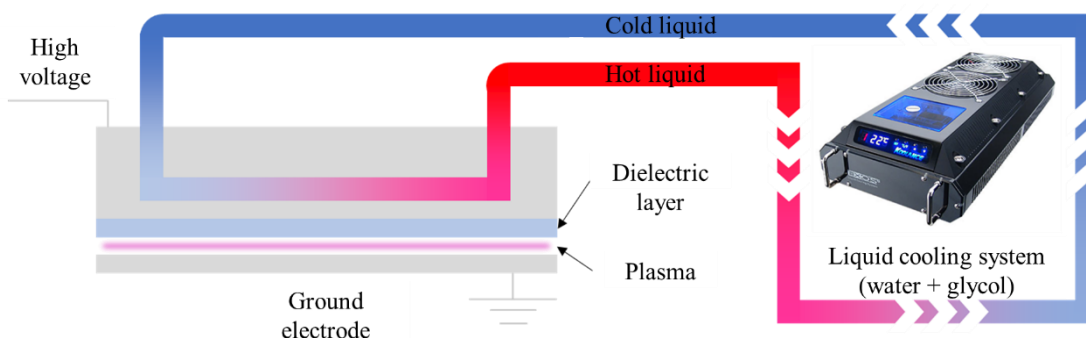


Figure 5.7 Rendering of the liquid cooled DBD (top), section view (bottom): 1. Gres layer; 2. Resin; 3. O-Ring; 4. Cooling system connection; 5. High voltage electrode.

Lastly, a schematic of the cooling system is reported; to pump the liquid in the electrode and to cool it, the Koolance EX2-755 was used.



*Figure 5.8 Cooling system*

## 5.6 Chemistry analysis

Temperature and electrical investigations allowed to define the best performing DBD layout; once fixed the geometry and materials of the plasma source, research activities must look for the best plasma operative conditions. Starting from the inactivation results obtained earlier (reported in chapter 3), the aim was to find a connection between biological results and the chemistry involved in the process, parametrizing the operating conditions of the plasma process over treatment time and power density.

This inquiry started from a literature analysis, to understand which were the most relevant chemical processes and physical parameters which lead to microbial inactivation; later, the chemical kinetics of biocidal reactive species were observed by means of Optical Absorption Spectroscopy (OAS).

As soon as research showed interest in cold air plasmas, a lot of effort was made to study and understand the chemistry governing these processes; interest grew together with its industrial applications. Companies interested in producing ozone for disinfection purposes, found in CAP a viable and efficient alternative; this is the reason why the greatest part of scientific papers of the last century dealing with the chemistry of air plasma were focused to ozone production and how to maximize it [6–9].

The chemistry of air plasma consists mainly in oxygen and nitrogen-based reactions; consequently, the most produced species are those connected to these elements. In plasma processes there are three main types of species that are produced: excited species, radicals (and ions) and neutral reactive species. Excited species have usually low energy compared to other species; therefore, their reactions affect only marginally the discharge. On the contrary, radicals and ions are extremely energetic and reacts faster than any other species involved in the discharge. Radicals and ions have a strong impact on the plasma chemistry and are also known to have a strong biocidal effect. Due to their high energy and aggressiveness, radicals and ions are short-living species; consequently, their concentrations measurements are based on highly sophisticated methods which cannot be used in an industrial environment. Neutral reactive species

are long-living species (from minutes to hours), more stable than radicals; some of these species have a biocidal effect and it is interesting to measure their concentration. In air plasmas, excited species are mainly vibrational and rotational excited species of nitrogen and oxygen molecules; as it was already said, such species are not interesting in this frame. The most important radicals are atomic oxygen and the hydroxyl radical; both these species are known to have a huge biocidal effect. On the side of neutral reactive species, usually called RONS (reactive oxygen and nitrogen species), it is worth reporting:  $O_3$ ,  $NO$ ,  $NO_2$ ,  $NO_3$ ,  $N_2O$ ,  $N_2O_3$ ,  $N_2O_4$  and  $N_2O_5$ . Among long-living species  $O_3$ ,  $NO$  and  $NO_2$  are known to have the stronger impact on microbial inactivation.

A lot of work was put to describe minutely the chemistry of ozone production and the species governing this process were easily predictable; however, the dynamic of their production was not trivial to guess. Mainly thanks to the works of Kogelschatz *et alii* [7,8] we know that there are two different chemical regimes governing an air plasma discharge; moreover, he discovered that the chemical regime is defined by the power density involved in the discharge. To understand this fact, it is necessary to analyze the chain reactions describing this chemistry.

Table 5.9 Main RONS reaction involved in air plasma discharge

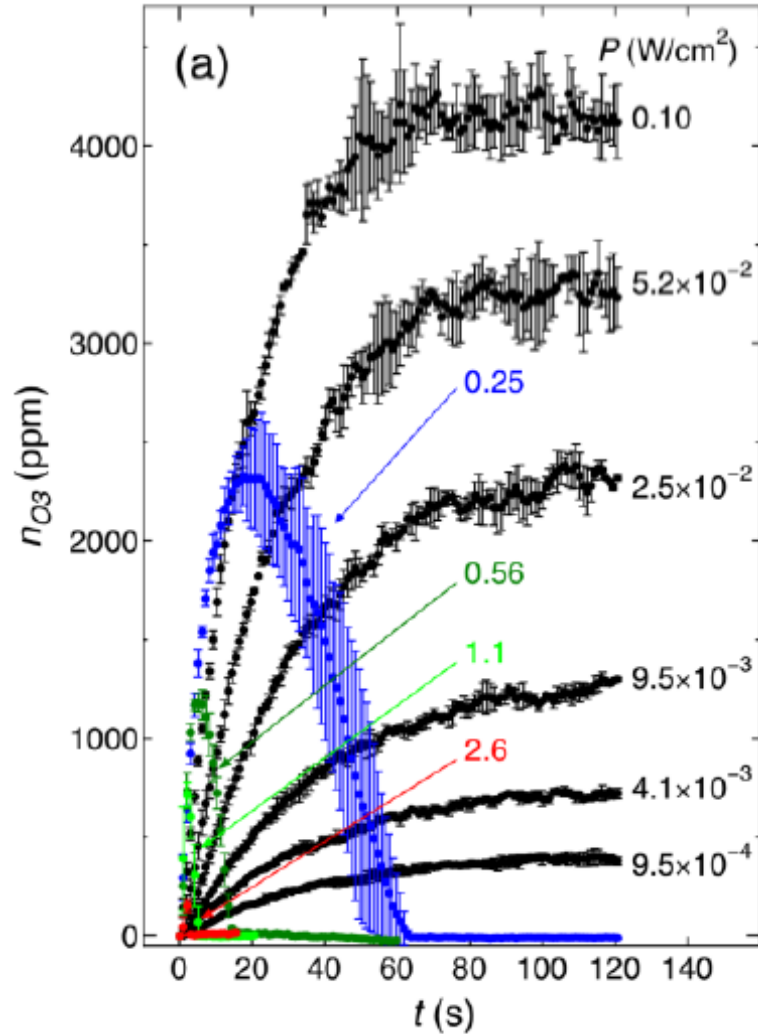
Ozone					
Production	R1	$O_2+O+M\rightarrow O_3+M$	(10 <sup>-21</sup> )		
	R2	$O_3+e\rightarrow O+O_2^-$	(10 <sup>-15</sup> )	R7	$O_3+N\rightarrow NO+O_2$ (10 <sup>-21</sup> )
Destruction	R3	$O_3+H\rightarrow OH+O_2$	(10 <sup>-17</sup> )	R8	$O_3+HO_2\rightarrow OH+2O_2$ (10 <sup>-21</sup> )
	R4	$O_3+OH\rightarrow HO_2+O_2$	(10 <sup>-19</sup> )	R9	$O_3+NO_2\rightarrow NO_3+O_2$ (10 <sup>-23</sup> )
	R5	$O_3+O\rightarrow 2O_2$	(10 <sup>-20</sup> )	R10	$O_3+M\rightarrow O_2+O+M$ (10 <sup>-32</sup> )
	R6	$O_3+NO\rightarrow NO_2+O_2$	(10 <sup>-20</sup> )		
NO					
Production	R10	$O+HNO\rightarrow OH+NO$	(10 <sup>-16</sup> )	R16	$O+NO_2\rightarrow NO+O_2$ (10 <sup>-17</sup> )
	R11	$OH+HNO\rightarrow NO+H_2O$	(10 <sup>-16</sup> )	R17	$HNO+O_2\rightarrow NO+HO_2$ (10 <sup>-17</sup> )
	R12	$N+O_2\rightarrow NO+O$	(10 <sup>-17</sup> )	R18	$N+NO_2\rightarrow 2NO$ (10 <sup>-18</sup> )
	R13	$H+HNO\rightarrow NO+H_2$	(10 <sup>-17</sup> )	R19	$N+O_3\rightarrow NO+O_2$ (10 <sup>-22</sup> )
	R14	$N+OH\rightarrow H+NO$	(10 <sup>-17</sup> )	R20	$2HNO_2\rightarrow NO+NO_2+H_2O$ (10 <sup>-26</sup> )
	R15	$N+HO_2\rightarrow NO+OH$	(10 <sup>-17</sup> )	R21	$N+O+M\rightarrow NO+M$ (10 <sup>-45</sup> )
Destruction	R22	$N+NO\rightarrow N_2+O$	(10 <sup>-17</sup> )	R26	$NO+OH+M\rightarrow HNO_2+M$ (10 <sup>-42</sup> )
	R23	$NO+NO_3\rightarrow 2NO_2$	(10 <sup>-17</sup> )	R27	$O+NO+M\rightarrow NO_2+M$ (10 <sup>-43</sup> )
	R24	$NO+HO_2\rightarrow OH+NO_2$	(10 <sup>-18</sup> )	R28	$NO+NO_2+M\rightarrow N_2O_3+M$ (10 <sup>-46</sup> )
	R25	$NO+HO_2\rightarrow O_2+NO_2$	(10 <sup>-19</sup> )		
NO <sub>2</sub>					
Production	R29	$NO_3+O\rightarrow NO_2+O_2$	(10 <sup>-17</sup> )	R37	$N_2O_4\rightarrow 2NO_2$ (10 <sup>-20</sup> )
	R30	$NO+NO_3\rightarrow 2NO_2$	(10 <sup>-17</sup> )	R38	$HNO+O_2\rightarrow NO_2+OH$ (10 <sup>-21</sup> )
	R31	$NO+HO_2\rightarrow NO_2+OH$	(10 <sup>-17</sup> )	R39	$O+HNO_2\rightarrow NO_2+OH$ (10 <sup>-21</sup> )
	R32	$NO_3+OH\rightarrow NO_2+HO_2$	(10 <sup>-17</sup> )	R40	$2NO_3\rightarrow NO_2+O_2$ (10 <sup>-22</sup> )
	R33	$O+NO\rightarrow NO_2$	(10 <sup>-18</sup> )	R41	$HNO_2+HNO_3\rightarrow 2NO_2+H_2O$ (10 <sup>-23</sup> )
	R34	$OH+HNO_2\rightarrow NO_2+H_2O$	(10 <sup>-18</sup> )	R42	$N_2O_5\rightarrow NO_2+NO_3$ (10 <sup>-25</sup> )
	R35	$O_3+NO\rightarrow NO_2+O_2$	(10 <sup>-20</sup> )	R43	$2HNO_2\rightarrow NO_2+NO+H_2O$ (10 <sup>-26</sup> )
	R36	$N_2O_3+HO_2\rightarrow NO_2+NO$	(10 <sup>-20</sup> )		
Destruction	R44	$NO_2+H\rightarrow OH+NO$	(10 <sup>-16</sup> )	R49	$2NO_2\rightarrow N_2O_4$ (10 <sup>-20</sup> )
	R45	$NO_2+N\rightarrow N_2O+O$	(10 <sup>-17</sup> )	R50	$NO_2+NO\rightarrow N_2O_3$ (10 <sup>-21</sup> )
	R46	$NO_2+NO_3\rightarrow N_2O_5$	(10 <sup>-17</sup> )	R51	$NO_2+O\rightarrow NO+O_2$ (10 <sup>-21</sup> )

	R47	$\text{NO}_2 + \text{O} \rightarrow \text{NO}_3$	(10 <sup>-18</sup> )	R52	$\text{NO}_2 + \text{O}_3 \rightarrow \text{O}_2 + \text{NO}_3$	(10 <sup>-23</sup> )
	R48	$\text{NO}_2 + \text{OH} \rightarrow \text{HNO}_3$	(10 <sup>-18</sup> )			
<hr/> <b>NO<sub>3</sub></b> <hr/>						
Production	R53	$\text{NO}_2 + \text{O} \rightarrow \text{NO}_3$	(10 <sup>-18</sup> )	R55	$\text{NO}_2 + \text{O}_3 \rightarrow \text{NO}_3 + \text{O}_2$	(10 <sup>-23</sup> )
	R54	$\text{OH} + \text{HNO}_3 \rightarrow \text{NO}_3 + \text{H}_2\text{O}$	(10 <sup>-21</sup> )	R56	$\text{N}_2\text{O}_5 \rightarrow \text{NO}_3$	(10 <sup>-25</sup> )
Destruction	R57	$\text{NO}_3 + \text{O} \rightarrow \text{NO}_2 + \text{O}_2$	(10 <sup>-17</sup> )	R60	$\text{NO}_3 + \text{OH} \rightarrow \text{H}_2\text{O} + \text{NO}_2$	(10 <sup>-17</sup> )
	R58	$\text{NO}_3 + \text{NO} \rightarrow 2\text{NO}_2$	(10 <sup>-17</sup> )	R61	$\text{NO}_3 + \text{HO}_2 \rightarrow \text{HNO}_3$	(10 <sup>-18</sup> )
	R59	$\text{NO}_3 + \text{NO}_2 \rightarrow \text{N}_2\text{O}_5$	(10 <sup>-17</sup> )	R62	$2\text{NO}_3 \rightarrow \text{NO}_3 + \text{O}_2$	(10 <sup>-22</sup> )

Reactions in table 5.9 were found in papers published by different authors [7,8,10]; although their works differ in various details, a crucial concept can be found through them: the atmosphere generated by DBDs (e.g. ozonisers) is directly affected by the surface power density in case of a stationary process. Moreover, at low power density (<0.2W/cm<sup>2</sup>) CAP treatment produces an ozone enriched atmosphere; while at higher power density, the atmosphere shifts into a NO<sub>x</sub> regime, due to a phenomenon called *ozone poisoning* [6,7,10–17]. It has been observed that, the ozone poisoning is a time-dependent effect occurring at high power density, and affect the kinetics of NO<sub>x</sub> (NO, NO<sub>2</sub>, NO<sub>3</sub> and N<sub>2</sub>O<sub>5</sub> molecules) concentrations in a time-dependent way. Many studies demonstrated the direct correlation between the ozone concentration and the antimicrobial efficacy of CAP treatment [10,15]; fewer authors analysed the efficacy of RONS in general [18,19].

For the sake of simplicity, low-power density regime will be called *ozone-regime* and the high-power density regime will be called *NO<sub>x</sub>-regime*. Above all, Shimitzu *et alii* [10] reported and explained the difference between these two regimes and the reasons of the ozone poisoning. In graph 5.10 they reported the ozone concentration as a function of time; they obtained several curves depending on the power density applied to a surface DBD. The authors highlighted that, increasing power density from 0 to 0.10 W/cm<sup>2</sup> (black lines) increased the ozone production rate; additionally, the maximum concentration of ozone increased as well. As soon as the power density reached a value of 0.25 W/cm<sup>2</sup>(blue line), a new phenomenon could be noticed: the ozone concentration reached a maximum after a few seconds of operation and then decreased, going below the sensibility of the instrument. This phenomenon (i.e. ozone poisoning) was faster and faster as power density increased.

Shimitzu also gave an explanation to this behaviour which requires the analysis of the reactions of production and destruction of RONS.



Graph 5.10 Ozone chemical kinetics in an air surface DBD [10]

Ozone is mainly produced by reaction R1 between oxygen molecules and oxygen atoms. O is formed by electron impact dissociation of  $O_2$ ; its formation is directly proportional to the power density, as Yagi and Tanaka showed in their study on air-fed ozonisers [11]. This relation between the production of O and the power density explains the behaviour of ozone kinetics during the first seconds of plasma treatment, with ozone production rate increasing linearly with power density.

There are several pathways which may cause the depletion of ozone; in air plasmas, as for air-fed ozonisers, the main contribution in the destruction of ozone is given by  $NO_x$  molecules forming the catalytic cycle represented by R6 and R9 [7,11], which consume directly ozone and by R47 that reduces the density of O atoms, a reagent which is needed for  $O_3$  formation. Several studies on air ozonisers [6,11,12] describe this phenomenon as the ozone poisoning effect and suggest that it is caused by an increase of nitrogen oxides as NO and  $NO_2$ . Increasing power density, reactions R33 and R51 become faster than R1 and thus remove O atoms.

Biological results show different inactivation levels and trends for the two power densities tested; in order to understand if the chemistry involved in the process was

effectively responsible for this behaviour, OAS measurements were performed. Ozone and nitrogen dioxide concentrations were analysed to assess which regime was governing the discharge: ozone or nitrogen oxides.

### 5.6.1 OAS

OAS is a technique relying on the Lambert-Beer (Johann Heinrich Lambert and August Beer) law that can be used to derive the absolute concentrations of several species, measuring the reduction of intensity of light passing through a certain volume of gas. This technique is non-intrusive and calibration-free; it can be on-line used during treatments to observe the kinetics of reactive species produced by CAPs [17,20].

The OAS set up used in this work is shown in figure 5.11; as light source: a deuterium-halogen lamp was used, characterized by a broadband spectrum from UV to NIR radiation. The light emitted from the lamp is directed to a fused silica lens through an optical fiber. This lens collimates the light beam travelling inside the plasma generation volume and reaches a second lens. This lens converges the light beam to another optical fiber that brought the signal to a 500 mm spectrometer (Acton SP2500i, Princeton Instruments). The grating of the spectrometer disperses the spectral components of impinging light at slightly varying angles and this allowed to separate photons reaching the target at different wavelengths; by means of an outlet slit only photons of selected wavelengths reached the detector. A photomultiplier (PMT - Princeton Instruments PD439) increased and converted the light output signal of the spectrometer to an electrical signal. The PMT amplification factor was kept constant for all acquisitions. In order to ensure equal gas initial conditions, the discharge chamber was opened and flushed for 30 seconds before every measurement. The signal could be monitored with a fast oscilloscope.

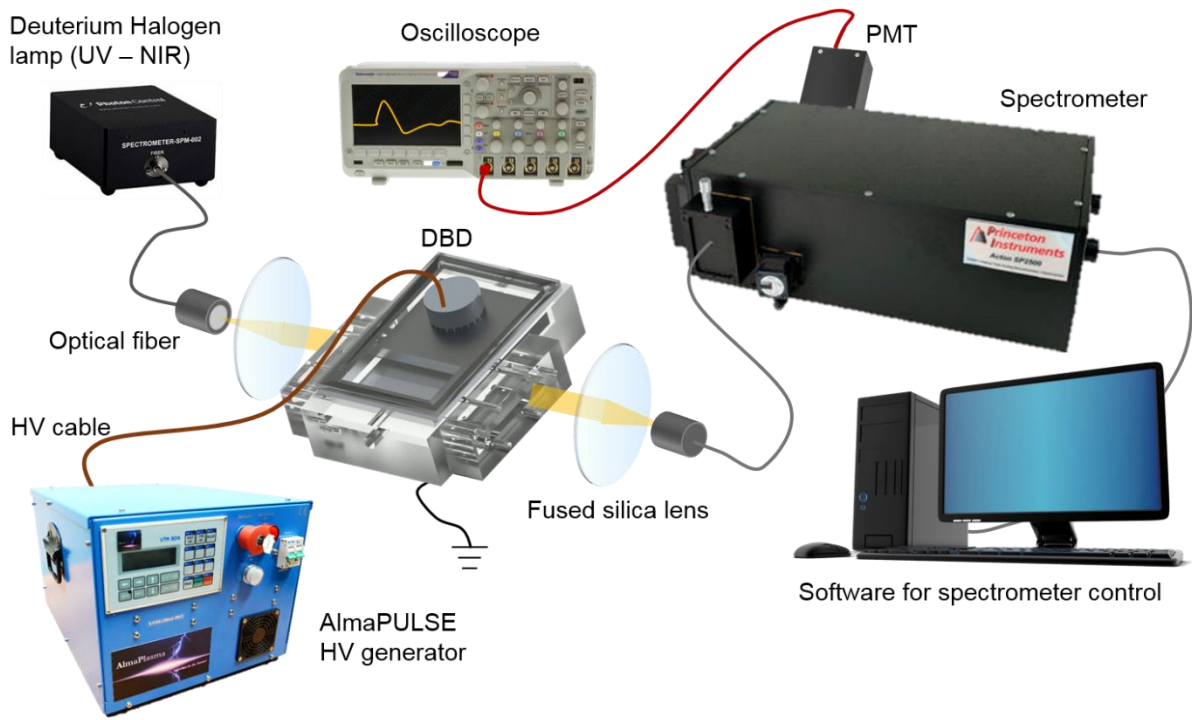


Figure 5.11 OAS setup

To quantitatively evaluate O<sub>3</sub> and NO<sub>2</sub> concentrations from absorption measurements, the Lambert-Beer law was used; this relation describes the light absorbed by a homogeneous medium as a function of the species density  $n$  in the medium:

$$\frac{I}{I_0} = e^{(-L\sigma n)}$$

where  $I$  is the light intensity,  $I_0$  is the initial light intensity and  $\sigma$  is the absorption cross-section.

In order to minimize the external influence on the treatment atmosphere during measurements, a case was created to contain the DBD (figure 5.12). The optical path of this reactor was of 8.0 cm. The reactor was made with 2 quartz windows to be transparent to any radiation (borosilicate glass blocks radiation with a wavelength lower than 300 nm); these windows were 7 cm wide to allow a spatial analysis of concentrations. Four different distances from the electrode were investigated, to analyse the diffusion of reactive species.



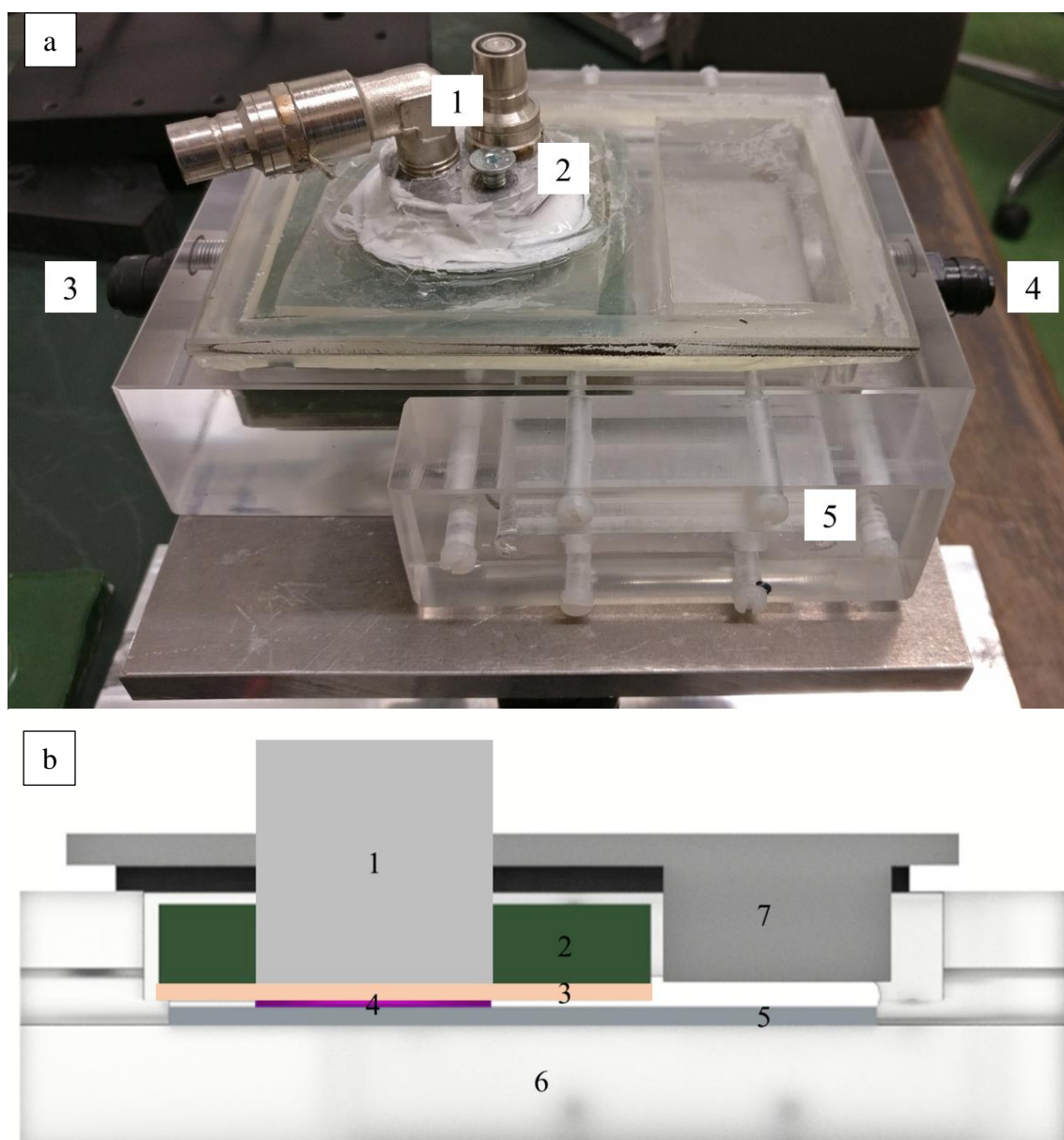


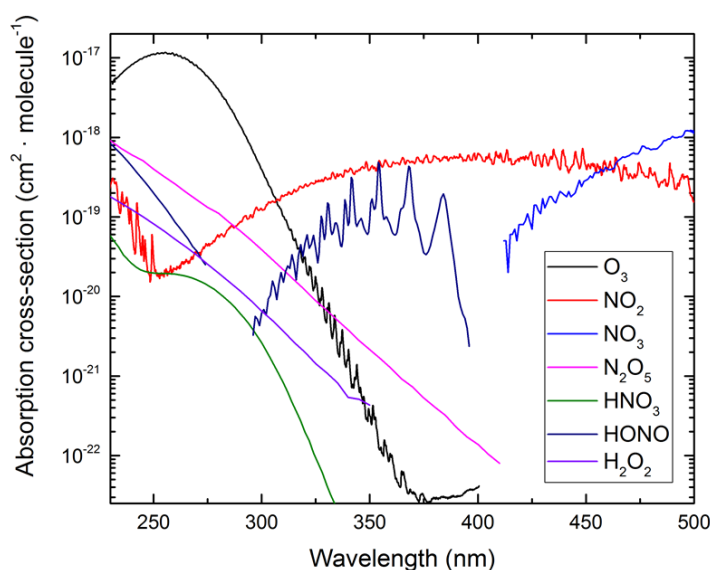
Figure 5.12 a) DBD reactor: 1. Cooling connection; 2. High voltage connection; 3. Gas inlet; 4. Gas outlet; 5. Quartz optical window. B) cross section of the DBD reactor rendering: 1. HV electrode; 2. Resin; 3. Gres; 4. Plasma; 5. Ground electrode; 6. Container bottom; 7. Container top.

The wavelength range, specific for  $O_3$  and  $NO_2$  has been chosen according to Moiseev's studies [17] and integrated with the spectral resolution of the instrumentations used in this work (1.2 nm). Values for the absorption cross-sections are found by averaging data from the MPI-Mainz UV/VIS Spectral Atlas database [21]. Absorption cross-sections are presented in table 5.13:

Table 5.13 Ozone and nitrogen dioxide cross-sections

Wavelength range [nm]	O <sub>3</sub> cross-section [cm <sup>2</sup> ]	NO <sub>2</sub> cross-section [cm <sup>2</sup> ]
253 ± 1.2	(1.12 ± 0.02) E-17	(1.1 ± 0.3) E-20
400 ± 1.2	(1.12 ± 0.08) E-23	(6.4 ± 0.2) E-19

As reported by Moiseev, these two wavelength ranges are suitable for OAS investigation; in fact, as can be seen in graph 5.14, the cross-sections of O<sub>3</sub> and NO<sub>2</sub> are at least two orders of magnitude greater than those of any other species; consequently the absolute concentrations may be calculated without making a significant error.



Graph 5.14 Absorption cross-sections of main RONS [17]

To make experiment faster and more repeatable a MATLAB code was written to allow real time kinetics analysis converting the oscilloscope signal to the concentration value of the species under examination within the acquisition time. Furthermore, the code could be easily adjusted for the analysis of different species and geometries.

To allow a spatial analysis of O<sub>3</sub> and NO<sub>2</sub> kinetics, four distinct optical paths were used (as shown in figure 5.15). The first path used was located under the high voltage electrode, the second one, at the edge of the electrode; the third and fourth paths were placed outside the plasma generation volume to assess the diffusion of chemical species.

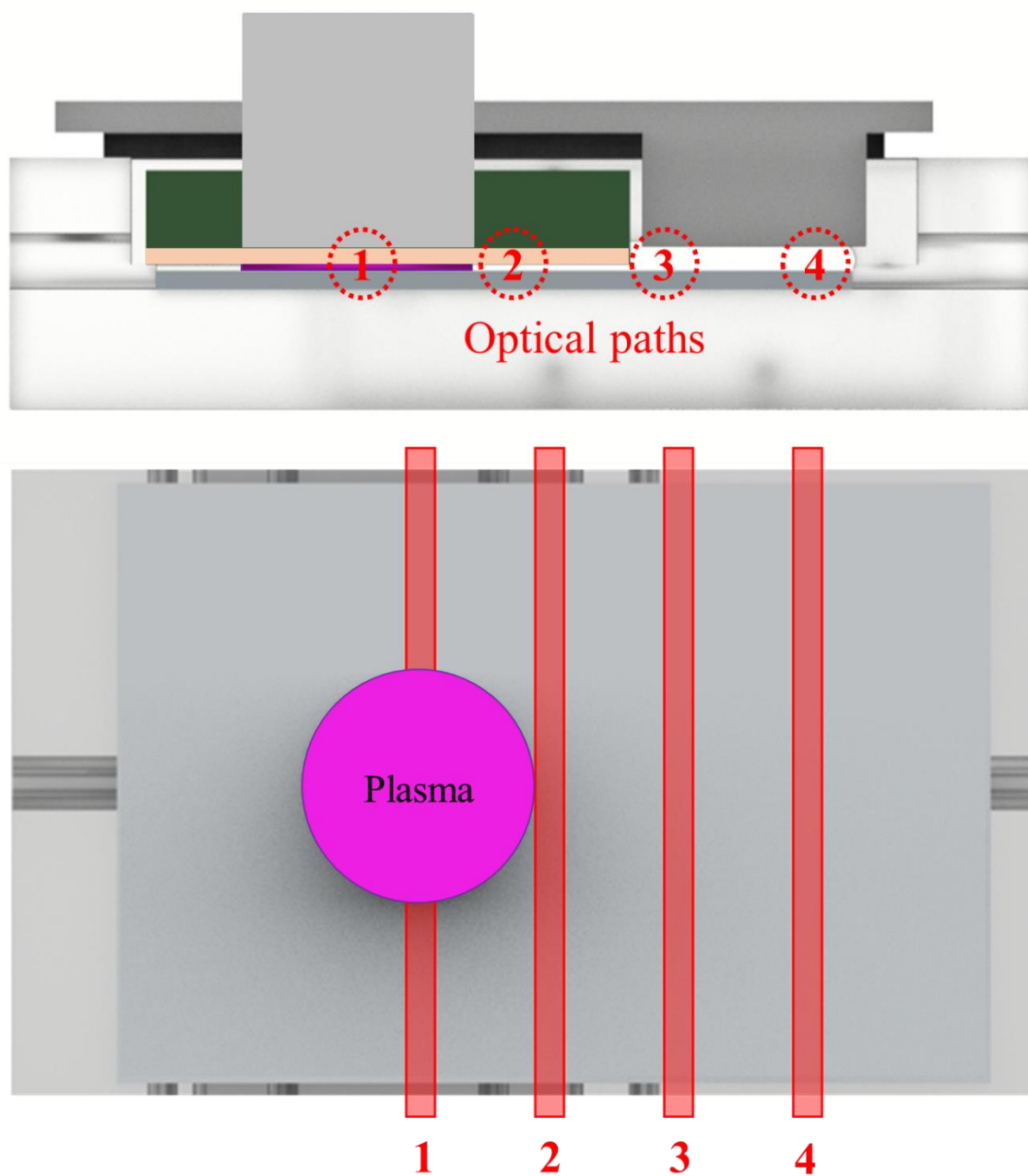


*Figure 5.15 Schematic of OAS optical paths*

## 5.6.2 OAS results and discussion

Experiments were performed with 3 different values of power density to better understand the role of ozone poisoning in the process. Measurements were acquired 3 times (and averaged) for each optical path. The DBD container was flushed with compressed air for 30 seconds before any measure; the relative humidity of the air was measured and found at 21%. Acquisitions lasted 400 seconds: 30 seconds of plasma discharge and 370 seconds of post discharge.

Data were imported in Origin and plotted in 3D graphs reporting  $O_3$  and  $NO_2$  kinetics as function of time and distance from the electrode.

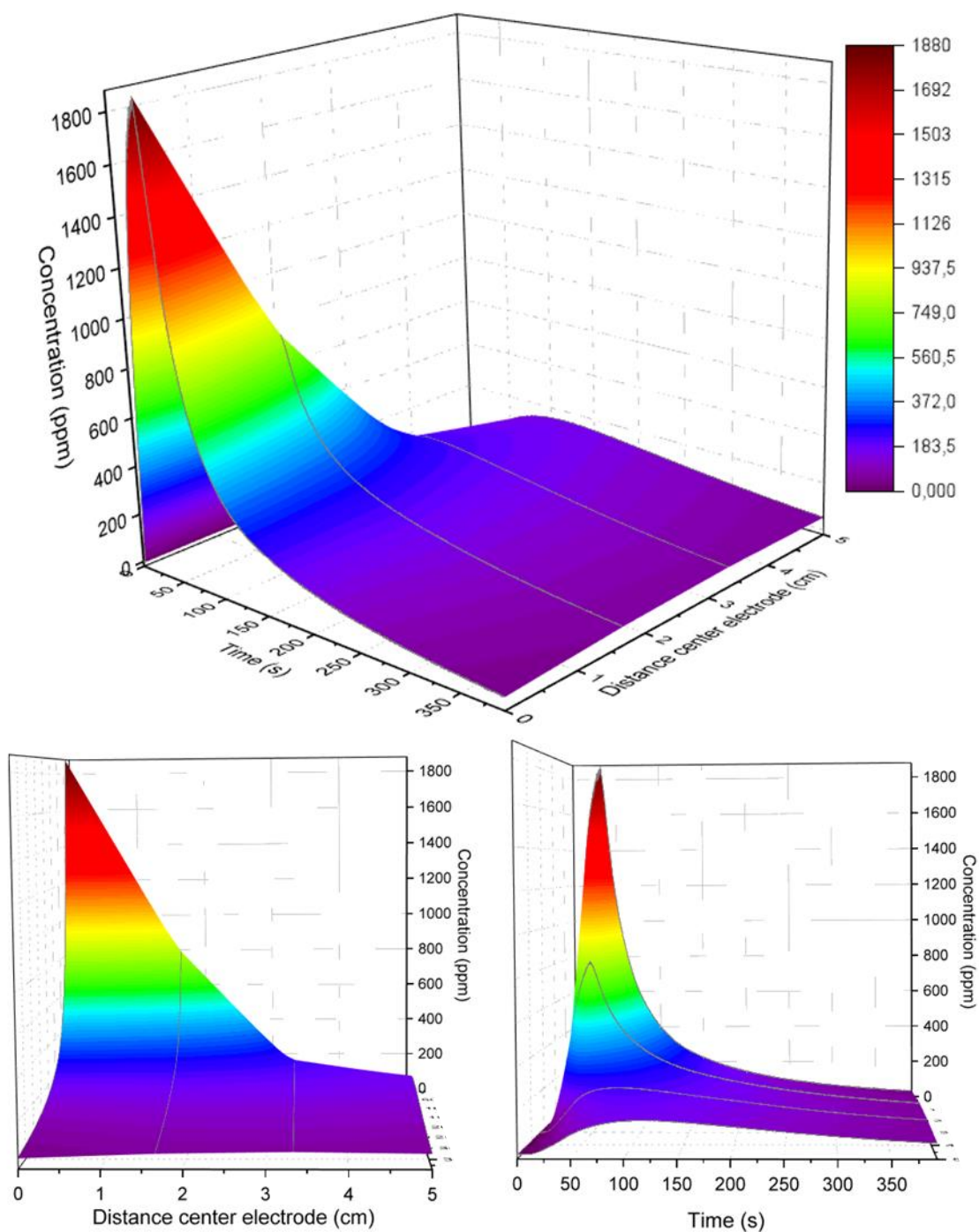
### *Ozone regime*

The first three graphs reported here show the ozone kinetic obtained with a power density of  $0.13 \text{ W/cm}^2$ ; the ozone concentration increased during the 30 seconds of plasma discharge and reached a peak value of 1880 ppm in correspondence of the electrode, at the end of the treatment, implying that higher concentrations could be reached for longer treatment time. After the switch off of the plasma there was a fall-off of  $O_3$  both in space and time. After about 350 seconds the concentration was distributed fairly homogeneously in space; the average concentration under the electrode was of 32 ppm, whereas the rest of the chamber contained about 55 ppm. Furthermore, there was still an overall decline in concentration noticeable over the whole volume after 400 seconds, presumably caused by the leakages of the reactor. The data at the peak value had a standard deviation 2% of the mean concentration. The rest of the data points had a higher ratio of standard deviation to mean concentration, about 5-20%.

Experiments were performed with the same power density to assess also the kinetic of nitrogen dioxide; no trace of  $NO_2$  was found in any condition.

Both  $O_3$  and  $NO_2$  analyses described the behaviour of a low-power density discharge, a regime in which there was not enough energy for reactions involving  $NO_x$ , hence only  $O_3$  was produced. The increase of  $O_3$  was stable during the discharge and tended to reach a plateau; this regime did not show any ozone poisoning effect.

It must be underlined that; measured concentrations of ozone are significantly higher than maximum values permitted by law in atmosphere; this fact implies the obligation to use an exhaust gas disposal system when using DBDs for industrial applications.



Graph 5.16 Visual representation of ozone kinetic obtained with a power density of  $0.13 \text{ W/cm}^2$ : global behaviour (top); spatial evolution (bottom left); temporal evolution (bottom right).

### *NO<sub>x</sub> regime*

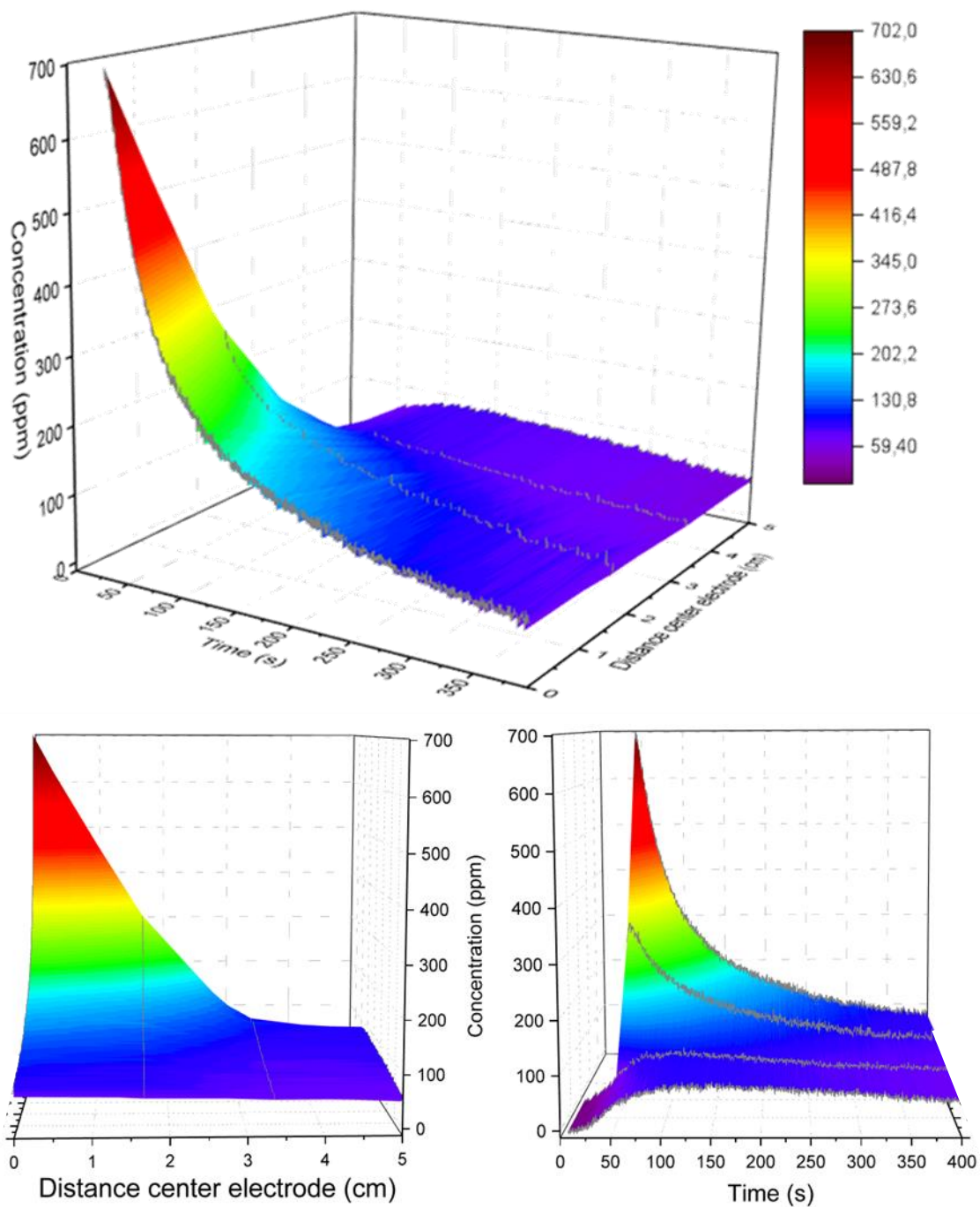
Graphs reported in this section show the nitrogen dioxide kinetic measured with a power density of 5.79 W/cm<sup>2</sup>. In this condition, the discharge was extremely intense and bright; in particular an intense radiation was emitted at 400 nm due to nitrogen reactions. Due to this fact, it was impossible to measure the concentration of NO<sub>2</sub> in the plasma discharge (under the electrode during the discharge time); the N<sub>2</sub> emission in that wavelength range covered the absorption of NO<sub>2</sub>. Consequently, the graph reported here shows no results for optical path 1 and 2 during the first 30 seconds of acquisition (discharge time).

After the plasma switch-off, the NO<sub>2</sub> concentration started to decrease; although we do not have any idea of the build-up trend, there must have been an increase in NO<sub>2</sub> concentration during the discharge time. The peak value reached from NO<sub>2</sub> was of 700 ppm and could be found at the end of the treatment time in correspondence of the electrode.

After about 350 seconds from the beginning of the treatment, the NO<sub>2</sub> concentration was distributed fairly homogeneously in space with an average of 65 ppm. This fact is remarkable, considering that in ozone regime, O<sub>3</sub> peak concentration was higher, while its final concentration was lower compared to the one measured in O<sub>3</sub> regime.

Standard deviation as a percentage of the mean concentrations ranged from 2% at the peak value, up to 60% for some data points 5 cm away for the electrode.

Experiments were performed with the same power density to assess also the kinetic of ozone; no trace of O<sub>3</sub> was found in any condition. The presence of NO<sub>2</sub> and the absence of O<sub>3</sub>, may lead to the conclusion that the plasma under examination was in a strong NO<sub>x</sub> regime. In this condition the ozone poisoning is extremely fast and forbade O<sub>3</sub> measurement.



Graph 5.17 Visual representation of nitrogen dioxide kinetic obtained with a power density of  $5.79 \text{ W/cm}^2$ : global behaviour (top); spatial evolution (bottom left); temporal evolution (bottom right).

### *Transition regime*

Results obtained at low- and high-power densities were interesting but non-conclusive; no poisoning effect was observed. To highlight ozone quenching and to assess if there was a relation between the poisoning effect and the NO<sub>2</sub> production, a new series of acquisitions has been made. The power density used was of 0.85 W/cm<sup>2</sup>; results are shown in graph 5.18.

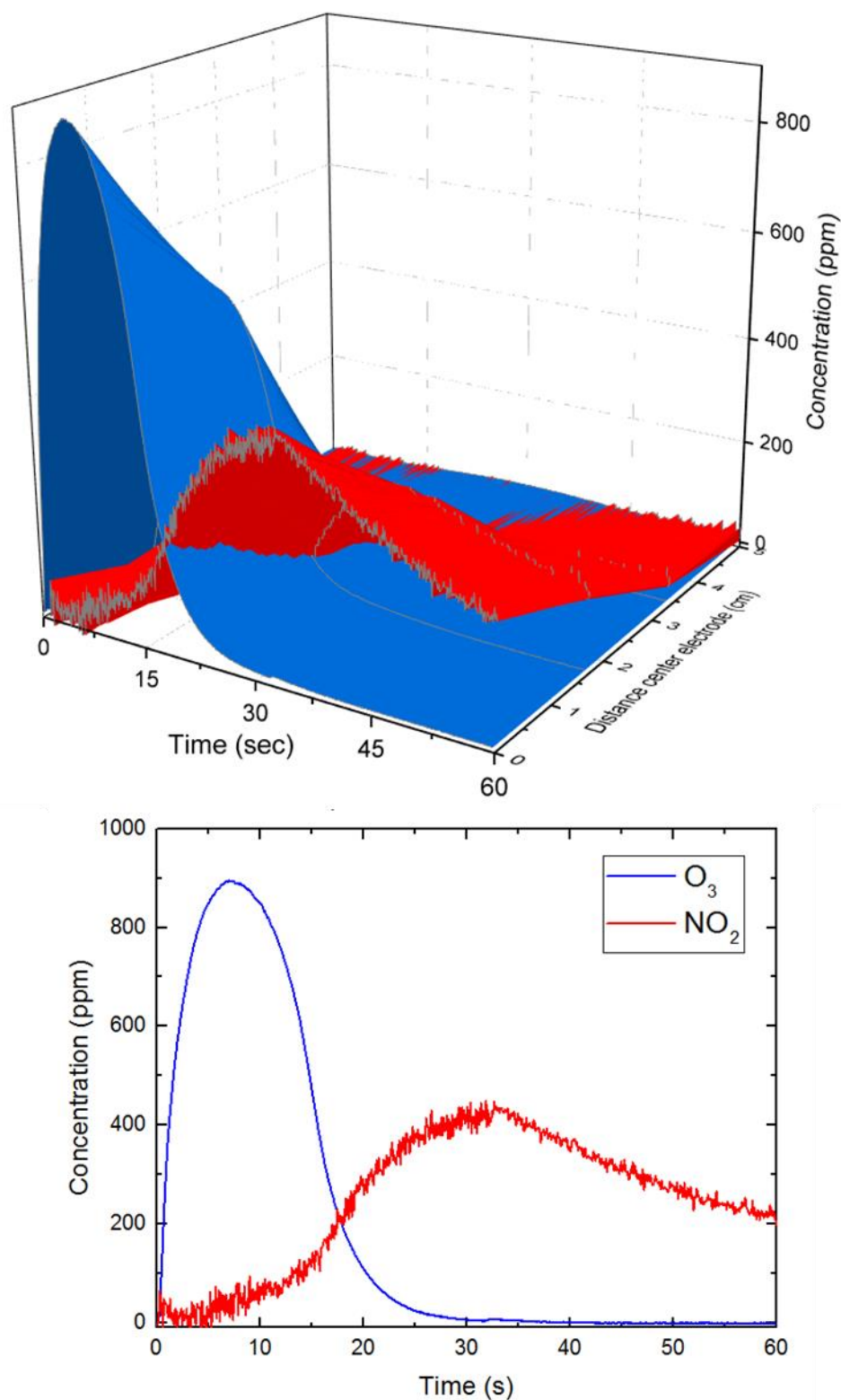
The plot has a shorter time interval than previous figures as the focus was on the kinetics of ozone quenching by nitrogen dioxide, which takes place during the treatment time. The plasma in the transition mode emitted a low intensity light at 400 nm; therefore, nitrogen dioxide and its concentration could have been investigated during the discharge time. This was done by adding a constant to the light intensities during the treatment time, equal to the emission of the plasma. For some data points at the beginning and at the end of the treatment, adding a constant was not possible as these measures were partly affected by the emission of the plasma. Therefore, those points have been excluded.

Ozone concentration grew for the first seconds of the plasma treatment and reached its peak after 7 seconds. The growth in concentration decreased when relatively small concentrations of nitrogen dioxide started to form. This was followed by a steep fall-off of ozone when a relatively small amount nitrogen dioxide was present. After 30 seconds the ozone was depleted. Ozone reached its peak concentration considerably faster in the transition mode, when compared to the ozone regime. The production rate of ozone is higher in the transition mode, due to the higher power density. However, in transition mode, ozone reached a lower peak concentration, as it was quenched.

Nitrogen dioxide in the transition mode reached its peak at the end of the discharge time; this peak value was almost two time lower than the peak reached with the highest power density. In the post discharge phase, only nitrogen dioxide remained, with a lower concentration compared to the results in the NO<sub>x</sub> regime.

The standard deviation as a percentage of the mean concentration of ozone and nitrogen dioxide is up to 4% and 12% for the peak values, respectively.



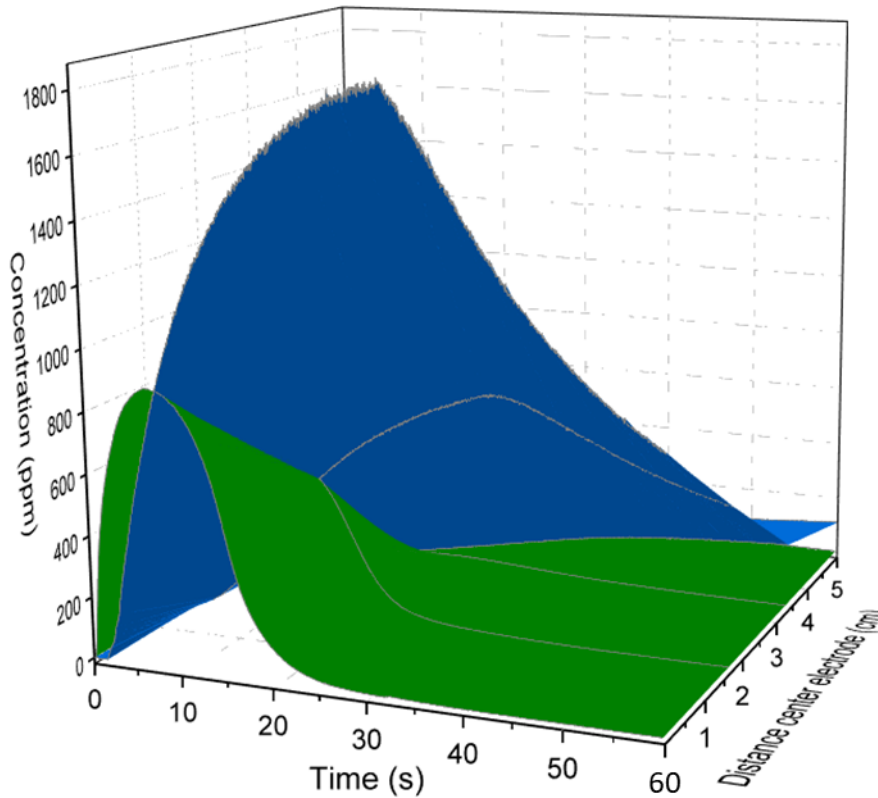


Graph 5.18 Visual representation of nitrogen dioxide and ozone kinetics obtained with a power density of  $0.85 \text{ W/cm}^2$ : global behaviour (top); temporal evolution under the high voltage electrode (bottom).

Finally, another graph is reported plotting together the ozone kinetics obtained in ozone mode and in transition mode; observing the ozone evolution under the electrode, there are mainly two remarks that is worth highlighting. Firstly, the ozone production

rate was greater in the transition mode, i.e. with the higher power density applied to the discharge. On the other hand, the peak concentration was almost double with the low-power density regime; this fact was related to the ozone poisoning effect, which started to quench the ozone a few seconds after the beginning of the discharge.

These trends are in perfect agreement with what showed by Moiseev [17].



*Graph 5.19 Visual representation of ozone kinetics obtained in ozone mode (blue curve) and in transition mode (green curve)*

O<sub>3</sub> and NO<sub>2</sub> data were also used to evaluate the diffusion inside the plasma reactor, which was thought to govern the distribution of species. The time needed for a species to diffuse over a certain length can be estimated by:

$$t \sim \frac{L^2}{D}$$

in which  $t$  is the time,  $L$  the distance and  $D$  the diffusion coefficient which depends of pressure (0.15 cm<sup>2</sup>/s for ozone and 0.17 cm<sup>2</sup>/s for nitrogen dioxide at atmospheric pressure[10]). Approximately, the time it took for the bulk of the ozone and nitrogen dioxide to travel 4 cm was 107 and 94 seconds respectively. In previous results, it was observed that it took about 100 seconds to reach a maximum in concentration 5 cm away from the centre of the electrode (which was about 4 cm from the edge of the electrode, the nearest place where species were produced). This rough estimation showed that, the movement of the species were dominated by diffusion. The approximation gave a close estimation but did not fully cover the propagation of species, as it neglected the concentration gradient.

## 5.7 Process characterization conclusions

The characterization phase of this project relied mainly on three types of investigation: temperature, electrical and OAS measurements.

The thermal analysis along with electrical measurements was fundamental to identify the optimal design of the DBD plasma source. In the frame of this work, four different materials have been tested as dielectric layer: PMMA, glass, mica and gres. PMMA was excluded due to its low thermal resistance for long treatment. Glass was found unusable in the conditions involved in this project: the glass layer broke after few minutes of operation due to thermal expansion. Although mica and gres showed similar results, both from a thermal and an electrical point of view, gres was chosen due to its better mechanical properties.

Electrical measurements were essential in two contexts: firstly, to measure the power density while trying different dielectric materials and thicknesses, hence the power conveyed from the plasma to the substrate. Later, electrical measurements were implied to parametrize on plasma conditions; in the frame of this work the plasma dose was defined by two quantities: treatment time and power density. By means of the electrical analysis the power density was calculated and used to compare different operative conditions.

OAS was by far the most sophisticated and useful characterization technique used. By analysing the absolute concentrations of ozone and nitrogen dioxide and their evolution, the chemistry involved in the discharge was studied. According to what was found in literature, two different chemical regimes were identified: a low-power density regime, in which the main reaction governing the chemistry was the one of production of ozone. This regime (called ozone regime) was described by a power density of  $0.13 \text{ W/cm}^2$ ; a stable production of ozone and no trace of nitrogen dioxide. On the contrary, at high power density ( $5.79 \text{ W/cm}^2$ ) no trace of ozone were detected, while a consistent production of nitrogen dioxide was observed; this condition was called nitrogen oxides regime. Finally, a transition regime was studied in between low- and high-power density regimes ( $0.85 \text{ W/cm}^2$ ); this analysis allowed to recognize the ozone poisoning effect. This phenomenon relies on two factors: the first is that, the ozone production rate grows increasing the power density applied to the discharge; secondly, if the power density exceed a certain threshold, the ozone concentration reaches a maximum level and starts to decrease after a precise time length; this time length is shorter for greater power densities.

The observation of this double chemistry, together with biological results reported in chapter 4, led to the conclusion that a  $\text{NO}_x$  enriched atmosphere has a greater biocidal effect if compared to a  $\text{O}_3$  enriched atmosphere.

## 5.8 References

- [1] Anon <https://www.thermoworks.com/emissivity-table>
- [2] Pipa A V., Hoder T and Brandenburg R 2013 On the Role of Capacitance Determination Accuracy for the Electrical Characterization of Pulsed Driven Dielectric Barrier Discharges *Contrib. to Plasma Phys.* 53 469–80
- [3] Pipa A V., Koskulics J, Brandenburg R and Hoder T 2012 The simplest equivalent circuit of a pulsed dielectric barrier discharge and the determination of the gas gap charge transfer *Rev. Sci. Instrum.* 83
- [4] Gibalov V I and Pietsch G J 2004 Properties of dielectric barrier discharges in extended coplanar electrode systems *J. Phys. D. Appl. Phys.* 37 2093–100
- [5] Okazaki S, Kogoma M, Ueharaj M and Kimura Y 1993 Appearance of stable glow discharge in air, argon, oxygen and nitrogen at atmospheric pressure using a 50 hz source *J. Phys. D. Appl. Phys.* 26 889–92
- [6] Fridman A 2008 *Plasma Chemistry*
- [7] Kogelschatz U and Baessler P 1987 Determination Of Nitrous Oxide And Dinitrogen Pentoxide Concentrations In The Output Of Air-Fed Ozone Generators Of High Power Density *Ozone Sci. Eng.* 9 195–206
- [8] Eliasson B, Hirth M and Kogelschatz U 1987 Ozone synthesis from oxygen in dielectric barrier discharges *J. Phys. D. Appl. Phys.* 20 1421–37
- [9] Anon Kogelshatz\_1988\_Brown\_Boveri\_Ozone\_generation.pdf
- [10] Shimizu T, Sakiyama Y, Graves D B, Zimmermann J L and Morfill G E 2012 The dynamics of ozone generation and mode transition in air surface micro-discharge plasma at atmospheric pressure *New J. Phys.* 14
- [11] Yagi S and Tanaka M 1979 Mechanism of ozone generation in air-fed ozonisers *J. Phys. D. Appl. Phys.* 12 1509–20
- [12] Kogelschatz U, Eliasson B and Hirth M 1988 Ozone generation from oxygen and air: discharge physics and reaction mechanisms
- [13] Kogelschatz U 2004 Atmospheric-pressure plasma technology *Plasma Phys. Control. Fusion* 46 B63
- [14] Kogelschatz U 2003 Dielectric-barrier Discharges: Their History , Discharge Physics , and Industrial Applications 23 1–46
- [15] Pavlovich M J, Chang H W, Sakiyama Y, Clark D S and Graves D B 2013

- Ozone correlates with antibacterial effects from indirect air dielectric barrier discharge treatment of water *J. Phys. D. Appl. Phys.* 46
- [16] Sakiyama Y, Graves D B, Chang H W, Shimizu T and Morfill G E 2012 Plasma chemistry model of surface microdischarge in humid air and dynamics of reactive neutral species *J. Phys. D. Appl. Phys.* 45
- [17] Moiseev T, Misra N N, Patil S, Cullen P J, Bourke P, Keener K M and Mosnier J P 2014 Post-discharge gas composition of a large-gap DBD in humid air by UV-Vis absorption spectroscopy *Plasma Sources Sci. Technol.* 23
- [18] Vinogradov I P and Wiesemann K 1997 Classical absorption and emission spectroscopy of barrier discharges in/NO and mixtures *Plasma Sources Sci. Technol.* 6 307
- [19] Gibson A R, McCarthy H O, Ali A A, O'Connell D and Graham W G 2014 Interactions of a non-thermal atmospheric pressure plasma effluent with PC-3 prostate cancer cells *Plasma Process. Polym.* 11 1142–9
- [20] Pavlovich M J, Clark D S and Graves D B 2014 Quantification of air plasma chemistry for surface disinfection *Plasma Sources Sci. Technol.* 23
- [21] Keller-Rudek H, Moortgat G K, Sander R and Sörensen R 2013 The MPI-Mainz UV/VIS spectral atlas of gaseous molecules of atmospheric interest *Earth Syst. Sci. Data* 5 365–73



## Chapter 6

# Numerical simulation

The analysis of the processes reported in chapter 5, together with biological results showed in chapter 4, highlighted that the efficacy of the DBD treatment under examination was strongly linked to the chemistry governing the process. A direct relation was found between the concentration of  $\text{NO}_x$  species and the biocidal effect of plasma.

Anyway, it was not fully clear was if  $\text{NO}_x$  were directly killing microbes or else if  $\text{NO}_x$  were just the marker of a strong antimicrobial process; some other agents being responsible for microbial inactivation s. From literature, it is known that fast reacting species (radicals and ions) have a strong effect on microbial inactivation [1–3]; moreover, some authors mentioned a possible biocidal effect of free electrons [4–6]. Unfortunately, these characteristics of plasma are not easy to detect and analyse; this is the reason why numerical simulation was involved in the final part of this work. Numerical simulation allows, after validation, to assess the physical and chemical behaviour of a discharge by means of a model. “A model in physics is a system of mathematical equations that are adapted, combined and solved to describe some aspects of reality. The solution of the model equations is intended to reproduce observed and measured phenomena, thus explaining these in terms of fundamental physics” [7]. Furthermore, a model can be used to predict the behaviour of a discharge, favouring experimental procedures.

Depending on the research field, several different models can be used; in the frame of this work two of them were implemented: a grand model and a specific model. A grand model (or global model) simulates the plasma discharge as a whole. The input of the model consists in the set of plasma control parameters such as materials and geometry, gas composition, gas mass flow and pressure, electrical power. The output of the model is formed by plasma properties and characteristics: electron density and temperature, density of chemical species. Outputs can later be used to calculate other secondary quantities, such as the heat flux or the emitted light. On the other hand, a specific model deals with the relation between internal quantities.

In the frame of this project, models were implemented in PLASIMO; the PLASIMO platform developed by Plasma Matters (<https://plasimo.phys.tue.nl/>) can be seen as a toolkit that facilitates the construction of specific and grand models. The greater part of plasma models is built upon the Boltzmann equation together with the Maxwell equations. These equations cannot be solved without making significant simplifications. There are mainly two methods for solving the Boltzmann equation: the kinetic approach and the fluid approach.

Kinetic models are time and spatially resolved; these models (e.g. Monte Carlo models) give kinetic information by following the trajectories of a large number of individual particles; consequently, this approach is extremely expensive in terms of computational cost, limiting dimensionality.

The alternative is to use a fluid model, which describes plasma species in terms of average quantities like the particle, momentum and energy densities. Fluid models solve the moments of the Boltzmann equation in time and space. The fluid approach, although being less accurate than the kinetic method, requires shorter computational effort. That allows higher dimensionality (2D, 3D).

The PLASIMO code was initially created by Hagelaar [8] and later developed by Van Dijk and Brok [9]. The code has been used for many different plasma modelling studies, such as DBD discharges [10], the plasma needle for biomedical applications [11], and simulations of plasma breakdown of a parabolic electrodes configuration [12].

In this thesis, two models are presented: a global model aimed to simulate the chemistry governing the plasma discharge and a fluid model to assess the fluid dynamics involved in the process.

## 6.1 Global model

This model is based on the solution of the particle balance equation for each species  $p$  included in the parameter definition:

$$\frac{\partial n_p}{\partial t} + \nabla \cdot \Gamma_p = S_p$$

Where  $\Gamma_p = n_p u_p$  is the flux density of the species  $p$ ;  $n_p$  is the density of the same species;  $u_p$  is the average velocity  $\mathbf{u}_p = \langle \mathbf{v} \rangle_p$ ;  $S_p$  is the net source term. However, in the global model the flux density term is neglected; therefore, the density of species relies only on the reaction occurring in the discharge:

$$S_p = \sum_r c_{p,r} R_r$$

Where  $c_{p,r}$  is the net stoichiometric number of particles of species  $p$  created in the reaction  $r$ ;  $c_{p,r}$  is positive in reaction which leads to the production of the species  $p$ , negative if the reaction leads to the destruction of  $p$ .  $R_r$  is the reaction rate and is proportional to the densities of reacting particles, this proportionality depends on the nature of the reaction (one, two or three body reactions).

The models of this kind are aimed to the evaluation of the chemistry governing a discharge, without considering the fluid dynamics of the process; this simplifies both the input parameters required to run the model and the solution of the model itself, hence reducing the computational effort.



### 6.1.1 Input parameters

In this paragraph the input parameters used to run the global model in PLASIMO will be presented; these inputs can be divided in two groups: gaseous and electrical parameters.

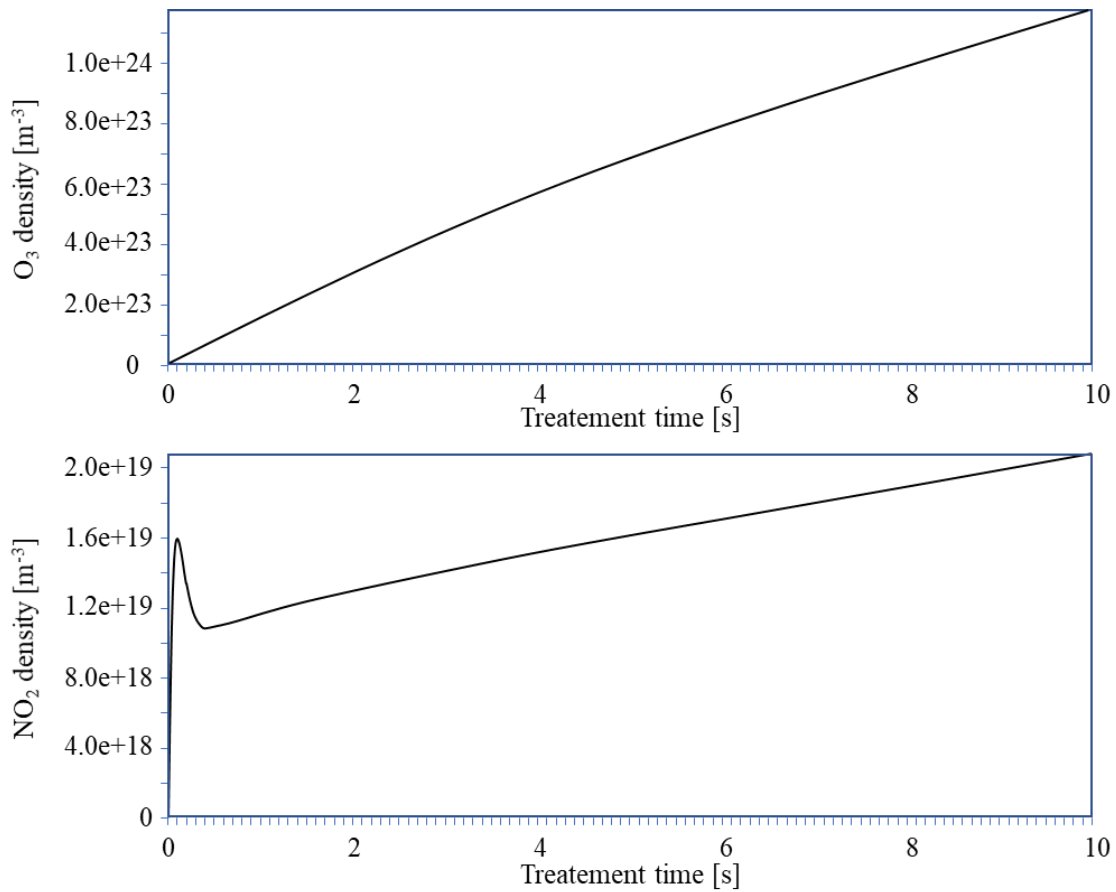
Gaseous parameters were the most complex to define and included:

- Initial gas composition: dealing with an open-air application, initial gas composition was defined by means of three main species nitrogen, oxygen and water (78%, 21% and 1% respectively, 1% of water correspond approximately to a 30% or relative humidity at 25°C).
- Species definition: at the beginning, more than 200 species were included in the model and this fact led to extremely long simulation. For this reason, several species were left out of the simulation, after verifying their hopefully negligible impact on the overall chemistry. The final set consisted of 48 species, including nitrogen, oxygen and hydrogen derivatives.
- Reaction list: the set of reaction occurring in the process had to be defined along with their reaction constants. These values were taken mainly from the *Plasma kinetic in atmospheric gases* [13], while other chemical parameters came from the NIST chemistry webbook [14].

The electrical input was defined as a constant volumetric power density defined over the plasma discharge volume ( $\text{W}/\text{m}^3$ ); this input was varied in different simulations to assess the ozone poisoning effect. DBD discharge is composed by streamers with drastic pressure and temperature gradients; consequently, assuming the electrical power as a constant is a strong approximation, however an initial step had to be taken. Three distinct results are reported here: ozone and nitrogen dioxide concentrations are shown as function of time; these results were obtained with three different power density inputs, here defined as: low, medium and high power. Treatment time was kept constant at 10 seconds to assess the ozone poisoning effect.

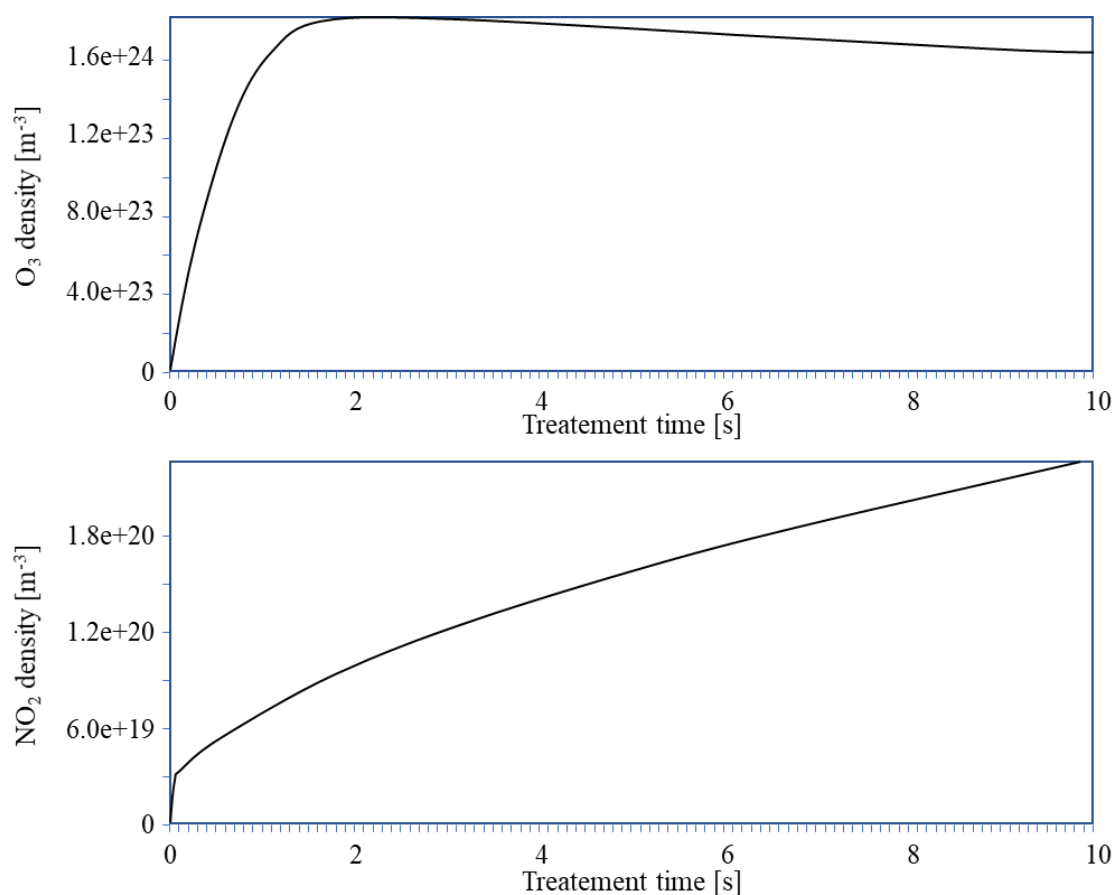
### 6.1.2 Global model results

The first graphs reported, show  $\text{O}_3$  and  $\text{NO}_2$  kinetics at low power density: the ozone concentration showed a constant increase over the 10 seconds of treatment.  $\text{NO}_2$  concentration grew as well; however, the final concentration reached was order of magnitude smaller; this fact is in good agreement with what has been observed with the OAS analysis. During the first tenths of second a spike is present in the  $\text{NO}_2$  trend; this fact cannot be explained with any reaction path, probably that spike relates to miscalculation connected to the beginning of the simulation.



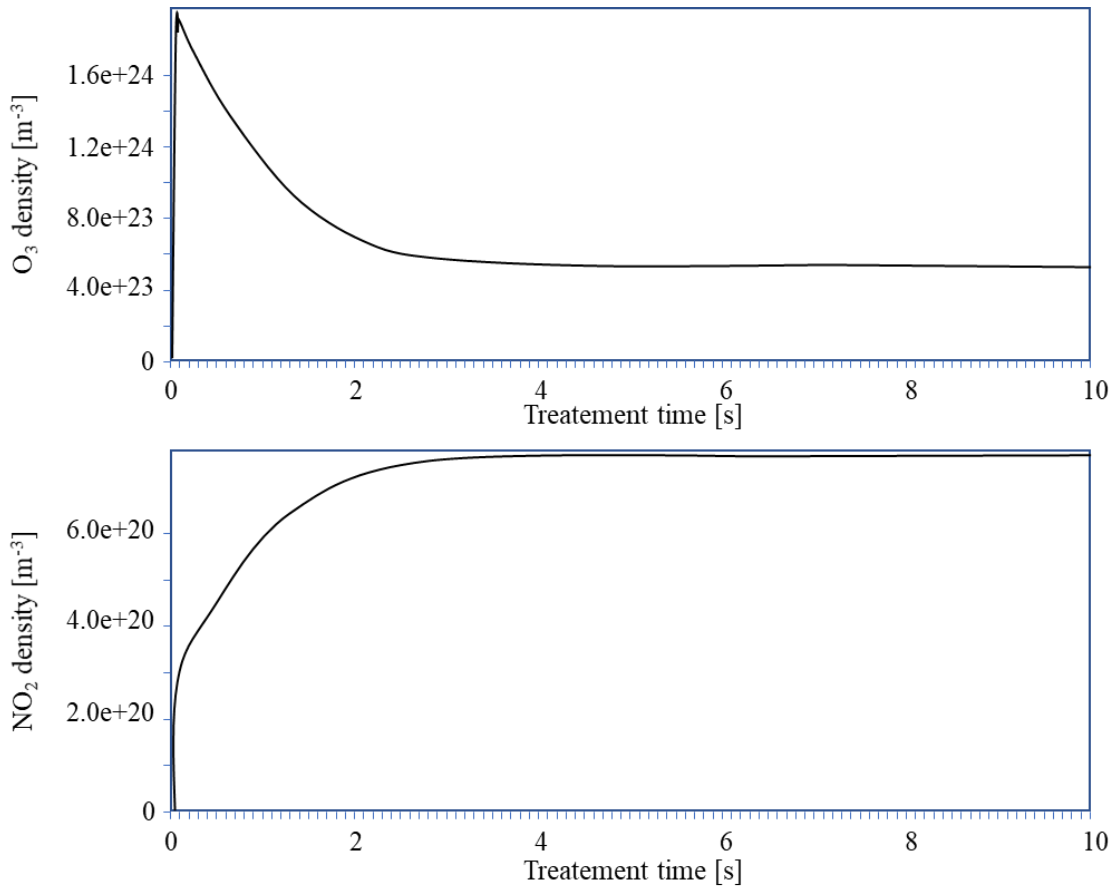
*Graph 6.1 O<sub>3</sub> and NO<sub>2</sub> evolution at low power density*

The second set of results was obtained with a medium power density; O<sub>3</sub> kinetics showed the poisoning effect: after an initial raise in the concentration, the ozone density started to decrease. The NO<sub>2</sub> concentration showed a steady growth; moreover, its concentration was higher than the one calculated for the low power density case; this fact, along with the ozone trend, confirmed the qualitative agreement between simulation and measurements.



*Graph 6.2 O<sub>3</sub> and NO<sub>2</sub> evolution at medium power density*

Finally, results at high power density are reported in graphs 6.3. There are two facts in these kinetic behaviours that need to be highlighted: first, the ozone quenching was faster than the one observed when using the medium power density; moreover the intensity of the ozone poisoning was also greater: as it can be seen the density dropped of more than one order of magnitude in about 2 seconds. A second interesting remark has to be made regarding the NO<sub>2</sub> concentration: NO<sub>2</sub> density raised for almost 2 seconds and then maintained that value until the end of the simulation; this behaviour is in good agreement with what reported in the chemistry analysis of chapter 5. NO<sub>2</sub> raised faster for greater power density; moreover, as soon as ozone was depleted the NO<sub>2</sub> density stabilized.



*Graph 6.3 O<sub>3</sub> and NO<sub>2</sub> evolution at high power density*

The global model allowed to define the chemistry governing the process; the set of inputs used with this model were included in the fluid model used to spatially analyse the plasma discharge.

## 6.2 Fluid model

As the global model, the fluid model relies on the iterative solution of the particle balance equation; unlike the global model, the flux density is not neglected. The most common definition of the flux density of a species  $p$  is here reported:

$$\Gamma_p = \mu_p \mathbf{E} n_p - D_p \nabla n_p$$

Where  $\Gamma$  is the flux density,  $\mathbf{E}$  is the electrical field,  $n$  is the density,  $\mu$  is the mobility and  $D$  is the diffusion coefficient. The first term at the right-hand side of this equation represent the flux due to the electric field (drift); while the second term represent the flux connected to the density gradients (diffusion). Accordingly, this type of model is also known as drift-diffusion model. The transport coefficients can be explained:

$$\mu_p = \frac{q_p}{m_{p0} v_{p0}} \quad D_p = \frac{k_B T_p}{m_{p0} v_{p0}}$$

Where  $m_{p0}$  and  $v_{p0}$  are the mass and the velocity of the buffer gas respectively;  $k_B$  is the Boltzmann constant and  $T_p$  is the temperature of the species  $p$ . Rearranging the transport coefficients, the Einstein relation can be derived:

$$D_p = \frac{k_B T_p \mu_p}{q_p}$$

This relation can be used to deduce the diffusion coefficient from the mobility; consequently, to solve the flux density equation, it is required to know the mobility of each species included in the model. Mobility data are reported in literature as a function of the reduced electric field ( $\mathbf{E}/N$ ); moreover, the mobility of a certain species is measured over a buffer gas; here is reported the equation to calculate the mobility of a species in a mixture:

$$\frac{1}{K} = \sum_j \frac{X_j}{K_j} + \frac{1}{2} \sum_j \frac{X_j}{K_j} (1 - \Delta_j) \frac{d \ln(K_j)}{d \ln(\frac{\mathbf{E}}{N})} \times \left[ 1 + \frac{d \ln(K_j)}{d \ln(\frac{\mathbf{E}}{N})} \right]^{-1}$$

Where  $K$  is the mobility coefficient over a buffer mixture,  $K_j$  is the mobility coefficient over a buffer gas and  $X_j$  is the molar fraction of the species  $j$  over the buffer gas. Although this equation is not particularly difficult to solve, mobility data are rare to find in literature; additionally, available data are defined over a small range of  $\mathbf{E}/N$  and often approximations must be taken. The most consistent work in this field was carried out by Ellis *et alii*; their measurements were widely used in this project [15–18].

## 6.2.1 Input parameters

The only change in the definition of the mixture, switching from the global model to the fluid model, was the inclusion of the mobility coefficient; these coefficients are needed only for ions; in fact, only charged species are affected by the electrical field (assumed as Laplacian). While the global model is a dimensionless model, the implementation of a drift-diffusion model required the definition of a geometry; a one-dimensional geometry was chosen. The DBD configuration under examination was not a highly complex one; therefore, a mono-dimensional approximation could be used without compromising similarity with the reality. The definition of the geometry in PLASIMO is done by individual squared blocks; thus, the size of the block must be consistent with the smallest dimension which allows to represent the geometry of the plasma source. In this case, the smallest dimension is the one of the interelectrode gap (1 mm); consequently 3 blocks are needed to describe the gres layer and two blocks are needed to represent walls (i.e. the electrodes).

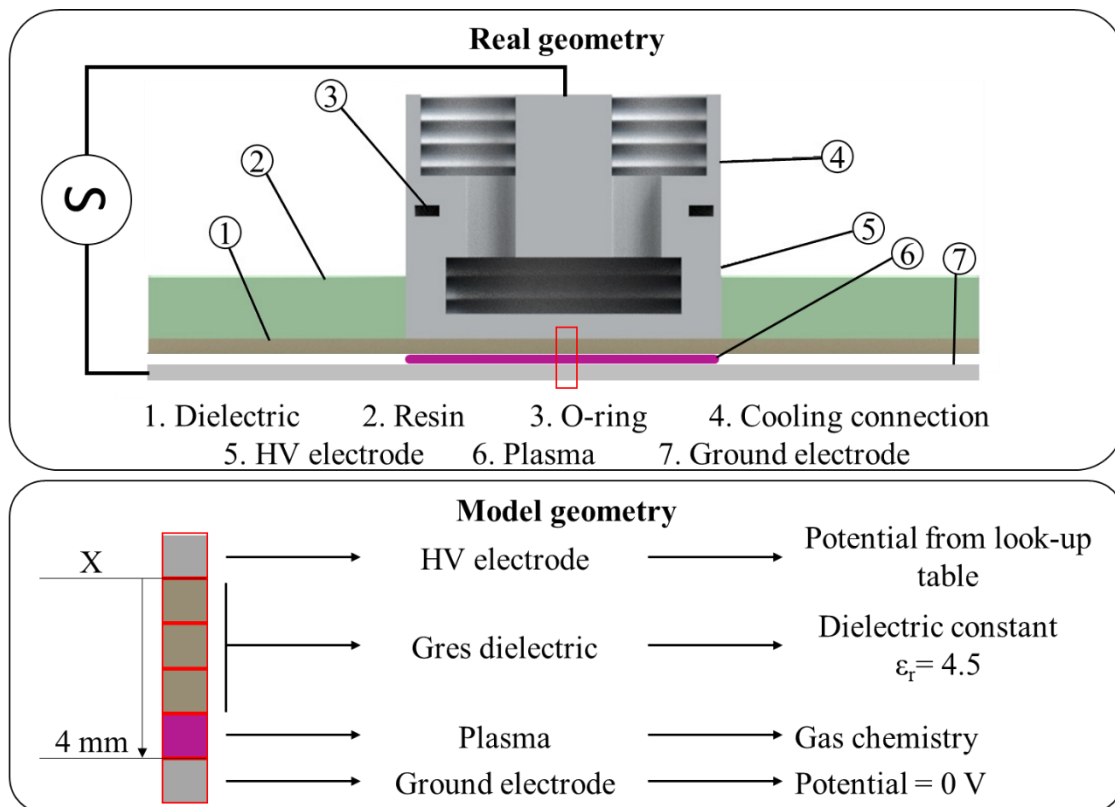
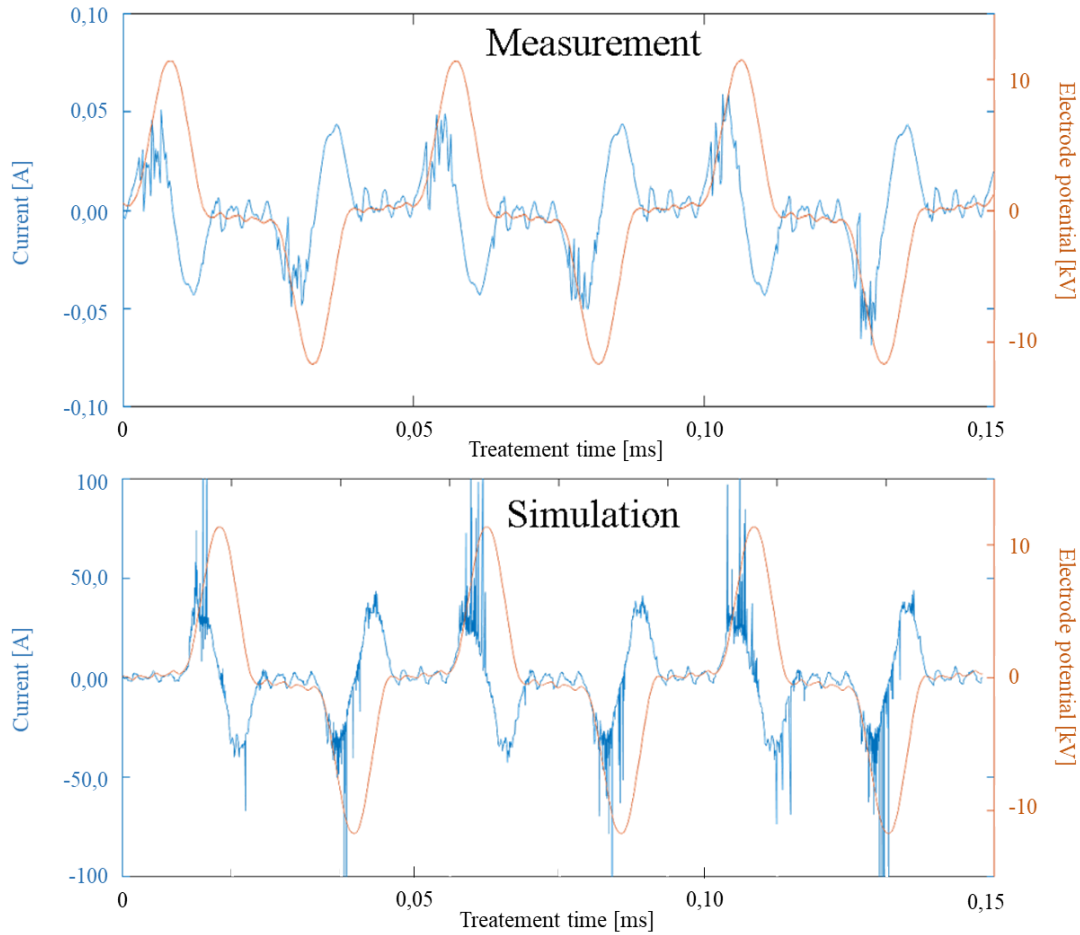


Figure 6.4 Schematic of the mono-dimensional geometry used for the fluid model implementation

Finally, the fluid model requires the definition of electrodes potential, differently from the global model which required the power density of the whole process. For this reason, a look-up table has been drawn with the potential measurements of the high voltage electrode; while the potential of the ground electrode was set to zero.

## 6.2.2 Fluid model results

In graph 6.5 a comparison between electrical measurements and numerical simulation results is shown; the orange line represents the potential waveform, which was measured and later used as input in the fluid model. The blue lines represent the current flowing through the high voltage electrode: a good similarity can be seen between measurements and calculated values. It must be underlined that, the orders of magnitude of the two current waveforms are extremely different. This fact can be explained introducing how PLASIMO deals with mono-dimensional simulation. PLASIMO must assume standard values to simulate a 3-D process. In the mono-dimensional model, equally shaped squares are defined; the software assigns to each square a cross-section of  $1 \text{ m}^2$ . Consequently, in this model, electrodes were defined with a generating surface of  $1 \text{ m}^2$ ; however, in realty electrodes had an active area of  $0.0011 \text{ m}^2$ . This surface discrepancy must be considered and can be solved using a scaling factor. In this case, the scaling factor was 0.0011. Multiplying current results by this factor, the order of magnitude of measurements and simulation results coincide.



*Graph 6.5 comparison between electrical measurements and numerical simulation using the drift-diffusion model*

### 6.3 Conclusions

A global model was created, and simulations of the plasma treatment under development were performed by means of PLASIMO. In this model, a complex mixture was defined consisting in 48 species derived from nitrogen oxygen and hydrogen; a set of hundreds of reactions was implemented to describe the, chemistry governing the plasma discharge. The  $O_3$  and  $NO_2$  kinetics were observed using three different levels of power density. With the lowest power density input no ozone quenching was observed:  $O_3$  concentration raised steadily in the whole simulation. Increasing the power density, the ozone poisoning effect was noticed: ozone concentration raised to a maximum and then started to decrease. The ozone poisoning effect was paired with an increase in  $NO_2$  concentration values. With the highest power density input, the ozone quenching was completed in about 2 seconds; the depletion of ozone led to a plateau in  $NO_2$  concentration.



The chemistry defined for the global model was expanded and implemented in a drift-diffusion model; by adding mobility data for charged species, the fluid dynamics of the plasma discharge could be modelled in a 1-D simulation. Although further investigation must be performed, preliminary results are promising: the electrical current of the discharge was calculated starting from electrodes potential waveforms with a good level of approximation.

In the frame of this project, numerical simulation of DBD air discharge was used to study the plasma process; although this investigation showed promising results, a lot of effort still has to be put in this analysis. Final results from the fluid model are not achieved yet; moreover, there are some traits of plasma that should be analysed more deeply. In the current model, only the temperature of the electrons is calculated, while the temperature of any other species is fixed. Considering that the temperature of the process is not constant, a parametric study about heating effect onto the chemistry of the discharge should be performed. Furthermore, the investigation performed so far included only ozone and nitrogen dioxide, while many other species are present in the model. An analysis on the kinetics of different species should be performed as well: starting from fast reacting species, such as nitrogen oxide, the hydroxyl radical and atomic oxygen.

Once refined the model, simulation should be used to identify the set of operating conditions that maximize the production of defined species; this work would lead to a deeper understanding of which chemical agents are connected with the microbial inactivation, and later with the optimization of the process.

## 6.4 References

- [1] Dobrynin D, Friedman G, Fridman A and Starikovskiy A 2011 Inactivation of bacteria using dc corona discharge: Role of ions and humidity *New J. Phys.* 13
- [2] Muranyi P, Wunderlich J and Heise M 2007 Sterilization efficiency of a cascaded dielectric barrier discharge *J. Appl. Microbiol.* 103 1535–44
- [3] Hähnel M, Von Woedtke T and Weltmann K D 2010 Influence of the air humidity on the reduction of Bacillus spores in a defined environment at atmospheric pressure using a dielectric barrier surface discharge *Plasma Process. Polym.* 7 244–9
- [4] Muranyi P, Wunderlich J and Langowski H C 2010 Modification of bacterial structures by a low-temperature gas plasma and influence on packaging material *J. Appl. Microbiol.* 109 1875–85
- [5] Xu X 2001 Dielectric barrier discharge - Properties and applications *Thin Solid Films* 390 237–42
- [6] Pavlovich M J, Clark D S and Graves D B 2014 Quantification of air plasma chemistry for surface disinfection *Plasma Sources Sci. Technol.* 23

- [7] Diana Borisova Mihailova 2010 *Sputtering Hollow Cathode Discharges designed for Laser Applications; Experiments and Theory*
- [8] Hagelaar G J M 2000 *Modeling of microdischarges for display technology*
- [9] Brok W J M 2005 *Modelling of transient phenomena in gas discharges*
- [10] Martens T, Bogaerts A, Brok W and van Dijk J 2007 Computer simulations of a dielectric barrier discharge used for analytical spectrometry *Anal. Bioanal. Chem.* 388 1583–94
- [11] Brok W J M, Bowden M D, Van Dijk J, der Mullen J and Kroesen G M W 2005 Numerical description of discharge characteristics of the plasma needle *J. Appl. Phys.* 98 13302
- [12] Brok W J M, Wagenaars E, van Dijk J and van der Mullen J 2007 Numerical description of pulsed breakdown between parabolic electrodes *IEEE Trans. Plasma Sci.* 35 1325–34
- [13] Capitelli M, Ferreira C M, Gordiets B F and Osipov A I 2013 *Plasma kinetics in atmospheric gases*
- [14] Linstrom P J and Mallard W G 2001 The NIST Chemistry WebBook: A chemical data resource on the internet *J. Chem. Eng. Data* 46 1059–63
- [15] Viehland L A and Mason E A 1995 Transport properties of gaseous ions over a wide energy range, IV *At. Data Nucl. Data Tables* 60 37–95
- [16] Ellis H W, Pai R Y, McDaniel E W, Mason E A and Viehland L A 1976 Transport Properties of Gaseous Ions Over a Wide Energy Range\* 17 177–210
- [17] Ellis H W, and others 1984 Transport properties of gaseous ions over a wide energy range, Part III, *At. Data Nucl. Data Tables* 31 113–51
- [18] Ellis H W, McDaniel E W, Albritton D L, Viehland L A, Lin S L and Mason E A 1978 Transport properties of gaseous ions over a wide energy range. Part II *At. data Nucl. data tables* 22 179–217

## Chapter 7

# Conclusions

In this 3 years Ph.D. project, a CAP process for microbial inactivation of packaging materials has been developed. During the first year of work, a thorough study of state of the art of standard disinfection treatments and plasma processes has been done, with the aim of identifying the most suitable plasma-assisted disinfection process in the framework examined.

The goal was to develop a process able to reduce the microbial load present on films used in food packaging procedures. Materials involved were both plastic and metallic; consequently, the temperature of the treatment had to be controlled, in order not to induce damage to the substrate. Additionally, treatment times were dictated by the particular type of industrial application and could not exceed ten seconds of duration.

Literature analysis, together with first biological results, showed that an open air DBD treatment would have been the best choice. After proving the feasibility of this concept using a PMMA DBD, a complete set of disinfection experiments was performed varying the process operative conditions. Biological results showed two different trends of microbial reduction for two distinct electrical input sets to the process; in particular, using a lower power density the influence of treatment time on microbial inactivation was almost negligible; additionally, the microbial reduction never exceeded the log 2. On the contrary, using a higher power density, the microbial inactivation showed a linear growing trend with increasing treatment time.

After biological tests, the characterization of the plasma discharge was accomplished; the aim of this phase of the project was to understand which reactive agents of the plasma were responsible for the antimicrobial effect of the treatment. These activities led to assess the most efficient operative conditions and later to an optimization of the process. To analyse the plasma discharge, three different methods have been used: thermal, electrical and OAS analysis.

Thermal and electrical analysis were involved mainly to study the behaviour of different materials used to realize the DBD source. Gres was found to be the best material to use as dielectric layer in the DBD layout; its electrical and mechanical properties were judged better than those of PMMA, glass and mica under stress tests.

OAS analysis was used to gain information about the chemistry governing the plasma discharge; in this frame, the concentration ozone and nitrogen dioxide were measured during treatments. In good agreement with literature, two distinct regimes were observed; the crucial parameter which allowed to switch from one regime to the other is the power density. At lower power density the O<sub>3</sub> concentration grew steadily

while no trace of  $\text{NO}_2$  has been detected. On the contrary, at higher power density no trace of  $\text{O}_3$  has been detected while  $\text{NO}_2$  grew steadily. Finally, a medium-power density was used to investigate a transition regime; in this condition the poisoning effect was observed: the concentration of  $\text{O}_3$  raised quickly as soon as the discharge was ignited; after a few seconds, the  $\text{O}_3$  reached a maximum and its concentration started to decrease; the complete depletion was achieved in 30 seconds. On the other hand,  $\text{NO}_2$  concentration started to rise a few seconds after the ignition of the discharge; its growth reached a plateau in correspondence of the  $\text{O}_3$  depletion.

OAS and biological results together led to the conclusion that the atmosphere produced by a high-power density has a stronger biocidal effect compared to the atmosphere produced by a low-power density one. Although OAS analysis led to the definition of the most efficient discharge regime, it was not clear which reactive agents of the plasma was directly responsible for the disinfection; consequently, numerical simulation has been involved to evaluate the behaviour of the different biocidal species of the treatment.

Two distinct models were created in PLASIMO: a global model and a fluid model. The global model was used to define the chemistry involved in the plasma discharge; this type of model neglects the importance of the drift and the diffusion of species allowing 0-D fast simulations. By means of this model, the chemical behaviours of both lower and higher power density discharges were assessed; furthermore, the ozone poisoning effect was observed. A fluid model was also created (using the chemistry defined for the global model) to assess the fluid dynamics governing the discharge. Conclusive results could not be achieved in the frame of this project; preliminary results obtained from simulations are promising since the electrical behaviour of the discharge was modelled almost perfectly; further investigation is needed to evaluate the different roles of reactive species present in the plasma.

## 7.1 Further investigations

An efficient open-air DBD disinfection process has been developed and further investigations are needed to optimize its treatment. Although the biocidal effect of the discharge was found to be linked with the chemistry involved in the process, there is still no direct relation between the microbial disinfection and the concentration of a reactive species. It would be interesting to identify new operative conditions able to maximize the presence of single reactive species (e.g.  $\text{NO}$ ,  $\text{OH}$ ,  $\text{O}$ ,  $\text{NO}_2$ ) and to perform biological experiment to assess the efficacy of those species. To do this, a more extensive use of numerical simulation must be involved; in fact, only this type of investigation may analyse the behaviour of each reactive species.

It would be interesting to analyse the efficacy of plasma in combination with another disinfection treatment such as ethylene oxide.

Finally, a lot of effort must be spent in order to realize each new industrial application; although at the moment the process is efficient on a lab scale, many changes have to be done to be able to use this technology on an industrial level. DBD dimensions must be scaled to allow a reasonable production rate; additionally, the

power supply has to be redesigned to satisfy the needs of an industrial process. Moreover, a gas flow system must be designed; species involved in the plasma discharge are toxic if reach a certain threshold; therefore, their use cannot be underestimated.

## 7.2 About disinfection treatment

In the frame of this project, an open-air DBD disinfection treatment has been developed. The efficacy of this process was already highlighted; however, in the industrial field several different disinfection treatments can be used and it is important to understand when it is worth to use a plasma assisted one instead of a conventional one. Plasma has several advantages compared to other inactivation methods: fast antimicrobial activity, moderate temperature reached during operation, easily removable gaseous residues.

Thermal disinfection methods are the most used, when applicable, due to their cost effectiveness. It is clear that this kind of methods cannot be involved in the disinfection of thermo-sensitive materials; applications that involve low thermal resistant material usually rely on chemicals or electromagnetic radiation to achieve disinfection. In this frame the plasma technology could be the best choice; using plasma instead of chemicals gives great advantages from the point of view of operation safety and environment concern. At the same time, the costs associated with electromagnetic radiation treatment are higher compared to those of a plasma assisted process.

To summarize, CAP disinfection treatments showed promising results both in terms of microbial reduction and of productivity rate; moreover, this technology could be the best disinfection method when materials with low thermal resistances are involved.



## Abstract

In this dissertation are reported the most relevant results obtained during my three years Ph.D. project. An open-air plasma source has been developed to treat plastic and metallic films typically used in food packaging manufacturing. Among others, the DBD configuration was chosen due to its many advantages such as high intensity and uniformity of the treatment, possibility of operating in ambient air as well as ease of scale up.

Biological experiments were performed to assess the microbial reduction induced by the plasma treatment. Different operative conditions have been tested in order to identify the most efficient configuration and two distinct behaviours have been observed: low-power density treatment allowed to achieve microbial inactivation values below  $\log 2$  independently on treatment time; high-power density treatment where the microbial reduction grew with increasing treatment time.

Subsequently, the plasma discharge has been characterized by means of three investigation methods: thermal, electrical and optical absorption spectroscopy (OAS) analysis. The thermal and electrical analyses were employed to identify the best dielectric materials for food packaging manufacturing purposes. Once defined the optimal DBD configuration, OAS was used to measure the absolute concentration of ozone and nitrogen dioxide. Results showed that at low-power density the chemistry is governed by ozone; while at high-power density ozone is consumed by the poisoning effect and only nitrogen dioxide is detectable.

Lastly, a numerical simulation has been used to deeper investigate the chemistry governing the plasma discharge; by means of PLASIMO a global model and a fluid model were implemented.





## Appendix

In this section are reported the data sheets of pathogens used in this dissertation and data sheets of materials used for the production of plasma sources.



Product Sheet

## *Escherichia coli* (ATCC® 11775™)

Please read this FIRST

Storage Temp.  
**Frozen: -80°C or colder**  
**Freeze-Dried: 2°C to 8°C**  
**Live Culture: See Propagation Section**

---

Biosafety Level  
**2**

### Intended Use

This product is intended for research use only. It is not intended for any animal or human therapeutic or diagnostic use.

### Citation of Strain

If use of this culture results in a scientific publication, it should be cited in that manuscript in the following manner: *Escherichia coli* (ATCC® 11775™)

American Type Culture Collection  
PO Box 1549  
Manassas, VA 20108 USA  
[www.atcc.org](http://www.atcc.org)

800.638.6597 or 703.365.2700  
Fax: 703.365.2750  
Email: [Tech@atcc.org](mailto:Tech@atcc.org)

Or contact your local distributor

Page 1 of 2

### Description

**Designation:** NCTC 9001  
**Deposited Name:** *Escherichia coli* (Migula) Castellani and Chalmers  
**Antigenic Properties:** Serovar O1:K1:H7  
**Product Description:** Type strain.

### Propagation

#### Medium

ATCC® Medium 3: Nutrient agar or nutrient broth

#### Growth Conditions

**Temperature:** 37°C

**Atmosphere:** Aerobic

#### Propagation Procedure

1. Open vial according to enclosed instructions.
2. Using a single tube of #3 broth (5 to 6 mL), withdraw approximately 0.5 to 1.0 mL with a Pasteur or 1.0 mL pipette. Rehydrate the entire pellet.
3. Aseptically transfer this aliquot back into the broth tube. Mix well.
4. Use several drops of the suspension to inoculate a #3 agar slant and/or plate.
5. Incubate the tubes and plate at 37°C for 24 hours.

### Notes

Additional information on this culture is available on the ATCC® web site at [www.atcc.org](http://www.atcc.org).

### References

References and other information relating to this product are available online at [www.atcc.org](http://www.atcc.org).

### Biosafety Level: 2

Appropriate safety procedures should always be used with this material. Laboratory safety is discussed in the current publication of the *Biosafety in Microbiological and Biomedical Laboratories* from the U.S. Department of Health and Human Services Centers for Disease Control and Prevention and National Institutes for Health.

### ATCC Warranty

ATCC® products are warranted for 30 days from the date of shipment, and this warranty is valid only if the product is stored and handled according to the information included on this product information sheet. If the ATCC® product is a living cell or microorganism, ATCC lists the media formulation that has been found to be effective for this product. While other, unspecified media may also produce satisfactory results, a change in media or the absence of an additive from the ATCC recommended media may affect recovery, growth and/or function of this product. If an alternative medium formulation is used, the ATCC warranty for viability is no longer valid.

### Disclaimers

This product is intended for laboratory research purposes only. It is not intended for use in humans. While ATCC uses reasonable efforts to include accurate and up-to-date information on this product sheet, ATCC makes no warranties or representations as to its accuracy. Citations from scientific literature and patents are provided for informational purposes only. ATCC does not warrant that such information has been confirmed to be accurate.

This product is sent with the condition that you are responsible for its safe storage, handling, and use. ATCC is not liable for any damages or injuries arising from receipt and/or use of this product. While reasonable effort is made to insure authenticity and reliability of materials on deposit, ATCC is not liable for damages arising from the misidentification or misrepresentation of such materials.

Please see the enclosed Material Transfer Agreement (MTA) for further details regarding the use of this product. The MTA is also available on our Web site at [www.atcc.org](http://www.atcc.org)




Product Sheet

***Escherichia coli* (ATCC®  
11775™)**


Additional information on this culture is available on the ATCC web site at [www.atcc.org](http://www.atcc.org).  
© ATCC 2017. All rights reserved. ATCC is a registered trademark of the American Type Culture Collection. [06/15]

Please read this FIRST



Storage Temp.  
**Frozen: -80°C or  
colder**  
**Freeze-Dried: 2°C  
to 8°C**  
**Live Culture: See  
Propagation  
Section**

---



Biosafety Level  
**2**

**Intended Use**

This product is intended for research use only. It is not intended for any animal or human therapeutic or diagnostic use.

**Citation of Strain**

If use of this culture results in a scientific publication, it should be cited in that manuscript in the following manner: *Escherichia coli* (ATCC® 11775™)

American Type Culture Collection  
PO Box 1549  
Manassas, VA 20108 USA  
[www.atcc.org](http://www.atcc.org)

800.638.6597 or 703.365.2700  
Fax: 703.365.2750  
Email: [Tech@atcc.org](mailto:Tech@atcc.org)

Or contact your local distributor




Product Sheet


## *Aspergillus brasiliensis* (ATCC® 16404™)

Please read this FIRST

Storage Temp.  
**Frozen: -80°C or colder**  
**Freeze-Dried: 2°C to 8°C**  
**Live Culture: See Propagation Section**



---

 Biosafety Level  
**1**

### Intended Use

This product is intended for research use only. It is not intended for any animal or human therapeutic or diagnostic use.

### Citation of Strain

If use of this culture results in a scientific publication, it should be cited in that manuscript in the following manner: *Aspergillus brasiliensis* (ATCC® 16404™)

American Type Culture Collection  
PO Box 1549  
Manassas, VA 20108 USA  
[www.atcc.org](http://www.atcc.org)

800.638.6597 or 703.365.2700  
Fax: 703.365.2750  
Email: [Tech@atcc.org](mailto:Tech@atcc.org)

Or contact your local distributor

Page 1 of 2

### Description

**Strain Designation:** WLRI 034(120) [CBS 733.88, DSM 1387, DSM 1988, IFO 9455, IMI 149007, NCPF 2275]

**Deposited Name:** *Aspergillus niger* van Tieghem

**Product Description:** An ampoule containing viable cells (may include spores and mycelia) suspended in cryoprotectant.

### Propagation

The information recommended in this section is to assist users in obtaining living culture(s) for their studies. The recommendation does not imply that the conditions or procedures provided below are optimum. Experienced researchers may initiate the growth of a culture in their own way.

ATCC® Medium 336: Potato dextrose agar (PDA)

ATCC® Medium 325: Malt extract agar (Blakeslee's formula)

ATCC® Medium 28: Emmons' modification of Sabouraud's agar

### Growth Conditions

**Temperature:** 20°C to 25°C

**Atmosphere:** Typical aerobic

### Recommended Procedure

For **freeze-dry (lyophilized) ampoules:**

1. Open an ampoule according to enclosed instructions.
2. From a single test tube of **sterile distilled water** (5 to 6 mL), withdraw approximately 0.5 to 1.0 mL with a sterile pipette and apply directly to the pellet. Stir to form a suspension.
3. Aseptically transfer the suspension back into the test tube of sterile distilled water.
4. Let the test tube sit at room temperature (25°C) undisturbed for **at least 2 hours**; longer (e.g., overnight) rehydration might increase viability of some fungi.
5. Mix the suspension well. Use several drops (or make dilutions if desired) to inoculate recommended solid or liquid medium. Include a control that receives no inoculum.
6. Incubate the inoculum at the propagation conditions recommended.
7. Inspect for growth of the inoculum/strain regularly. Viability is typically noticeable after 2 to 3 days of incubation. However, the time necessary for significant growth will vary from strain to strain.

**Colony and Cell Morphology:** Colonies initially white or yellowish, mycelium growing rapidly producing a dense layer of erect smooth-stiped, conidiophores terminated by globose vesicles bearing phialides (uniseriate) or metulae with phialides (biseriate) which produce dry chains of conidia. Reverse pale to grayish or greenish yellow. Vesicles radiate, initially pale, becoming dark brown to black. Conidia spherical, mid-to-dark brown, highly roughened with ridges and blunt or pointed protuberances, (3-4-5(-6) µm in diameter. Sporulation may be inhibited when grown in vessels with reduced gas exchange. Colonies may exhibit sectoring with areas of varying levels of sporulation. Use of freshly produced spores as inoculum should reduce sectoring.

### Notes

This strain was identified as belonging to the new species *Aspergillus brasiliensis* (see Varga et al. 2007 and Houseknecht et al., 2008.)

Additional, updated information on this product may be available on the ATCC® web site at [www.atcc.org](http://www.atcc.org).

### DNA Sequence

18S ribosomal RNA gene, partial sequence; internal transcribed spacer 1, 5.8S ribosomal RNA gene, and internal transcribed spacer 2, complete sequence; and 28S ribosomal RNA gene, partial sequence.  
GGTTCCGTAAGTGAACCTGCGGAAGGATCATTACCGAGTGC GGTCCTTTGGGCCAACCTCCATCC  
GTGTCATTGTACCCTGTTGCTTCGGCGGGCCCGCCGCTTGTGCGCCGCCGGGGGGCGCCTCTGCCCC  
CCGGGCCCGTGCCCGCGGAGACCCCAACACGAACCCTGTCTGAAAGCGTGCAGTCTGAGTCGATTGT  
TTGCAATCAGTTAAACTTTCAACAATGGATCTCTGGTTCCGGCATCGATGAAGAACGCAGCGAAAT  
GCGATAACTAATGTGAATTGCAGAATTCAGTGAATCATCGAGTCTTTGAACGCACATTGCGCCCCCTGG  
TATTCGGGGGGCATGCCTGTCGAGCGTCATTGCTGCCCTCAAGCCCGGCTTGTGTTGGGTCCGCCG  
TCCCCTCTCCGGGGGACGGGCCCGAAAGGCAGCGCGCCACCCGGTCCGATCCTCGAGCGTATG  
GGCCTTTGCACATGCTCTGTAGGATTGGCCGGCCCTGCCGACGTTTTCCAACATCTTTCCAGGTTG  
ACCTCGGATCAGGTAGGATACCCGCTGAACCTTAAGCATATCAATAA




Product Sheet

## *Aspergillus brasiliensis* (ATCC® 16404™)

Please read this FIRST

Storage Temp.  
**Frozen: -80°C or colder**  
**Freeze-Dried: 2°C to 8°C**  
**Live Culture: See Propagation Section**

---

 Biosafety Level  
**1**

### Intended Use

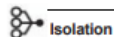
This product is intended for research use only. It is not intended for any animal or human therapeutic or diagnostic use.

### Citation of Strain

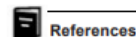
If use of this culture results in a scientific publication, it should be cited in that manuscript in the following manner: *Aspergillus brasiliensis* (ATCC® 16404™)

D1D2 region of the 28S Ribosomal RNA gene

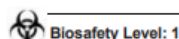
```
ATATCAATAAGCGGAGGAAAAGAAACCAACCGGGATTGCCTCAGTAACGGCGAGTGAAGCGGCAAG
AGCTCAAATTTGAAAGCTGGCTCCTTCGGAGTCCGCATTGTAATTTGCAGAGGATGCTTTGGGTGCGGC
CCCCGTCTAAGTGCCCTGGAACGGGCCGTCAGAGAGGGTGAGAATCCCGTCTTGGGCGGGGTGCCGT
GCCCGTGTAAAGCTCCTTCGACGAGTCGAGTTGTTGGGAATGCAGCTCTAAATGGTGGTAAATTTCA
TCTAAAGCTAAATACCTGGCCGGAGACCGATAGCGCACAAAGTAGAGTATCGAAAGATGAAAAGCAC
TTTGAAAAGAGAGTTAAACAGCACGTGAAATTTGAAAGGGAAGCGCTTGGCACCAGACTCGCCCG
CGGGGTTTCAGCCGCGCATCGTGCCGGTGTACTTCCCGTGGGCGGGCCAGCGTCGGTTTGGGCGGCC
GTCAAAGGCCCTTGGAAATGATGTGCCCTCCGGGGCACCTTATAGCCAGGGGTGCAATCGGGCCAGCCT
GGACCAGGAACCGCTTCGGCACGGACGCTGGCATAATGTCGTAAACGAC
```



Blueberry, North Carolina



References and other information relating to this product are available online at [www.atcc.org](http://www.atcc.org).



Appropriate safety procedures should always be used with this material. Laboratory safety is discussed in the current publication of the *Biosafety in Microbiological and Biomedical Laboratories* from the U.S. Department of Health and Human Services Centers for Disease Control and Prevention and National Institutes for Health.

### ATCC Warranty

ATCC® products are warranted for 30 days from the date of shipment, and this warranty is valid only if the product is stored and handled according to the information included on this product information sheet. If the ATCC® product is a living cell or microorganism, ATCC lists the media formulation that has been found to be effective for this product. While other, unspecified media may also produce satisfactory results, a change in media or the absence of an additive from the ATCC recommended media may affect recovery, growth and/or function of this product. If an alternative medium formulation is used, the ATCC warranty for viability is no longer valid.

### Disclaimers

This product is intended for laboratory research purposes only. It is not intended for use in humans. While ATCC uses reasonable efforts to include accurate and up-to-date information on this product sheet, ATCC makes no warranties or representations as to its accuracy. Citations from scientific literature and patents are provided for informational purposes only. ATCC does not warrant that such information has been confirmed to be accurate. This product is sent with the condition that you are responsible for its safe storage, handling, and use. ATCC is not liable for any damages or injuries arising from receipt and/or use of this product. While reasonable effort is made to insure authenticity and reliability of materials on deposit, ATCC is not liable for damages arising from the misidentification or misrepresentation of such materials. Please see the enclosed Material Transfer Agreement (MTA) for further details regarding the use of this product. The MTA is also available on our Web site at [www.atcc.org](http://www.atcc.org)

Additional information on this culture is available on the ATCC web site at [www.atcc.org](http://www.atcc.org).  
© ATCC 2018. All rights reserved. ATCC is a registered trademark of the American Type Culture Collection. [08/17]

American Type Culture Collection  
PO Box 1549  
Manassas, VA 20108 USA  
[www.atcc.org](http://www.atcc.org)

800.638.6597 or 703.365.2700  
Fax: 703.365.2750  
Email: [Tech@atcc.org](mailto:Tech@atcc.org)

Or contact your local distributor



Product Sheet

## ***Candida albicans* (ATCC® 10231™)**

Please read this FIRST

Storage Temp.  
**Frozen: -80°C or colder**  
**Freeze-Dried: 2°C to 8°C**  
**Live Culture: See Propagation Section**

---

Biosafety Level  
**1**

### Intended Use

This product is intended for research use only. It is not intended for any animal or human therapeutic or diagnostic use.

### Citation of Strain

If use of this culture results in a scientific publication, it should be cited in that manuscript in the following manner: *Candida albicans* (ATCC® 10231™)

American Type Culture Collection  
PO Box 1549  
Manassas, VA 20108 USA  
[www.atcc.org](http://www.atcc.org)

800.638.6597 or 703.365.2700  
Fax: 703.365.2750  
Email: [Tech@atcc.org](mailto:Tech@atcc.org)

Or contact your local distributor

### Description

**Strain Designation:** 3147 [CBS 6431, CCY 29-3-106, CIP 48.72, DSM 1386, IFO 1594, NCPF 3179, NCYC 1363, NIH 3147, VTT C-85161]

**Deposited Name:** *Candida albicans* (Robin) Berkhout

**Antigenic Properties:** Serotype A

**Product Description:** An ampoule containing viable cells (may include spores and mycelia) suspended in cryoprotectant.

### Propagation

The information recommended in this section is to assist users in obtaining living culture(s) for their studies. The recommendation does not imply that the conditions or procedures provided below are optimum. Experienced researchers may initiate the growth of a culture in their own way.

ATCC® Medium 200: YM agar or YM broth

ATCC® Medium 28: Emmons' modification of Sabouraud's agar

ATCC® Medium 1245: YEPD

### Growth Conditions

**Temperature:** 24°C to 26°C

**Atmosphere:** Typical aerobic

### Recommended Procedure

For **freeze-dry (lyophilized) ampoules:**

1. Open an ampoule according to enclosed instructions.
2. From a single test tube of **sterile distilled water** (5 to 6 mL), withdraw approximately 0.5 to 1.0 mL with a sterile pipette and apply directly to the pellet. Stir to form a suspension.
3. Aseptically transfer the suspension back into the test tube of sterile distilled water.
4. Let the test tube sit at room temperature (25°C) undisturbed **for at least 2 hours**; longer (e.g., overnight) rehydration might increase viability of some fungi.
5. Mix the suspension well. Use several drops (or make dilutions if desired) to inoculate recommended solid or liquid medium. Include a control that receives no inoculum.
6. Incubate the inoculum at the propagation conditions recommended.
7. Inspect for growth of the inoculum/strain regularly. The sign of viability is noticeable typically after 1-2 days of incubation. However, the time necessary for significant growth will vary from strain to strain.

**Colony and Cell Morphology:** On YEPD agar after 2 days at 25°C, colonies are cream-colored, shiny, and smooth. Older colonies show filaments-like structure at the margin and may have ridges or folds. Cells are ovoid (3.0-6.0 x 4.0-8.0 µm), budding, mostly singly and rarely clustered in young culture. Cells will elongate and form chain-like branched pseudohyphae in older culture.

### Notes

This strain is recommended by ATCC for use in the tests described in ASTM Standard Test Method E979-91 where only the taxon is specified; For sterility testing, not more than five passages from the ATCC culture should be used; Purified genomic DNA of this strain is available as ATCC 10231D-5™.

Additional, updated information on this product may be available on the ATCC® web site at [www.atcc.org](http://www.atcc.org).

### DNA Sequence

18S ribosomal RNA gene, partial sequence; internal transcribed spacer 1, 5.8S ribosomal RNA gene, and internal transcribed spacer 2, complete sequence; and 26S ribosomal RNA gene, partial sequence  
GGTTCCGTAGGTGAACCTGGGAAGGATCACTACTGATTGGCTTAATTGCACCACATGTTTCTTT  
GAAACAACTTGCTTTGGCGGTGGGCCAGCCTGCCGCCAGAGGTCTAAACTTACAACCAATTTTTAT  
CAACTGTACACACAGATTACTAATAGTCAAACTTTCAACAACGGATCTCTTGGTCTCGCATCGA  
TGAAGAAGCGCAGCGAAATGCGATACGTAATATGAATTGCAGATATTCGTGAATCATCGAATCTTGAA  
CGCACATTGCGCCCTCTGGTATTCGGAGGGCATGCCTGTTTGAGCGTCTTTCTCCCTCAAACCGCTGG  
GTTTGGTGTGAGCAATACGACTTGGGTTTGGCTTGAAGACGGTAGTGGTAAGCGGGATCGCTTGA  
CAATGGCTTAGGTCTAACCAAAAACATTGCTTGCGGCGTAACGTCCACCACGTATATCTTCAAACCTT  
GACCTCAAATCAGGTAGGACTACCCGCTGAACCTAAGCATATCAATAA

D1D2 region of the 26S ribosomal RNA gene  
ATATCAATAAGCGGAGGAAAAGAAACCAACAGGGATTGCCTCAGTAGCGGGAGTGAAGCGGCAAA




Product Sheet

## ***Candida albicans* (ATCC® 10231™)**

Please read this **FIRST**

Storage Temp.  
**Frozen: -80°C or colder**  
**Freeze-Dried: 2°C to 8°C**  
**Live Culture: See Propagation Section**

---

 Biosafety Level  
**1**

### **Intended Use**

This product is intended for research use only. It is not intended for any animal or human therapeutic or diagnostic use.

### **Citation of Strain**

If use of this culture results in a scientific publication, it should be cited in that manuscript in the following manner: *Candida albicans* (ATCC® 10231™)

American Type Culture Collection  
PO Box 1549  
Manassas, VA 20108 USA  
[www.atcc.org](http://www.atcc.org)

800.638.6597 or 703.365.2700  
Fax: 703.365.2750  
Email: [Tech@atcc.org](mailto:Tech@atcc.org)

Or contact your local distributor

Page 2 of 2

```
AGCTCAAATTTGAAATCTGGCGTCTTTGGCGTCGAGTTGTAATTTGAAGAAGGTATCTTTGGGCCCGG
CTCTTGCTATGTTCTTGGAACAGGACGTACAGAGGGTGAGAATCCCGTGCGATGAGATGACCCGG
GTCTGTGTAAAGTTCCCTCGACGAGTCGAGTTGTTTGGGAATGCAGCTCTAAGTGGGTGTAATTTCCA
TCTAAAGCTAAATATTGGCGAGAGACCGATAGCGAAACAAGTACAGTGATGGAAAGATGAAAAGAAC
TTTGAAAAGAGAGTGAAAAGTACGTGAAATTGTTGAAAGGGAAGGGCTTGAGATCAGACTTGGTAT
TTTGATGCTGCTCTCGGGGGCCGCGCTGCGGTTTACCGGGCCAGCATCGGTTTGGAGCGGCAGG
ATAATGGCGGAGGAATGTGGCACGGCTTCTGCTGTGTATAGCCTCTGACGACTGCCAGCCCTAG
ACCGAGGACTGCGGTTTTAACCTAGGATGTTGGCATAATGATCTTAA
```

### **Isolation**

Man with bronchomycosis

### **References**

References and other information relating to this product are available online at [www.atcc.org](http://www.atcc.org).

### **Biosafety Level: 1**

Appropriate safety procedures should always be used with this material. Laboratory safety is discussed in the current publication of the *Biosafety in Microbiological and Biomedical Laboratories* from the U.S. Department of Health and Human Services Centers for Disease Control and Prevention and National Institutes for Health.

### **ATCC Warranty**

ATCC® products are warranted for 30 days from the date of shipment, and this warranty is valid only if the product is stored and handled according to the information included on this product information sheet. If the ATCC® product is a living cell or microorganism, ATCC lists the media formulation that has been found to be effective for this product. While other, unspecified media may also produce satisfactory results, a change in media or the absence of an additive from the ATCC recommended media may affect recovery, growth and/or function of this product. If an alternative medium formulation is used, the ATCC warranty for viability is no longer valid.

### **Disclaimers**

This product is intended for laboratory research purposes only. It is not intended for use in humans. While ATCC uses reasonable efforts to include accurate and up-to-date information on this product sheet, ATCC makes no warranties or representations as to its accuracy. Citations from scientific literature and patents are provided for informational purposes only. ATCC does not warrant that such information has been confirmed to be accurate. This product is sent with the condition that you are responsible for its safe storage, handling, and use. ATCC is not liable for any damages or injuries arising from receipt and/or use of this product. While reasonable effort is made to insure authenticity and reliability of materials on deposit, ATCC is not liable for damages arising from the misidentification or misrepresentation of such materials. Please see the enclosed Material Transfer Agreement (MTA) for further details regarding the use of this product. The MTA is also available on our Web site at [www.atcc.org](http://www.atcc.org)


Additional information on this culture is available on the ATCC web site at [www.atcc.org](http://www.atcc.org).  
© ATCC 2019. All rights reserved. ATCC is a registered trademark of the American Type Culture Collection. [04/02]



Product Sheet


# *Staphylococcus aureus* *subsp. aureus* (ATCC® 6538™)

Please read this FIRST



Storage Temp.  
**Frozen: -80°C or colder**  
**Freeze-Dried: 2°C to 8°C**  
**Live Culture: See Propagation Section**

---



Biosafety Level  
**2**

## Intended Use

This product is intended for research use only. It is not intended for any animal or human therapeutic or diagnostic use.

## Citation of Strain

If use of this culture results in a scientific publication, it should be cited in that manuscript in the following manner: *Staphylococcus aureus subsp. aureus* (ATCC® 6538™)

American Type Culture Collection  
PO Box 1549  
Manassas, VA 20108 USA  
[www.atcc.org](http://www.atcc.org)

800.638.6597 or 703.365.2700  
Fax: 703.365.2750  
Email: [Tech@atcc.org](mailto:Tech@atcc.org)

Or contact your local distributor

Page 1 of 2

## Description

**Designation:** FDA 209

**Deposited Name:** *Staphylococcus aureus* subsp. *aureus* Rosenbach

**Product Description:** Used in testing media, sterility, sanitizers, disinfectants, antimicrobial preservatives, bacterial resistance in carpets and textiles, and as a control strain for Biosynth products. This strain is recommended by ATCC® for use in the tests described in military specification MIL G-13734B where only the taxon is specified.

## Propagation

### Medium

ATCC® Medium 18: Trypticase Soy Agar/Broth

### Growth Conditions

**Temperature:** 37°C

**Atmosphere:** Aerobic

### Propagation Procedure

1. Open vial according to enclosed instructions.
2. Using a single tube of #18 broth (5 to 6 mL), withdraw approximately 0.5 to 1.0 mL with a Pasteur or 1.0 mL pipette. Rehydrate the entire pellet.
3. Aseptically transfer this aliquot back into the broth tube. Mix well.
4. Use several drops of the suspension to inoculate a #18 agar slant and/or plate.
5. Incubate the tubes and plate at 37°C for 24 hours.

## Notes

Two colony types may be observed when growing ATCC® 6538™ on blood agar plates: Colony type 1 is yellow, circular, entire, low convex, and β-hemolytic; and colony type 2 is white, circular, entire, low convex, and β-hemolytic. Only colony type 1 has been observed on TSA maintenance medium.

This strain is also available as certified reference material ATCC® CRM-6538™.

Additional information on this culture is available on the ATCC® web site at [www.atcc.org](http://www.atcc.org).

## References

References and other information relating to this product are available online at [www.atcc.org](http://www.atcc.org).

## Biosafety Level: 2

Appropriate safety procedures should always be used with this material. Laboratory safety is discussed in the current publication of the *Biosafety in Microbiological and Biomedical Laboratories* from the U.S. Department of Health and Human Services Centers for Disease Control and Prevention and National Institutes for Health.

## ATCC Warranty

ATCC® products are warranted for 30 days from the date of shipment, and this warranty is valid only if the product is stored and handled according to the information included on this product information sheet. If the ATCC® product is a living cell or microorganism, ATCC lists the media formulation that has been found to be effective for this product. While other, unspecified media may also produce satisfactory results, a change in media or the absence of an additive from the ATCC recommended media may affect recovery, growth and/or function of this product. If an alternative medium formulation is used, the ATCC warranty for viability is no longer valid.

## Disclaimers

This product is intended for laboratory research purposes only. It is not intended for use in humans. While ATCC uses reasonable efforts to include accurate and up-to-date information on this product sheet, ATCC makes no warranties or representations as to its accuracy. Citations from scientific literature and patents are provided for informational purposes only. ATCC does not warrant that such information has been confirmed to be accurate.

This product is sent with the condition that you are responsible for its safe storage, handling, and use. ATCC





Product Sheet

***Staphylococcus aureus***  
***subsp. aureus*** (ATCC®  
6538™)

is not liable for any damages or injuries arising from receipt and/or use of this product. While reasonable effort is made to insure authenticity and reliability of materials on deposit, ATCC is not liable for damages arising from the misidentification or misrepresentation of such materials.


Please see the enclosed Material Transfer Agreement (MTA) for further details regarding the use of this product. The MTA is also available on our Web site at [www.atcc.org](http://www.atcc.org)

Additional information on this culture is available on the ATCC web site at [www.atcc.org](http://www.atcc.org).

© ATCC 2019. All rights reserved. ATCC is a registered trademark of the American Type Culture Collection. [10/01]


---

Please read this FIRST



Storage Temp.  
**Frozen: -80°C or colder**  
**Freeze-Dried: 2°C to 8°C**  
**Live Culture: See Propagation Section**

---



Biosafety Level  
**2**

---

**Intended Use**

This product is intended for research use only. It is not intended for any animal or human therapeutic or diagnostic use.

---

**Citation of Strain**

If use of this culture results in a scientific publication, it should be cited in that manuscript in the following manner: *Staphylococcus aureus subsp. aureus* (ATCC® 6538™)

American Type Culture Collection  
PO Box 1549  
Manassas, VA 20108 USA  
[www.atcc.org](http://www.atcc.org)

800.638.6597 or 703.365.2700  
Fax: 703.365.2750  
Email: [Tech@atcc.org](mailto:Tech@atcc.org)

Or contact your local distributor

# Ningbo LeadWin International Trade Co., LTD

## Omen Industrial Co., LTD

### Test Report of Muscovite Mica sheet

No.	Test items	Unit	Test results	Conclusion	
1	Mica Content	%	>ca.90	Pass	
2	Bond Content	%	<ca.10	Pass	
3	Density	g/cm <sup>3</sup>	1.6~2.0	Pass	
4	Heat Resistant	Continuous Services	℃	500~550	Pass
5		Intermittent Services	℃	800	Pass
6	Heat Loss at 500℃	%	<1	Pass	
7	Heat Loss at 700℃	%	<2	Pass	
8	Flexural Strength	MPa	<1	Pass	
9	Water Absorption	%		Pass	
10	Dielectric Strength	KV/mm	>15	Pass	
11	Insulation Resistance 23℃	Ω.cm		Pass	
12	Insulation Resistance 500℃	Ω.cm		Pass	
13	Flame Resistance		90V0	Pass	
14	Smoking Test	s		Pass	